

# **Investigating the Effect of Ageing and Substrate Variation on the Raman Spectrum of Equine Blood**

by

Christopher Wassell

A thesis submitted in partial fulfilment for the requirements for the degree of MSc (by  
Research) at the University of Central Lancashire

January 2016

## STUDENT DECLARATION FORM

### Concurrent registration for two or more academic awards

I declare that while registered as a candidate for the research degree, I have not been a registered candidate or enrolled student for another award of the University or other academic or professional institution



---

### Material submitted for another award

I declare that no material contained in the thesis has been used in any other submission for an academic award and is solely my own work



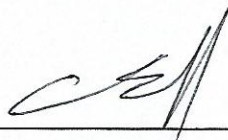
---

(state award and awarding body and list the material below):

### Collaboration

Where a candidate's research programme is part of a collaborative project, the thesis must indicate in addition clearly the candidate's individual contribution and the extent of the collaboration. Please state below:

Signature of Candidate



---

Type of Award

MSc by RESEARCH

---

School

FORENSIC AND INVESTIGATIVE SCIENCES

---

## **ABSTRACT**

Blood is one of the most common and useful evidence types found at the crime scene. Blood can indicate the number of suspects involved, the weapon used, the series of events, and can be used to generate DNA profiles. However, in some circumstances it can be difficult to identify blood on various substrates. Additionally other substances (such as paint and foodstuff) can be mistaken for blood. Current presumptive and confirmatory tests for blood used in forensic science (such as Luminol and Crystalline tests) have certain disadvantages including false positives and invasive testing. Raman spectroscopy is a method of non-invasive, confirmatory testing for blood and (with the recent development of handheld spectrometers) confirmation of blood at the crime scene is now possible

The aim of this research is to investigate the effect of ageing and substrate variation on the Raman spectrum of Equine blood. The main focus will be on the possible effects on the main peak intensities corresponding to blood. This paper will also discuss the reliability of Raman spectroscopy to identify blood in conditions to those similar to the crime scene environment.

Through analysis of spectra collected using Raman spectroscopy it was possible to demonstrate that the main peaks corresponding to blood undergo changes in intensity over time. The general change was an increase in intensity over time which did not correspond to the expectations of the study. However, decreases in intensity were seen at peaks  $1587\text{cm}^{-1}$  and  $1640\text{cm}^{-1}$  over time which did correspond to the expectations of the study and did correspond to haemoglobin degradation. Additionally, using Raman spectroscopy it was possible to demonstrate that the main peaks corresponding to blood undergo peak intensity fluctuations across various substrates. Initially, peak intensities

varied greatly with each other and then decreased over time. The most significant decrease in intensity was seen at peaks  $1587\text{cm}^{-1}$  and  $1640\text{cm}^{-1}$  which correspond to haemoglobin degradation.

Bought Equine (horse) blood was deposited on 6 substrates used for analysis: crystalline silicon (standard), a condom, brown leather, a ceramic tile, laminate flooring and blue denim. These substrates were chosen to represent similar substrates which blood may come into contact with at the crime scene. 3 droplets on each substrate were then analysed via Raman spectroscopy over a period of three months at time periods of:  $\leq 1\text{hr}$ , 2hrs, 5hrs, 24hrs, 1 week, 2 weeks, 1 month (28days), 2 months (56 days) and 3 months (84 days).

This research combines both ageing and substrate studies where previous research has only analysed the two separately. This research will also provide evidence for the use of Raman spectroscopy in a forensic context, specifically, when analysing blood at different stages of ageing and on different substrates.

## LIST OF CONTENTS

	<b>Page Number</b>
<b>ABSTRACT</b>	3
<b>LIST OF CONTENTS</b>	5
<b>ACKNOWLEDGEMENTS</b>	8
<b>LIST OF FIGURES</b>	9
<b>LIST OF TABLES</b>	13
<b>LIST OF ABBREVIATIONS</b>	15
<b>CHAPTER 1-INTRODUCTION</b>	17
<i>1.1 Blood Pattern Analysis</i>	17
<i>1.2 Denaturation of Blood Over time</i>	20
<i>1.3 Identification and Analysis of Blood at the Crime Scene</i>	22
<i>1.4 Raman Spectroscopy</i>	25
<i>1.5 Advantages of Raman Spectroscopy</i>	30
<i>1.6 Disadvantages of Raman Spectroscopy</i>	30
<i>1.7 Surface Enhanced Raman Spectroscopy (SERS)</i>	31
<i>1.8 Portable Raman Instruments</i>	31
<i>1.9 Previous Studies: Raman Analysis of Blood</i>	32
<i>1.10 Substrate Variation at the Crime Scene</i>	33
<i>1.11 Study Aims and Rationale</i>	35
<i>1.12 Pre-Processing Techniques and Multivariate Analysis</i>	36
(MVA) Review	
<b>CHAPTER 2-MATERIALS AND METHODS</b>	38

2.1 Blood Specimens	38
2.2 Substrates	39
2.3 Raman Spectroscopy Instrumentation	40
2.4 Methodology	42
2.5 Data Pre-Processing and MVA	42
<b>CHAPTER 3-SPECTRAL COMPOSITION</b>	44
3.1 Blood Spectrum	44
3.2 Blood Components	48
3.3 Substrate Spectra	52
3.4 Blood on Substrate	63
3.5 Conclusions	64
<b>CHAPTER 4-INVESTIGATING THE EFFECT OF AGEING ON</b>	65
<b>THE RAMAN SPECTRUM OF EQUINE BLOOD</b>	
4.1 Raw Spectrum of Blood	65
4.2 5 <sup>th</sup> Order Polynomial Fit Pre-Processing	68
4.3 5 <sup>th</sup> Order Polynomial Fit PCA Plots	72
4.4 5 <sup>th</sup> Order Polynomial Fit DFA Plots	74
4.5 5 <sup>th</sup> Order Polynomial Fit Early Against Late Spectra	79
4.6 2 <sup>nd</sup> Order Derivative DFA Plots	83
4.7 2 <sup>nd</sup> Order Derivative Early Against Late Spectra	88
4.8 Conclusions	92
<b>CHAPTER 5-INVESTIGATING THE EFFECT OF SUBSTRATE</b>	94
<b>VARIATION ON THE RAMAN SPECTRUM OF</b>	

<b>EQUINE BLOOD</b>	
<b>5.1 5<sup>th</sup> Order Polynomial Fit DFA Plots</b>	94
<b>5.2 Conclusions</b>	100
<b>CHAPTER 6- INVESTIGATING THE EFFECT OF AGEING AND</b>	102
<b>SUBSTRATE VARIATION ON THE RAMAN</b>	
<b>SPECTRUM OF BLOOD (PHOTO TIMELINE)</b>	
<b>6.1 Blood on Denim-Photo Timeline</b>	108
<b>6.2 Raman Microscopic Images</b>	109
<b>6.3 Conclusions</b>	110
<b>CHAPTER 7-CONCLUSIONS</b>	112
<b>CHAPTER 8-FUTURE WORK</b>	114
<b>BIBLIOGRAPHY</b>	115
<b>APPENDICES</b>	126
<b>Appendix 1</b>	126

## **ACKNOWLEDGEMENTS**

Firstly I would like to thank my Director of Studies, Dr Matt Baker, for letting me be part of the research team and for giving me the opportunity to carry out this research. I am gratefully appreciative of all the time, effort and expertise he has given me throughout this past year. Great supervisor, great guy.

Secondly, I would like to thank Dr Graeme Clemens for his help with MATLAB and all the time and effort he also put aside to make this research possible. It has been a pleasure to work with both Matt and Graeme.

Finally, I would like to thank my family; especially my parents and Naomi. They have given me lots of support and helped me out whenever I have needed it. They have even put up with me when I have been stressed; which is not a picnic. A special thanks to Naomi for helping me with money and buying the majority of the pizzas.

## LIST OF FIGURES

<b>Figure Number</b>	<b>Title</b>	<b>Page Number</b>
<b>Figure 1</b>	Raman spectra of pure blood acquired using 406.7 (A), 457.9 (B), 488 (C), 514.5 (D), 647.1 (E) and 785 (F) nm excitations. Extracted from [2].	17
<b>Figure 2</b>	Showing the Hb path in the human body. Adapted from [9].	21
<b>Figure 3</b>	Showing the process of Hb oxygenation and denaturation of a blood stain. Adapted from [9].	21
<b>Figure 4</b>	Photograph demonstrating the effect of spraying Luminol on blood at a crime scene. Extracted from [12].	23
<b>Figure 5</b>	Energy level diagram. Raman fits in the UV-visible.	26
<b>Figure 6</b>	Mechanism of Raman spectroscopy. Adapted from [17].	26
<b>Figure 7</b>	The fundamentals of Raman scattering. Adapted from [19].	27
<b>Figure 8</b>	The vibrational modes of CO <sup>2</sup> Adapted from [17].	29
<b>Figure 9</b>	Ceramic tile substrate and Equine blood.	39
<b>Figure 10</b>	Blue denim substrate and blood.	39
<b>Figure 11</b>	Brown leather substrate and blood.	39
<b>Figure 12</b>	Condom substrate and blood.	39
<b>Figure 13</b>	Crystalline silicon substrate and blood.	40
<b>Figure 14</b>	Laminate tile substrate and blood.	40
<b>Figure 15</b>	The Horiba Jobin-Yvon LabRAM HR800 confocal Raman	40

Spectrometer used to take blood and substrate scans.

<b>Figure 16</b>	Blood droplet showing line scan points.	45
<b>Figure 17</b>	Raw line scan of blood droplets dried <1hr.	45
<b>Figure 18</b>	Raw line scan of blood droplets dried >1hr.	46
<b>Figure 19</b>	Raw mean Raman spectrum of ceramic tile.	52
<b>Figure 20</b>	Raw mean Raman spectrum of blue denim.	54
<b>Figure 21</b>	Raw mean Raman spectrum of brown leather.	56
<b>Figure 22</b>	Raw mean Raman spectrum of Durex Thin Feel <sup>®</sup> Condoms.	58
<b>Figure 23</b>	Raw mean Raman spectrum of laminate flooring.	60
<b>Figure 24</b>	Raw mean Raman spectrum of crystalline silicon.	61
<b>Figure 25</b>	Mean raw spectra of blood on condom.	63
<b>Figure 26</b>	Spectrum of blood on condom after 5 <sup>th</sup> order polynomial fit pre-processing technique.	63
<b>Figure 27</b>	[A.] Mean raw Raman spectra of blood on denim. [B.] Mean raw Raman spectra of blood on leather. [C.] Mean raw Raman spectra of blood on laminate.	66
<b>Figure 28</b>	The mean raw Raman spectra of blood on condom.	67
<b>Figure 29</b>	The 5 <sup>th</sup> order polynomial fit pre-processed spectra of blood on: [A.] Denim [B.] Leather [C.] Condom.	70
<b>Figure 30</b>	PCA plot of blood on denim.	72
<b>Figure 31</b>	PCA plot of blood on leather.	73
<b>Figure 32</b>	PCA plot of blood on crystalline silicon.	73
<b>Figure 33</b>	5 <sup>th</sup> order polynomial fit DFA plot of blood on ceramic.	75
<b>Figure 34</b>	5 <sup>th</sup> order polynomial fit DFA plot of blood on condom.	75
<b>Figure 35</b>	5 <sup>th</sup> order polynomial fit DFA plots of blood on leather.	76

<b>Figure 36</b>	The mean 5 <sup>th</sup> order polynomial spectra of blood on ceramic against DFA spectrum.	77
<b>Figure 37</b>	The mean 5 <sup>th</sup> order polynomial spectra of blood on condom against DFA spectrum.	78
<b>Figure 38</b>	The mean 5 <sup>th</sup> order polynomial spectra of blood on leather against DFA spectrum.	78
<b>Figure 39</b>	The mean early and late spectra of blood on ceramic against DFA spectrum.	80
<b>Figure 40</b>	The mean early and late spectra of blood on condom against DFA spectrum.	80
<b>Figure 41</b>	The mean early and late spectra of blood on leather against DFA spectrum.	81
<b>Figure 42</b>	2 <sup>nd</sup> order derivative DFA plot of blood on ceramic.	83
<b>Figure 43</b>	2 <sup>nd</sup> order derivative DFA plot of blood on leather.	84
<b>Figure 44</b>	2 <sup>nd</sup> order derivative DFA plot of blood on crystalline silicon.	84
<b>Figure 45</b>	Mean 2 <sup>nd</sup> order derivative spectra of blood on ceramic against DFA spectrum.	86
<b>Figure 46</b>	Mean 2 <sup>nd</sup> order derivative spectra of blood on leather against DFA spectrum.	86
<b>Figure 47</b>	Mean 2 <sup>nd</sup> order derivative spectra of blood on silicon against DFA spectrum.	87
<b>Figure 48</b>	The mean early and late spectra of blood on ceramic against DFA spectrum.	89
<b>Figure 49</b>	The mean early and late spectra of blood on leather against DFA spectrum.	89

<b>Figure 50</b>	The mean early and late spectra of blood on silicon against DFA spectrum.	90
<b>Figure 51</b>	DFA plot of blood on substrates at $\leq 1$ hr.	95
<b>Figure 52</b>	Mean 5 <sup>th</sup> order polynomial Raman spectra of blood on substrates at $\leq 1$ hr against DFA spectrum.	95
<b>Figure 53</b>	DFA plot of blood on substrates at 24hr.	96
<b>Figure 54</b>	Mean 5 <sup>th</sup> order polynomial Raman spectra of blood on substrates at 24hr against DFA spectrum.	96
<b>Figure 55</b>	DFA plot of blood on substrates at 3m.	97
<b>Figure 56</b>	Mean Raman 5 <sup>th</sup> order polynomial spectra of blood on substrates at 3m against DFA spectrum.	97
<b>Figure 57</b>	Photo timeline of blood on ceramic tile from $\leq 1$ hr to 2m.	103
<b>Figure 58</b>	Photo timeline of blood on brown leather from $\leq 1$ hr to 2m.	104
<b>Figure 59</b>	Photo timeline of blood on condom from $\leq 1$ hr to 2m.	105
<b>Figure 60</b>	Blood on blue denim at $\leq 1$ hr and 2m.	108
<b>Figure 61</b>	Microscopic images of blood on substrates at 10x magnification.	110

## LIST OF TABLES

<b>Table Number</b>	<b>Title</b>	<b>Page Number</b>
<b>Table 1</b>	Laser type and power for substrate standard scans.	41
<b>Table 2</b>	The main components of blood, their Raman shifts and their vibrational modes <sup>[14], [29], [31], [41]</sup> .	48
<b>Table 3</b>	Description of phenylalanine.	49
<b>Table 4</b>	Description of tryptophan.	49
<b>Table 5</b>	Description of haemoglobin.	50
<b>Table 6</b>	Description of fibrin.	50
<b>Table 7</b>	Description of glucose.	51
<b>Table 8</b>	The main Raman shifts and vibrational modes of ceramic tile.	52
<b>Table 9</b>	The Raman shifts, components and vibrational modes of blue denim.	53
<b>Table 10</b>	Description of indigo dye.	54
<b>Table 11</b>	Description of cellulose.	55
<b>Table 12</b>	The Raman shifts, components and vibrational mode of brown leather.	56
<b>Table 13</b>	Description of collagen.	57
<b>Table 14</b>	The Raman shifts, components and vibrational modes of Durex Thin Feel <sup>®</sup> condoms.	58
<b>Table 15</b>	Description of latex and glycerine.	59
<b>Table 16</b>	The Raman shifts and vibrational modes of laminate flooring.	60
<b>Table 17</b>	The Raman shifts, components and vibrational modes of	61

crystalline silicon.

**Table 18** Description of crystalline silicon.

62

## LIST OF ABBREVIATIONS

<b>RBCs</b>	Red Blood Cells
<b>P.C.V</b>	Packed Cell Volume
<b>BPA</b>	Blood Pattern Analysis
<b>Hb</b>	De-Oxyhaemoglobin
<b>HbO<sub>2</sub></b>	Oxy-Haemoglobin
<b>Met-Hb</b>	Meth-haemoglobin
<b>HC</b>	Haemichrome
<b>NIR</b>	Near Infrared Spectroscopy
<b>WBC</b>	White Blood Cells
<b>LDH</b>	Lactate Dehydrogenase
<b>ELISA</b>	Enzyme Linked Immunosorbent Assay
<b>SERS</b>	Surface Enhanced Raman Spectroscopy
<b>CCD</b>	Charge-Coupled Device
<b>S/R</b>	Signal to Noise Ratio
<b>MVA</b>	Multivariate Analysis
<b>PCA</b>	Principal Component Analysis
<b>DFA</b>	Discriminative Function Analysis
<b>LDA</b>	Linear Discriminative Analysis
<b>≤1hr/1hr</b>	1 Hour (less than and equal to)
<b>2hr</b>	2 Hours
<b>5hr</b>	5 Hours
<b>24hr</b>	24 Hours
<b>1w</b>	1 Week

<b>2w</b>	2 Weeks
<b>1m</b>	1 Month
<b>2m</b>	2 Months
<b>3m</b>	3 Months
<b>PAH</b>	Phenylalanine Hydroxylase
<b>ATP</b>	Adenosine Triphosphate
<b>NADH</b>	Nicotinamide Adenine Dinucleotide

## CHAPTER 1

### INTRODUCTION

#### 1.1 Blood Pattern Analysis

Blood is a non-Newtonian visco-elastic fluid containing red blood cells (RBCs), plasma proteins and amino-acids suspended in plasma [1]. Wonder [1] defines blood as a “*vital, complex biological fluid containing RBCs which is present in vertebrates and may be shed during accidental, intentional or criminal acts*”. There are two major components of blood which are important in blood stain pattern analysis. These are: plasma and RBCs which combine to create a Haematocrit or P.C.V (packed cell volume) that varies between individuals and organs [1]. **Figure 1** (below) demonstrates the spectra and characteristic peaks which are gained from the Raman analysis of blood.

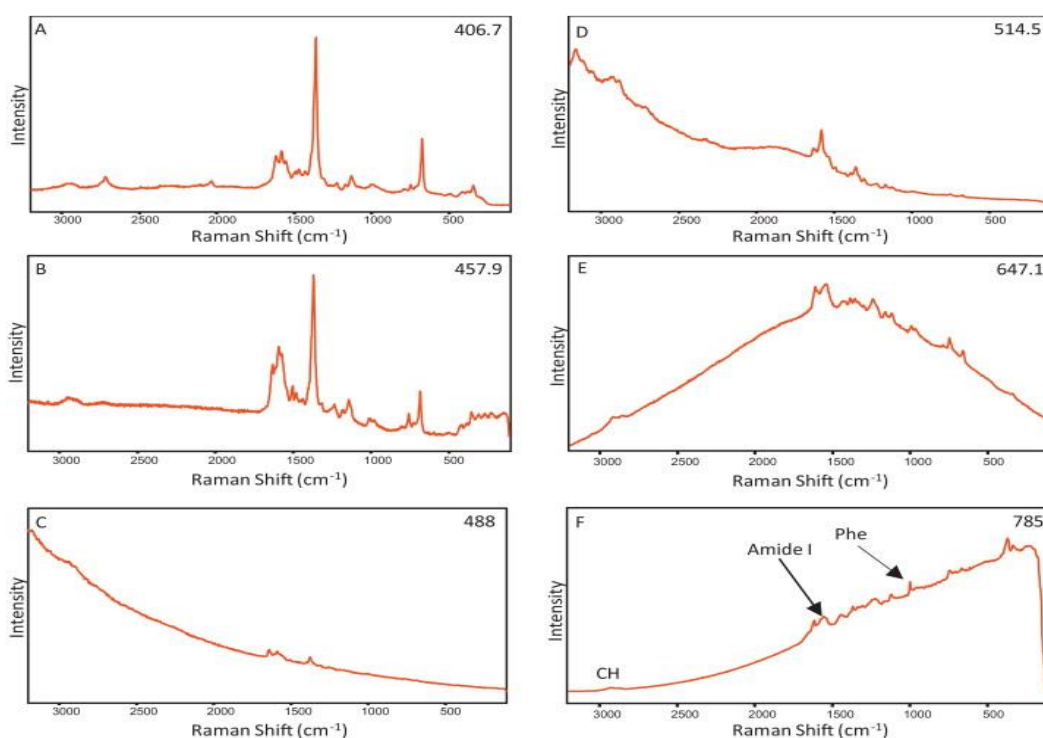


**Figure 1:** Raman spectra of pure blood acquired using: 406.7 (A), 457.9 (B), 488 (C), 514.5 (D), 647.1 (E) and 785 (F) nm excitations. Extracted from [2].

Blood pattern analysis (BPA) involves the study of blood found at the crime scene from discovery through to identification and further analysis. Blood is one of the most frequently discovered evidence types at a crime scene <sup>[3]</sup> and is found particularly in cases such as: accidents, assaults or murders. Although identifying and analysing the pattern caused by the deposition of blood at the crime scene is an important step, this is not the only information that can be gathered from finding blood. It can also provide essential and key information about the crime scene including:

- Identifying the number of individuals involved
- Spatter patterns can be utilised to determine the type of weapon used; position of the victim and assailant; and verify inflicted wounds
- Laboratory analysis of blood can be used to generate a full DNA profile
- Blood transfer to clothing and weapons can link suspects and victims to the crime scene
- Analytical analysis can be used to determine blood alcohol concentration; the presence of illegal or harmful substances and; recent studies have even shown that serum can be analysed to determine cancer and brain tumours <sup>[4], [5]</sup>

However, blood at the scene of the crime may not always have 100% purity as it may come into contact with other substances, surfaces and materials. Blood can mix with other materials which are split into physiological and non-physiological <sup>[1]</sup>. Physiological materials include bodily fluids such as semen and urine, whereas, non-physiological fluids include water, beer and disinfectants <sup>[1]</sup>. This provides an issue when attempting to identify blood using Raman spectroscopy as substance and surface interference may affect the Raman spectrum.

Sikirzhytski *et al.* <sup>[6]</sup> analysed blood and semen mixtures to investigate whether Raman spectroscopy could be used to identify and differentiate between the individual body fluids. Mixtures of blood and semen were prepared in different ratios and then left overnight to dry. Results showed that semen and blood could be identified and differentiated between reliably using Raman spectroscopy. Although, at 50% and higher blood concentrations blood appeared to dominate the spectrum over semen. The aims of this study are in close relation to this current study and it is also interesting to note the effect a mixed blood sample may have on the Raman spectrum. However, this study only investigates the effect of homogenous substance interference on the Raman spectrum of blood. Therefore more research needs to be carried out on substrate and heterogeneous substance interference.

Another very recent study by Sikirzhytskaya *et al.* <sup>[7]</sup> carried out further research to investigate the effect of contaminants on the Raman spectrum of blood. They tested blood with heterogeneous contaminants which included sand, dust and soil. Following statistical analysis of the results the outcome was that reliable identification of the bloodstains could be produced regardless of the heterogeneous contaminant.

[7] and [6] both produce similar outcomes and, although neither investigate the effect of substrates and surfaces on the Raman spectrum of blood, these results can be used as a guide in this current research when investigating the ageing and substrate effect on the Raman spectrum of blood.

## 1.2 Denaturation of Blood Over Time

In the human body Haemoglobin is present in two main forms which are: de-oxy-haemoglobin (Hb) and oxy-haemoglobin (HbO<sub>2</sub>). There is also a small presence of meth-haemoglobin (met-Hb) in the body as HbO<sub>2</sub> can auto-oxidize. However, met-Hb is incapable of binding oxygen and is reduced back to Hb by the reductase protein cytochrome *b5* <sup>[3]</sup> (**Figure 2**).

Outside the body, Hb saturates completely with oxygen to form HbO<sub>2</sub>. This is due to a decreasing availability of *b5* and therefore this process can no longer be reversed <sup>[3]</sup>. met-Hb will then denature to haemichrome (HC) caused by a conformation of the haemoglobin group <sup>[3]</sup> (**Figure 3**).

Blood plasma also goes through a process of denaturation as it contains serum proteins and clotting factors including: albumin, serum globulins, and hormones which all degrade after being deposited outside the body <sup>[3]</sup>.

This overall denaturation process can cause blood to alter its physical appearance and will often appear brown or black when dried. Therefore, it is essential that blood can be correctly identified and it essential to discover whether there is a link between the denaturation process of Hb and the time since deposition of the blood. This would provide key information about the time frame of a crime.

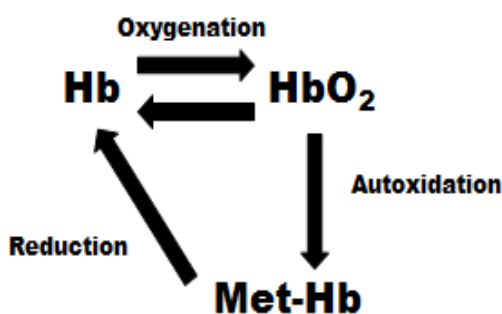


**Figure 2:** Showing the Hb path in the human body. Adapted from [9].

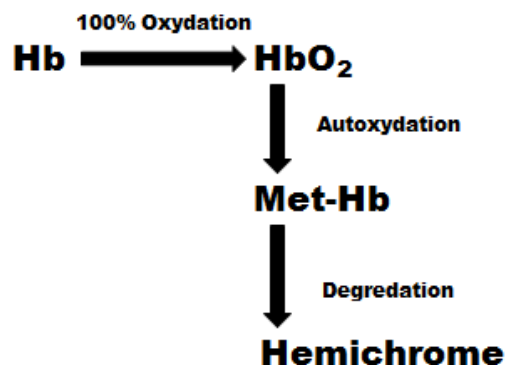


**Figure 3:** Showing the process of Hb oxygenation and denaturation of a blood stain. Adapted from [9].

Some previous studies have analysed how the ageing of blood can alter its appearance and whether this effects spectra gained from spectroscopic analysis. Lemler *et al.* [8] analysed the effect of *in vitro* haemoglobin denaturation and the Raman spectrum differences between liquid blood and dried blood. 5µl of blood was collected from healthy human donors and dried whole blood samples were analysed using an excitation emission wavelength of 785nm at stages of fresh blood, one week old and two weeks old blood. Whole liquid blood was also stored for periods of 1 hour, 24 hours and 2 weeks and then dried for 1-2 hours in an ambient environment. Results showed that there were changes in the Raman spectrum of blood for both groups due to HbO<sub>2</sub> denaturation products which attributed to haemoglobin aggregates and the conversion of HbO<sub>2</sub> to met-Hb.

Overall this study demonstrates that spectral heterogeneity at different times of ageing does exist and therefore suggesting Raman spectroscopy could be used to reliably identify blood at different stages of ageing and provide a time of deposition. However this study does not account for possible substrate interference affecting the Raman spectrum.

Botonjic-Sehic *et al.* <sup>[10]</sup> investigated the use of near-infrared spectroscopy (NIR) to determine the age of bloodstains. Human blood samples were measured on porous and non-porous surfaces and measured periodically over one month in ambient temperatures. Results showed that over the one month time period the bloodstains went through spectral changes as Hb was converted to HbO<sub>2</sub> and then to met-Hb.

This study investigates both the age determination of blood on two different substrates (gauze and glass). However more substrate materials need to be analysed which are relevant to the crime scene environment. Also this study's results were affected by water which is heavily detected by the infrared machine. Therefore a complimentary technique to use in conjunction with infrared would be Raman spectroscopy. This is also a non-invasive technique unlike NIR spectroscopy.

### **1.3 Identification and Analysis of Blood at the Crime Scene**

Before blood can be analysed it has to be located and its identity needs to be confirmed which requires a set of standard procedures carried out by the forensic examiner. These procedures include the use of presumptive and confirmatory tests.

#### **Presumptive Tests for Blood**

Presumptive tests are used to give the forensic examiner an indication that the substance they are collecting or analysing is that substance (in this case blood) which therefore saves time and cost. Presumptive tests work by a reaction with Hb which causes either a colour change or a fluorescent or chemiluminescent reaction <sup>[11]</sup>.

- **Colour change test:** testing chemical is added to the stain and then oxidant is applied (3% Hydrogen Peroxide) which is reduced due to contact with the Hb

and causes a colour change of the testing chemical. Common tests include *phenolphthalein* and *leucomalachite green* <sup>[11]</sup>

- ***Fluorescent and Luminescent test:*** to cover large areas the reacting chemical is sprayed onto a surface area and will react with the Hb, then will fluoresce or luminesce if blood is present. Common tests include *Luminol* (**Figure 4**) and *Fluorescein* <sup>[11]</sup>

Issues with presumptive tests are that colour change tests (e.g. phenolphthalein) can provide false positives with some substances such as vegetables and (if a colour change reaction is not instantaneous) then the oxidation reaction will occur naturally due to exposure to air <sup>[11]</sup>.

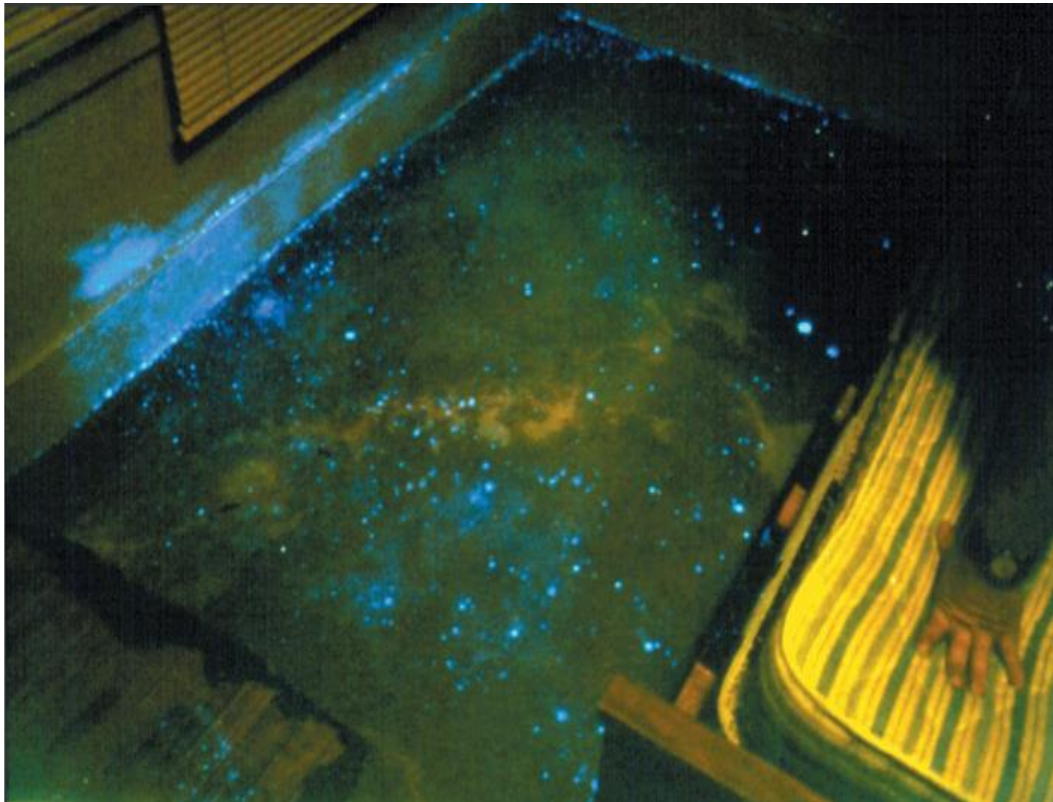


**Figure 4:** Photograph demonstrating the effect of spraying Luminol on blood at a crime scene. Extracted from [12].

Issues also arise with fluorescent and chemiluminescent tests (e.g. Luminol) as they too can provide false positives on reaction with plants or trees. Additionally, they have to be analysed in the dark to view the fluorescence or chemiluminescence. They may also cause streaking or bleeding of the pattern if re-applied excessively <sup>[11]</sup>.

### **Confirmatory Tests for Blood**

Confirmatory tests follow presumptive tests to give a definitive, absolute identification of the substance/stain (blood) which then enables further analysis, including, generating a DNA profile. Common confirmatory tests for blood are: *microscopic, crystal, immunological and spectroscopic*.

- ***Microscopic analysis***: involves identifying RBCs, white blood cells (WBC) and fibrin. However, the crystalline tests are used more commonly <sup>[13]</sup>
- ***Takayama and Teichman***: are two tests which use the formation of crystals to confirm the presence of blood. The Takayama test forms haemochromogen by heating a dried stain in the presence of pyridine and glucose (under alkaline conditions) forming needle-shaped crystals <sup>[13]</sup>. The Teichman test forms haematin by heating a dried stain (in the presence of halide and glacial acetic acid) forming brown, rhombic crystals <sup>[13]</sup>
- ***Immunological techniques***: include lactate dehydrogenase (LDH) which compares isozyme patterns in fluids and enzyme linked immunosorbent assay (ELISA) which identifies blood groups using antibodies <sup>[13]</sup>
- ***Spectroscopic techniques***: include *UV, Raman* and *IR*. All are non-destructive techniques and produce spectra which contain principal peaks which can be used to distinguish between Hb derivatives and can be used to reliably identify a substance as blood. Raman will be elaborated on further in this paper <sup>[13]</sup>.

An issue with confirmatory tests is that most are destructive and therefore once identification has been made then that sample is no longer available for further analysis. Therefore, this is unsuitable when working with very small amounts of evidence deposited at crime scenes.

Raman and FT-IR are newly developed confirmatory techniques. Lin *et al.* <sup>[14]</sup> proposed the use of IR spectroscopy to identify blood in 2007 and Virkler and Lednev <sup>[15]</sup> first published an article on the application of Raman to analyse blood in 2008. Further research into these techniques (in particular Raman spectroscopy due to its non-invasive nature) could revolutionise the presumptive and confirmatory testing of blood at the crime scene. Especially with the new introduction of hand held spectrometers which will be discussed further in Chapter 1.8.

#### **1.4 Raman Spectroscopy**

Raman spectroscopy involves the use of monochromatic light in the UV-visible region to irradiate a sample causing the scattered light to shift frequencies due to the sample's vibrational modes <sup>[16]</sup>. This scattered light is then usually observed perpendicular to the incident light ( $\nu_0$ ) (**Figure 6**).

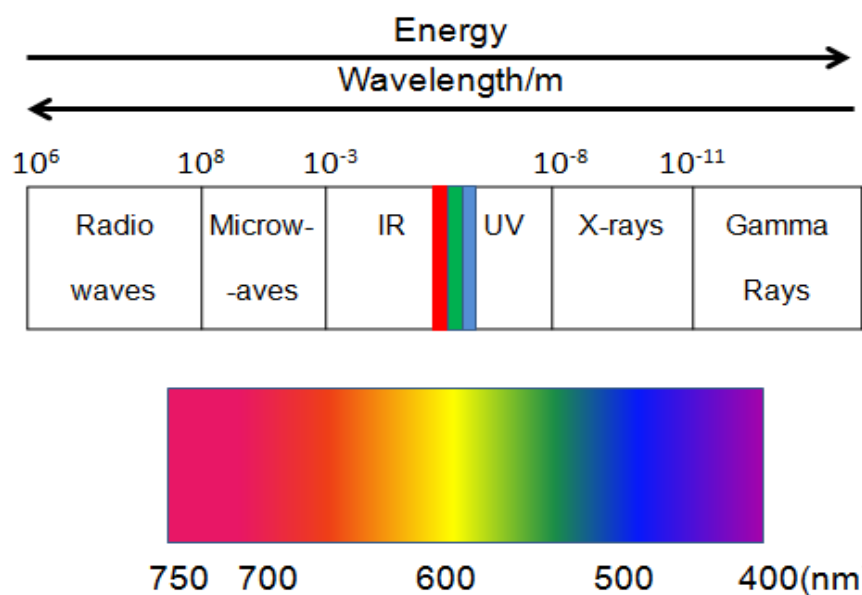


**Figure 5:** Energy level diagram. Raman fits in the UV-visible region.

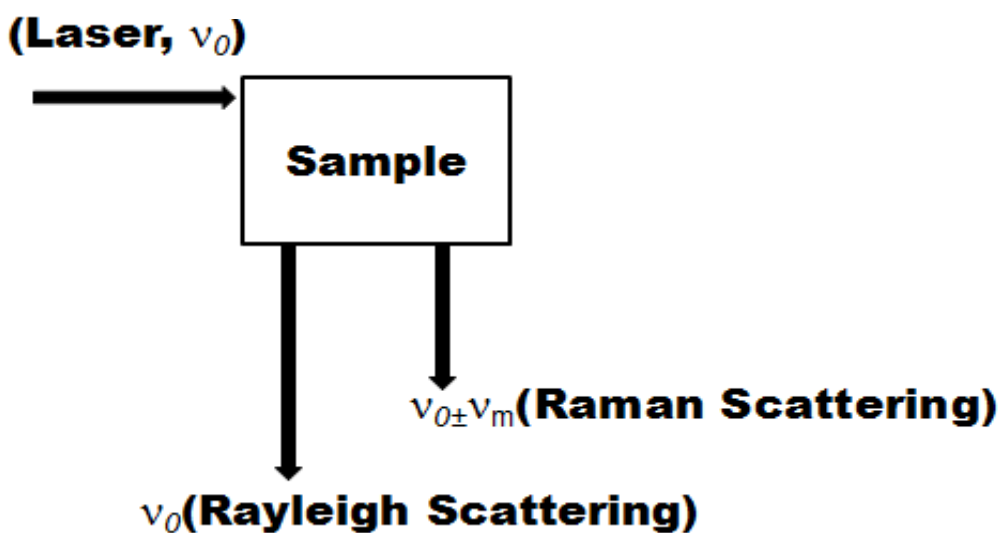


**Figure 6:** Mechanism of Raman spectroscopy. Adapted from [17].

Light is scattered in two forms: Rayleigh scattering and Raman scattering. Rayleigh scattering (elastic collisions) has a frequency equal to the incident beam, whereas, Raman scattering (inelastic collisions) has a frequency which is shifted higher or lower than that of the incident beam<sup>[18]</sup>. Raman scattering is very weak ( $\sim 10^{-5}$  of the incident beam) and possess the frequency  $\nu_0 \pm \nu_m$ ; where  $\nu_m$  equals the molecular frequency<sup>[17]</sup>.

*Stokes* lines equate to light which is scattered at a frequency lower than the frequency of the incident light ( $\nu_0 - \nu_m$ ). *Anti-Stokes* lines equate to light which is scattered at a frequency higher than the incident light ( $\nu_0 + \nu_m$ )<sup>[17]</sup>. Stokes lines appear when the molecule has  $\nu=0$  and is excited to  $\nu=1$ , whereas, anti-Stokes lines appear when the molecule starts at  $\nu=1$  and is demoted to  $\nu=0$ <sup>[18]</sup> (**Figure 7**).

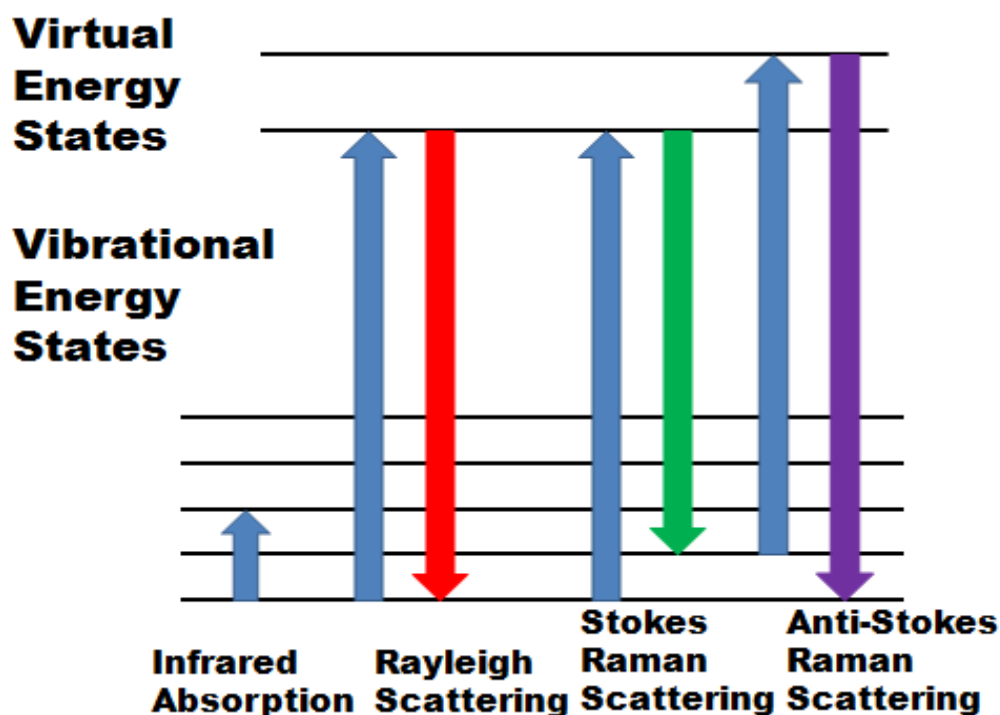


**Figure 7:** The fundamentals of Raman scattering. Adapted from [19].

More sample molecules exist in the ground state ( $\nu=0$ ) than in the excited state ( $\nu=1$ ) (Maxwell-Boltzmann distribution law). Thus, the Stokes lines are more prominent than anti-Stokes lines and therefore the Stokes side of the spectrum is used for analysis<sup>[17]</sup>.

For a molecule to be Raman-active there must be a change in the polarisability during the vibration, different to IR spectroscopy which must have a change in the dipole<sup>[17]</sup>. When a molecule is introduced into an electric field (laser beam) then a distortion undergoes due to the attraction of positively charged nuclei towards the negative pole

and electrons towards the positive pole. This produces an induced dipole moment ( $P$ ) given by:

$$P = \alpha E \text{ [20]}$$

This relationship does not exist in simple molecules as  $P$  and  $E$  are vectors consisting of three components in the directions  $x$ ,  $y$  and  $z$  therefore the equation becomes:

$$P_x = \alpha_{xx}E_x + \alpha_{xy}E_y + \alpha_{xz}E_z$$

$$P_y = \alpha_{yx}E_x + \alpha_{yy}E_y + \alpha_{yz}E_z$$

$$P_z = \alpha_{zx}E_x + \alpha_{zy}E_y + \alpha_{zz}E_z$$

And in matrix form becomes:

$$\begin{bmatrix} P_x \\ P_y \\ P_z \end{bmatrix} = \begin{bmatrix} \alpha_{xx} & \alpha_{xy} & \alpha_{xz} \\ \alpha_{yx} & \alpha_{yy} & \alpha_{yz} \\ \alpha_{zx} & \alpha_{zy} & \alpha_{zz} \end{bmatrix} \begin{bmatrix} E_x \\ E_y \\ E_z \end{bmatrix}$$

The first matrix on the right of the equals sign is the *polarizability tensor* and, according to quantum mechanics, the vibration is Raman active if one of these components is changed during the vibration <sup>[17]</sup>.

The vibration will be Raman active if the shape, size or orientation of the *polarizability ellipsoid* is changed. **Figure 8** shows the vibrational modes of CO<sub>2</sub> where  $\nu_1$  is Raman-active because the size of the ellipsoid changes and where  $\nu_2$  and  $\nu_3$  are Raman-inactive because at the two extreme displacements the ellipsoid remains the same size, shape and orientation <sup>[17]</sup>.

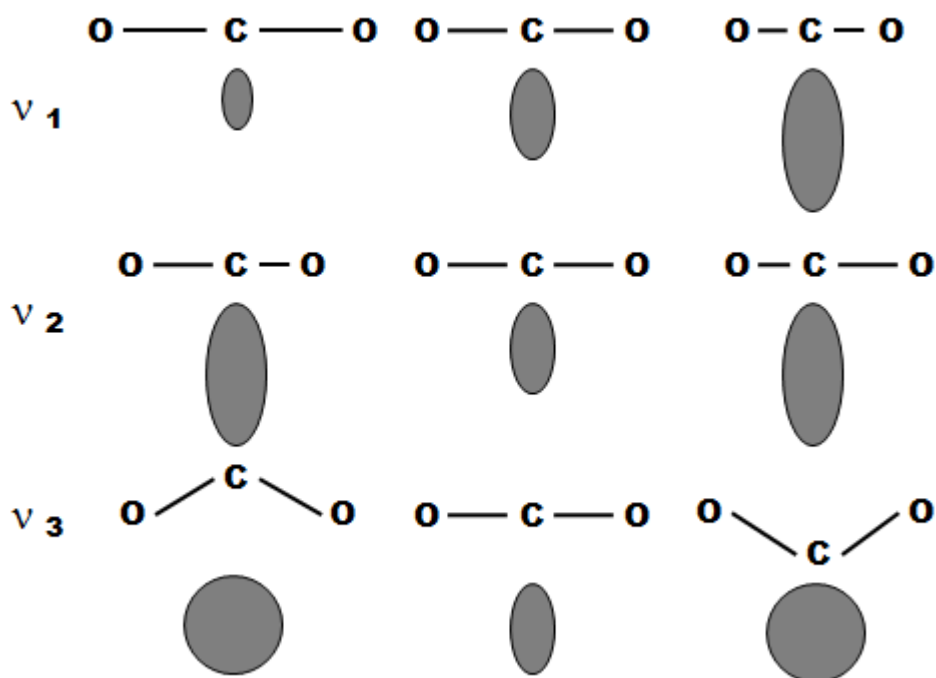


**Figure 8:** The vibrational modes of CO<sub>2</sub> Adapted from [17].

It can also be noted that as  $\nu_1$  is Raman-active and  $\nu_2$  and  $\nu_3$  are Raman-inactive, conversely,  $\nu_1$  will be IR- inactive and  $\nu_2$  and  $\nu_3$  will be IR-active. This is defined as the *mutual exclusion principle* and can be applied to any molecule having a centre of symmetry [17].

The Raman spectrum contains bands which are specific to individual compounds due to their modes of molecular vibration [20]. These bands are analysed to identify an unknown compound or material. Raman spectroscopy has already demonstrated great potential in its application in the field of forensics through analysis of: controlled substances [21], synthetic dyes in ball point pen inks [22], paint [23], and bodily fluids including blood [6], [13].

### **1.5 Advantages of Raman Spectroscopy**

The advantages of Raman spectroscopy should outweigh the disadvantages and be beneficial to the area of blood identification to make it a useful technique for this purpose. The advantages and disadvantages are described below.

- Some vibrations are stronger in Raman than they are in IR. For instance, the stretching vibrations ( $C\equiv C$ ,  $C=C$ ,  $P=S$ ,  $S-S$ , and  $C-S$ ). Covalent bonds are also stronger in Raman and ionic bonds are stronger in IR. In Raman, bending vibrations are also generally weaker than stretching vibrations <sup>[17]</sup>
- Due to the small diameter of the laser beam (1-2mm) only a small amount of the sample is needed for analysis <sup>[17]</sup>
- Acts as a molecular fingerprint containing highly unique and detailed features allowing highly selective determinations
- Can be applied to any sample which can be accessible by laser and the resulting emitted photons can be detected whether organic, inorganic or biological
- Can measure solid, liquid, gas, transparent and non-transparent samples
- Aqueous samples present no problems (unlike IR)
- Scanning is completely non-invasive and reproducible
- It is now available for field analysis <sup>[24]</sup>

### **1.6 Disadvantages of Raman Spectroscopy**

- Some compounds fluoresce when irradiated by the laser beam <sup>[17]</sup>
- It is more difficult to obtain rotational and rotation-vibration spectra with high resolution in Raman than IR as Raman spectra are observed in the UV-visible region where high resolving power is difficult <sup>[17]</sup>

### **1.7 Surface Enhanced Raman Spectroscopy (SERS)**

SERS involves molecules being attached to noble metal clusters (aluminium) which can be rough or smooth <sup>[12]</sup>. SERS allow for an improvement on Raman spectroscopy by minimising the effect of fluorescent backgrounds which can arise from fibres and dyes. In particular it can also enhance the Raman signal up to  $10^6$  times and allow reduction of the laser excitation to avoid sample damage <sup>[25]</sup>. This means that SERS can allow for the detection of even weak peaks that would not normally be noticeable using standard Raman spectroscopy.

A recent study carried out by Boyd *et al.* <sup>[26]</sup> studied the effects of using SERS for the detection of blood. The study used blood collected from two donors and used a commercial slide, covered in aluminium foil, for conventional Raman spectroscopy. For SERS, silicone substrates covered in nickel nanotips were used. Results showed that at a blood dilution of 1:100 on the Al substrate the signature peaks were barely measurable. However, the peaks in blood dilutions of up to 1:100,000 on SERS substrates were clearly identifiable. The results also showed that when SERS were used for swabbing on fabrics the spectrum did not show any luminescence arising from the fabrics. Overall, this study is effective at demonstrating that SERS is a very useful technique to use when analysing low dilutions of blood on highly luminescent fabrics.

### **1.8 Portable Raman Instruments**

Recent advances in the field of Raman spectroscopy have enabled portable technology to be used to analyse and identify unknown substances *in vitro* at the crime scene <sup>[27]</sup>. The use of Raman spectroscopy in this way is due to a compact, safe and reliable NIR solid-state laser source along with a high-resolution charge-coupled device (CCD) detector to detect the Raman emission <sup>[27]</sup>. Portable Raman instruments can also be used

in a forensic context for the analysis of unknown substances and the analysis of drugs without samples having to be sent to the lab before identification is possible. Small hand-held units such as: the DeltaNU Inspector Raman and the Ahura First Defender have now been developed which can be used to analyse substances through clear or translucent materials (e.g. glass bottles). This eliminates possible contamination through handling of the sample directly <sup>[28]</sup>.

Compact portable Raman spectrometers, incorporating the use of SERS, have been used in the field to detect bacillus spores (Anthrax bacterium) successfully giving a spectrum with high signal to noise ratio (S/N) and within five seconds <sup>[29]</sup>. This demonstrates that Raman spectroscopy is effective as a portable device.

### **1.9 Previous Studies: Raman Analysis of Blood**

Virkler and Lednev have carried out extensive research into the area of Raman identification for body fluids, including the identification of blood. In 2008 <sup>[15]</sup> the use of Raman spectroscopy to identify blood and other body fluids, including semen and saliva, was investigated. Samples were collected from volunteers and were analysed on microscopic slides and layered in aluminium foil to minimise reflectance. The results demonstrated that blood had several contributing components including: Hb, albumin, and glucose and proved these could be used to distinguish blood from other bodily fluids.

Virkler and Lednev <sup>[30]</sup> also investigated the effect that samples from different blood donors would have on the spectrum produced from Raman analysis and whether a multi-dimensional analysis can be used to better identify a sample. Blood was analysed from 14 donors and these were dried. Additionally, one liquid blood sample was analysed for comparison to the spectrum of dried blood and its components.

Statistical analysis was carried out on a dried sample from a single donor and the presence of three principal peaks was identified: fibrin, Hb and background fluorescence. Results demonstrated that fibrin was strongly present in dried blood more than liquid blood but the presence of Hb was abundant in both dried and liquid blood. Also, very little spectral heterogeneity was seen between spectra of dried blood from different donors. Overall, these two studies by Virkler and Lednev show that the principal components (Hb and fibrin) can be used as spectroscopic signatures for dried blood and proves that Raman spectroscopy is a reliable confirmatory tool for the non-destructive identification of blood.

#### **1.10 Substrate Variation at the Crime Scene**

Different substrates can be found at the scene of a crime due to the number of different types of: furniture, carpets, wall coverings, paints, clothes, surfaces and materials. Materials include fabrics such as: cotton, leather, nylon and denim and surfaces can include metals, glass and wood. The various types of substrates mean that blood can be deposited on any number and any type, therefore, affecting further analysis of blood. As Raman spectroscopy is used as a confirmatory technique for identifying blood it is essential that identification is reliable which can save time and expense.

Boyd *et al.* <sup>[31]</sup> was one of the first to study the effect of substrate interference on the Raman spectrum of blood. Substrates used for analysis were: a microscope slide, a silicon wafer, a polyethylene cup, and a microscope slide covered with aluminium foil. Common substrates used which are found at the crime scene included: plastic and metal utensils, dry wall, and fabrics. Common Raman substrates showed scattering peaks that were consistent with blood but also showed substrate peaks except for the aluminium foil. Common crime scene substrates showed characteristic blood peaks as long as the

substrate possessed low luminescence. Commercial fabrics proved difficult due to their luminescence. Overall the study showed that aluminium foil was the most ideal substrate to use and that Raman spectroscopy is not suited to analyse substrates which possess strong fluorescent properties.

McLaughlin *et al.* <sup>[2]</sup> also analysed substrate interference on the Raman spectrum of blood. They used un-dyed cotton swatches, a yellow bathroom tile, blue jean denim and a glass microscope as substrates. A full spectrum range (100-3200 $\text{cm}^{-1}$ ) was used for most spectra with the scan range set at 300-1645 $\text{cm}^{-1}$  (which is the fingerprint region for dilute blood). Also, in order to investigate which laser excitation wavelength worked best for each individual substrate, wavelengths/nm at 406.7, 457.9, 488, 514.5, 647.1 and 785 were used (**Figure 1**). Results showed that ability to identify blood depended on the nature of the substrate and excitation of the laser source. Glass and tile substrates demonstrated strong luminescence, interference was greater for cotton due to its absorption properties, and denim added a large fluorescent background. The study demonstrated that no-one laser excitation wavelength was ideal in all scenarios and the most problematic substrates were tile and glass and the best was cotton. Overall this study shows good investigation into using Raman as a confirmatory tool for blood.

Using different coloured substrates has also been investigated. Edelman *et al.* <sup>[32]</sup> used NIR to analyse blood stains on: white, black, red, green, and blue cotton. Absorption spectra maxima of the blood and the maxima related to blood components (Hb, met-Hb, albumin, globulin, triglycerides, glucose, cholesterol and urea) on cotton were compared to that of the standards. Results showed that using NIR to identify blood on coloured cotton backgrounds can prove to distinguish blood from substrates with 100% specificity and 100% sensitivity. Overall, this study has shown that NIR can be successful as a non-destructive technique for identifying blood on coloured

backgrounds. However, further study should be carried out using Raman on coloured backgrounds and also on other coloured/dyed substrates other than just cotton.

### **1.11 Study Aims and Rationale**

This study has two main aims: to assess the efficiency and reliability of Raman spectroscopy as a confirmatory technique for the identification of blood and to investigate the effect of ageing and substrate variation on the Raman spectrum of blood.

This aims will be carried out as such:

- Blood droplets will be deposited on various substrate materials
- These droplets will be aged for a period of time
- During this ageing process, Raman spectroscopy scans will be taken of the droplets at different stages of ageing
- Once scans at all stages of ageing, on all substrates, have been carried out and the spectra collected then the data will be analysed to highlight any changes in intensity of the main peaks of blood over time and across each substrate
- What is expected to be seen is a decrease of the main Raman peaks corresponding to blood over time. Demonstrating that ageing does have an effect on the blood spectrum and also that ageing stages of blood could be assumed
- Also results are expected to show variation in the intensity of the main Raman peaks corresponding to blood across different substrates. Demonstrating that substrate variation does have an effect on the Raman spectrum
- Other expected results of this stage would also be that fluorescent materials (commercial fabrics) would interfere with the intensity of the spectral principal peaks of blood making its identification difficult

The results of this research would help towards quicker and more reliable identification of blood at a crime scene and in the lab, therefore, allowing more time for further analysis. This research would particularly have great benefit to new handheld Raman spectroscopy instruments which are being implemented in the field and are used to analyse samples directly deposited on various substrates.

This research would also aid the forensic community and the field of BPA by providing a method to determine the time since blood was deposited at a crime scene, and therefore, an approximate time of when the crime was committed.

### **1.12 Pre-Processing Techniques and Multivariate Analysis (MVA) Review**

In some cases it is difficult to differentiate between changes in the Raman spectrum of blood over time and across different substrates. These difficulties are due to background fluorescence which can arise from the substrate material and can minimise the clarity of the characteristic peaks corresponding to blood. Pre-processing and MVA allow for the subtraction of background and substrate interference and demonstrate the patterns and separation of data. Polynomial fit, introduced by Lieber *et al.* <sup>[33]</sup>, is a baseline correction technique where low frequency, non-constant baselines are adjusted for by estimating the unknown background and has been used in previous literature <sup>[34]</sup>. Second order derivative is a technique which removes the baseline and any additions in the spectrum which are not the main peaks and has also been shown to be the best form of Raman data pre-processing in previous literature <sup>[35]</sup>.

Multivariate analysis was carried out on the raw spectral data employing Principal component analysis (PCA) and discriminative function analysis (DFA). PCA is an unsupervised technique of identifying patterns in data and expressing the data in a way so similarities and differences are highlighted. PCA has been used in Raman studies of a

similar nature to this [6], [36], [37]. These studies demonstrate that PCA is effective at showing the separation between groups of data. DFA is a supervised technique which maximises the intergroup variation and minimises the intra-group variance which allows for discrimination between the groups to be visualised. DFA, also referred to as Linear Discriminant Analysis (LDA), has also been used as a MVA technique in similar Raman studies [38], [39]. These studies demonstrate that DFA is effective at showing the separation between groups of data.

Vector normalisation is used in this study as blood is a heterogeneous sample and therefore variation can occur which can provide slight differences in spectra collected. Vector normalisation is a technique where the heterogeneity of the blood sample is accommodated for and spectra collected are normalised to a similar level. However, this will still allow for differences in the peaks of blood (over time and across different substrates) to be identified.

## CHAPTER 2

### MATERIALS AND METHODS

#### 2.1 Blood Specimens

Defibrinated equine (horse) blood (P.C.V 45%) was purchased from TCS Biosciences Ltd. Horse blood is characterized by more rapid aggregation and stronger adhesive forces between red blood cells than human blood <sup>[40], [41]</sup>. Horse and sheep blood are the most widely used blood products in clinical culture and a vacuum assisted defibrination process is the best method used to clump fibrinogen <sup>[42]</sup>. Additionally, horse blood is used because human blood can be hazardous due to HIV and hepatitis <sup>[43]</sup>. For these reasons equine blood was selected for analysis in this study over human blood. Defibrination is the process of removing fibrin from the blood to prevent clotting outside the body <sup>[44]</sup>. McLaughlin *et al.* demonstrated that the Raman spectrum of human blood could be distinguished from animal blood (including horse) <sup>[45]</sup>. These differences between animal and human blood were suggested to arise from the shape and intensity of the variations within the 1220-1300cm<sup>-1</sup> spectral range which corresponds to stretching and vibrational modes of haemoglobin <sup>[45]</sup>. Additionally, the concentration and chemical characteristics of some blood components (e.g. red blood cell count or total leucocytes) are different for animals and humans which again could be responsible for the spectral differences between the two <sup>[45]</sup>. However, more studies need to be carried out comparing human and equine blood using Raman spectroscopy. Research also needs to be carried out to analyse the difference between whole blood and defibrinated blood.

## 2.2 Substrates

Six substrates were used in the study. These were: ceramic tile, blue denim, brown leather, condom, laminate tile and crystalline silicon standard (Figures 9-14). All substrates were bought from local fabric and DIY stores, excluding crystalline silicon which was provided in the laboratory. Sections of denim, leather and condom were cut from a larger piece and were attached to glass slides using tape to give a greater stability to the substrate. Silicon was also attached to a glass slide for this same reason.



**Figure 9:** Ceramic tile substrate and blood.

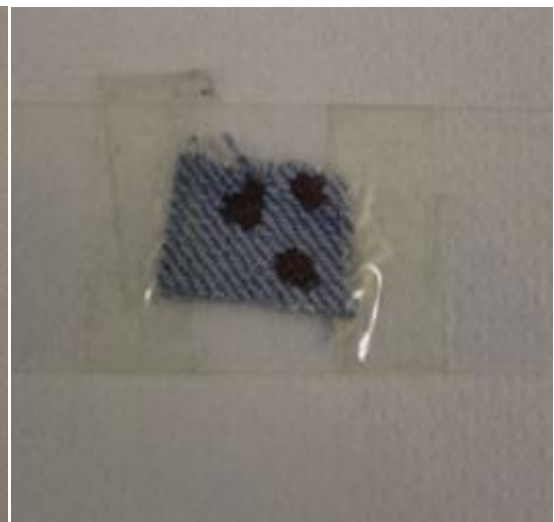


**Figure 10:** Blue denim substrate and blood.



**Figure 11:** Brown leather substrate and blood.



**Figure 12:** Condom substrate and blood.

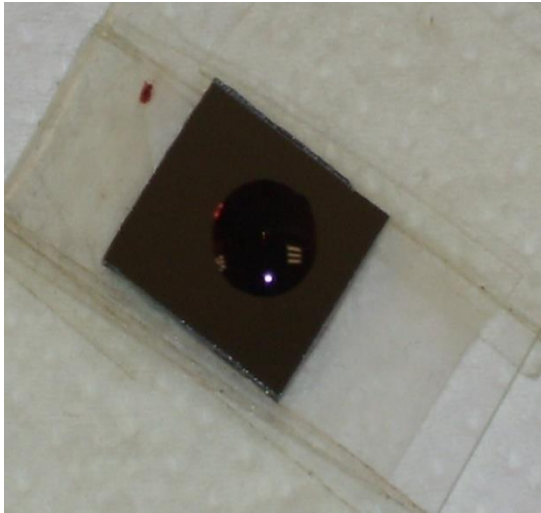


**Figure 13:** Crystalline silicon substrate and substrate and blood.



**Figure 14:** Laminate tile substrate and substrate and blood.

### 2.3 Raman Spectroscopy Instrumentation

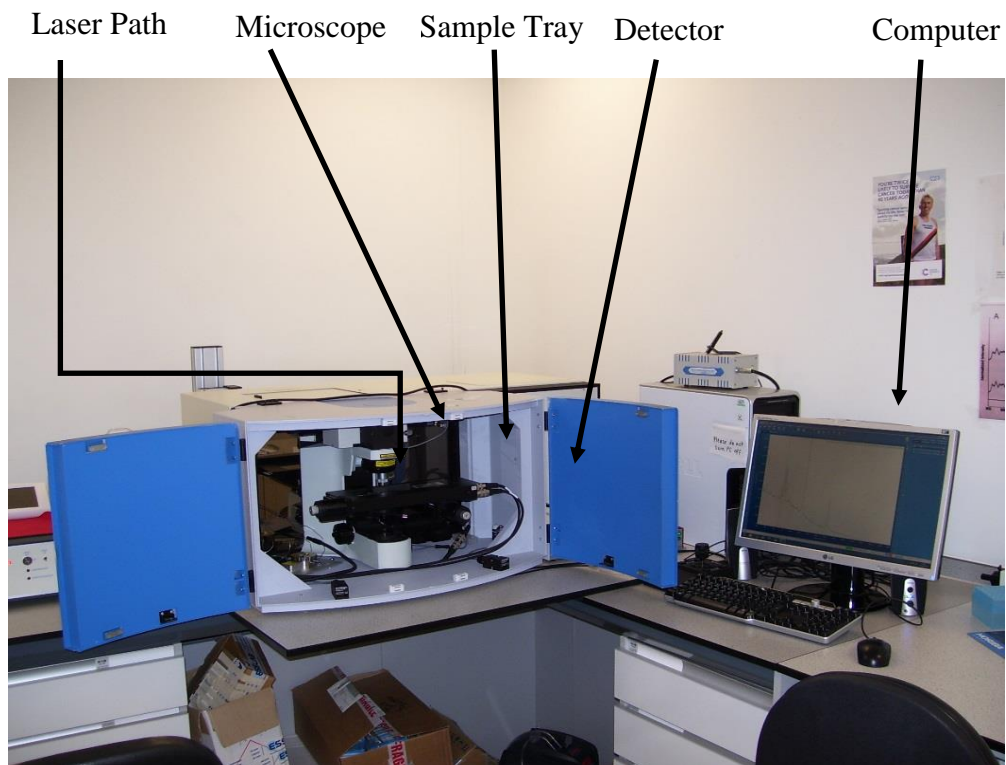


**Figure 15:** The Horiba Jobin-Yvon LabRAM HR800 confocal Raman Spectrometer used to take blood and substrate scans.

Spectroscopic analysis was carried out using a Horiba Jobin-Yvon LabRAM HR800 confocal Raman spectrometer (**Figure 15**). The detector used was an air-cooled open electrode 1024 x 256 pixel CCD detector. For measurements, a x50/0.55 long working distance microscope objective (PL FLUOTAR, leica) was employed. Spectral acquisitions were carried out for 2 seconds and with 20 accumulations and with a grating of 300gr/mm. Laser type (532nm/785nm) and power varied for the substrate standard scans depending on the type of substrate and the best laser to generate the clearest and optimal spectra (**Table 1**). Blood on substrate scans were carried out with a 532nm, 1% power laser. The spectra were measured across a wavelength range of  $500\text{cm}^{-1} - 3300\text{cm}^{-1}$ .

**Table 1:** Laser type and power for substrate standard scans.

Substrate	Laser Type/nm	Laser Power/%
Ceramic	532	100
Denim	785	100
Leather	532	1
Condom	532	10
Laminate	785	50
Silicon	785	100

The instrumentation was calibrated before use using crystalline silicon which gives a spectral line at  $520.8\text{cm}^{-1}$ . The detectors used were an Andor electromagnetic (EM) CCD and a Synapse CCD for the 785nm and 532nm lasers respectively.

## **2.4 Methodology**

Three 2 $\mu$ l droplets, of Equine blood, were deposited onto the substrate surface approximately <5mm from the surface. Scans were carried out at  $\leq$ 1 hour (1hr), 2 hours (2hr), 5 hours (5hr), 24 hours (24hr), 1 week (1w), 2 weeks (2w), 1 month (1m), 2 months (2m) and 3 months (3m). Ten scans were carried out for each droplet, with a total of thirty scans for each time point and an overall total of 270 spectra generated to enable the production of results that are representative for each time and substrate.

## **2.5 Data Pre-Processing and MVA**

Pre-processing and multivariate analysis were carried out on the raw data using Lab Spec 6 spectroscopy software suite (HORIBA Scientific) and Matlab version 7.8.0.347 (R2009a) (The MathWorks, Inc., USA) using in-house written software.

Minimal data pre-processing was carried out to allow for a better level of reproducibility. Data was initially subjected to a visual quality test to ensure only adequate spectra were included in the analysis. 5<sup>th</sup> order polynomial fit and 2<sup>nd</sup> order derivative were applied to the spectra. Both pre-processing techniques were carried out separately on the raw data which allowed comparison of the two and the ability to determine the best pre-processing technique for the data. After each technique, vector normalisation was carried out to account for the heterogeneity of blood.

Pre-processed spectra, firstly analysing the effect of ageing and secondly analysing the effect of substrate variation, were then compared against the DFA spectrum. DFA spectrum highlights the main peaks where changes take place over time and on different substrates respectively. Additionally, for analysing the effect of ageing, early ( $\leq$ 1hr to

5hr/24hr) and late (24hr/1w to 3m) spectra were compared against each other and the DFA spectrum to analyse the changes in the spectra.

## CHAPTER 3

### SPECTRAL COMPOSITION

Raman spectroscopy is typically utilized as a qualitative and quantitative, molecular fingerprinting analytical technique. This chapter utilizes Raman spectroscopy as a confirmatory technique for the identification of blood. Firstly, the optimal position on the blood droplet was investigated. Secondly, the main peaks and components of the Raman spectrum of blood were outlined and described. Finally substrate standard spectra were collected (30 scans for each substrate) and the main peaks were identified. Results from this chapter have been accepted and presented as a poster presentation at SciX 2014, Reno (**Appendix 1**).

#### 3.1 Blood Spectrum

To ensure the optimal spectra were collected when analysing the blood droplets, line scans across two droplets were carried out. This process involved scans at the outer edge, between the middle edge and outer edge, the middle edge and the middle of the droplet (**Figure 16**). This also indicated that the best laser to use was the 532nm with a power of 1%. A blood droplet with <1hr drying and a blood droplet with >1hr drying were analysed to determine the best area of analysis for drying and dried blood respectively. 10 scans were carried out for each area, meaning 40 scans each for <1hr and >1hr droplets, totalling 80 scans in all. The spectra were then analysed using Matlab R2013b software and compared to find the best area of the droplet to analyse.

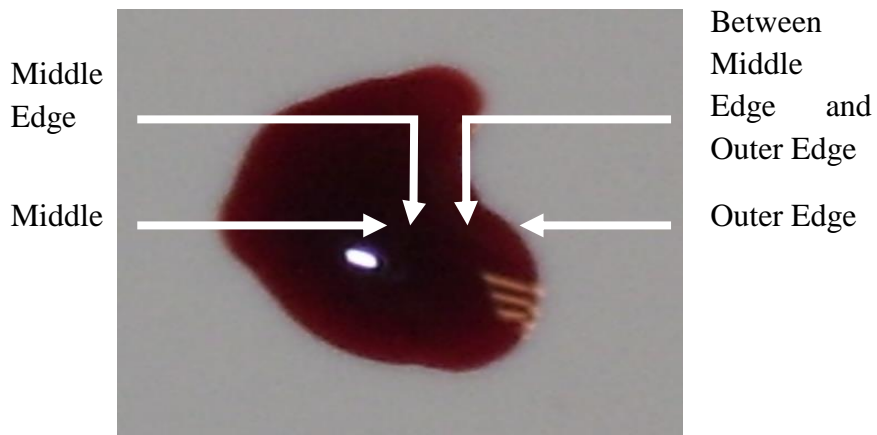


**Figure 16:** Blood droplet showing line scan points.

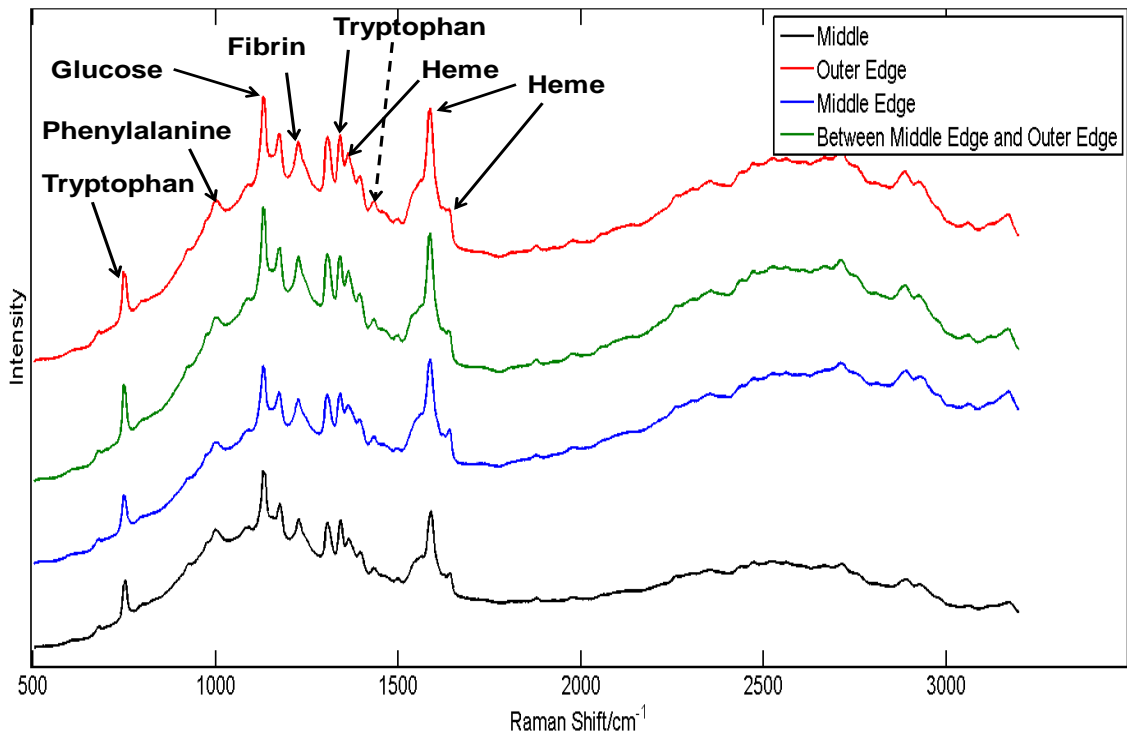


**Figure 17:** Raw line scan of blood droplets dried <1hr.

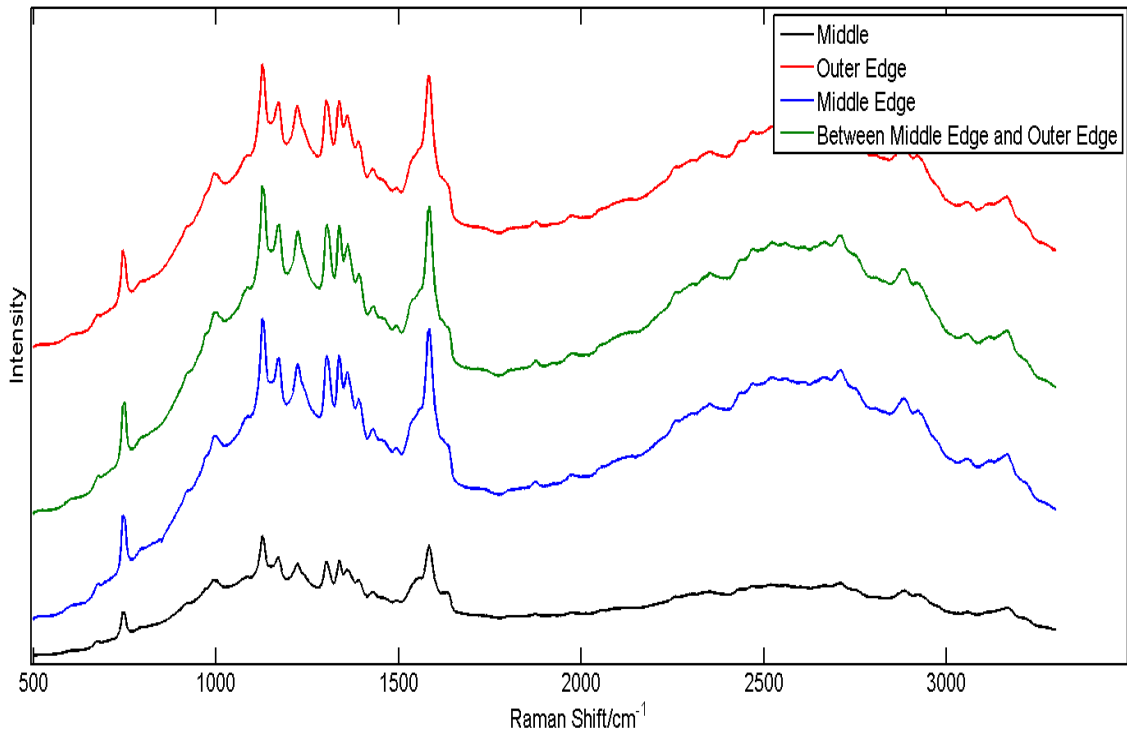


**Figure 18:** Raw line scan of blood droplets dried >1hr.

**Figure 17** shows the major highlighted peaks which are present in the Raman spectrum of blood: tryptophan ( $747.1\text{cm}^{-1}$ ), phenylalanine ( $1001\text{cm}^{-1}$ ), glucose ( $1129\text{cm}^{-1}$ ), fibrin ( $1225\text{cm}^{-1}$ ), tryptophan ( $1340\text{cm}^{-1}$ ), haemoglobin ( $1362\text{cm}^{-1}$ ), tryptophan ( $1434\text{cm}^{-1}$ ), haemoglobin ( $1587\text{cm}^{-1}$ ) and haemoglobin ( $1640\text{cm}^{-1}$ ).

From the raw line scan spectrum of blood dried <1hr (**Figure 17**) it can be seen that the spectrum from the “middle” and the “middle edge” of the droplet have a sharper peak at  $1640\text{cm}^{-1}$ , which relates to haemoglobin. It can also be seen that the spectrum from “between the middle edge and outer edge” and “outer edge” of the droplet have a higher intensity at  $1587\text{cm}^{-1}$  which also relates to haemoglobin.

From the raw spectrum of the line scan of blood dried >1hr (**Figure 18**) it can be seen that the spectrum from the “middle” of the droplet has lower intensity than spectrum taken from other areas of the droplet.

Overall from the line scans, the major peaks which characterise blood are visually clear at each position analysed on the droplets. This demonstrates when carrying out scans that no precise area of the droplet needs to be analysed and clear spectra can be gained as long as the blood can be visualised. Additionally, because of the nature of some of the substrates used in the study (i.e. denim and leather), blood may be soaked into the fabric and therefore will have to be analysed where it can be seen clearly. Also, in a forensic situation when trace blood is found then it will not be possible to divide the blood into different sections for analysis.

### 3.2 Blood Components

The main components of blood (**Table 2**) are described further. The chemical structures shown for blood were created using Symyx Draw 3.3 <sup>[46]</sup>.

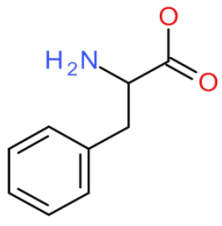
**Table 2:** The main components of blood, their Raman shifts and their vibrational modes <sup>[14], [29], [31], [47]</sup>.

Raman Shift/cm <sup>-1</sup>	Component	Vibrational Mode
747.1	tryptophan	Ring Vibrations
997.7	phenylalanine	Aromatic Ring Breathing
1129	glucose	C-O-C antisymmetric stretch
1225	protein (fibrin)	Amide III bend
1340	tryptophan	C-H bend
1362	haemoglobin	CH <sub>3</sub> symmetric stretch
1434	tryptophan	CH <sub>2</sub> , CH <sub>3</sub> bend
1587	haemoglobin	C=C stretch
1640	haemoglobin	C=N/C=C stretch

## Phenylalanine

**Table 3:** Description of phenylalanine.

Name	Molecular Formula	Description
DL-Phenylalanine	C <sub>9</sub> H <sub>11</sub> NO <sub>2</sub>	Phenylalanine (along with tyrosine) is one of the precursor amino acids required for synthesis of dopamine. Phenylalanine is converted to tyrosine via the phenylalanine hydroxylase (PAH) enzyme. High levels of phenylalanine have been linked to schizophrenia [48].

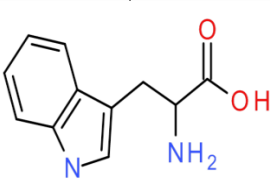


The chemical structure of DL-Phenylalanine is shown. It consists of a central chiral carbon atom bonded to a hydrogen atom (not explicitly shown), an amino group (H<sub>2</sub>N), a carboxyl group (COOH), and a benzyl group (a methylene group attached to a phenyl ring).

## Tryptophan

**Table 4:** Description of tryptophan.

Name	Molecular Formula	Description
DL-Tryptophan	C <sub>11</sub> H <sub>12</sub> N <sub>2</sub> O <sub>2</sub>	A dietary protein amino-acid which (along with phenylalanine and tyrosine) is crucially important for normal brain functions, pathophysiology of disease states, and in response to various drugs. It circulates in the blood and is taken up into the brain where they charge transfer RNAs and are subsequently converted into peptides and proteins. It can also be hydroxylated with neurons creating more amino acids which are converted to be used as neurotransmitters [49].



The chemical structure of DL-Tryptophan is shown. It consists of a central chiral carbon atom bonded to a hydrogen atom (not explicitly shown), an amino group (NH<sub>2</sub>), a carboxyl group (COOH), and a 3-(tryptophan-3-yl)propyl group (a propyl chain attached to the 3-position of an indole ring).

## Haemoglobin

**Table 5:** Description of haemoglobin.

Name	Molecular Formula	Description
Haemoglobin	$C_{34}H_{32}FeN_4O_4$	Haemoglobin is a pigment responsible for the red colour in blood. Haemoglobin is made up of four pyrrole groups. Molecules with a haemoglobin component are often responsible for transport of oxygen in the blood. In the blood the haemoglobin molecule is usually in the reduced form with a $H_2O$ covalently linked to the Iron molecule. In the presence of oxygen, this $H_2O$ molecule is replaced by $O_2$ to form $HbO_2$ [50].

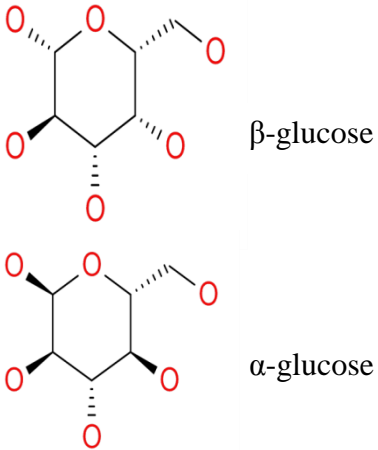
## Fibrin

**Table 6:** Description of fibrin.

Name	Molecular Formula	Description
Fibrin	$C_5H_{11}N_3O_2$	Fibrin is formed by the conversion of fibrinogen brought around through circulating blood in the presence of thrombin. Fibrin monomers then form polymeric fibrin structures which reinforce a plug of aggregated platelets to create a fibrin clot. Fibrin also acts as a temporary adhesion for cells to commence the regeneration of damaged vessels (e.g. fibroblasts and endothelial cells) [51].

## Glucose

**Table 7:** Description of glucose.

Name	Molecular Formula	Description
<p data-bbox="312 472 459 501">D-Glucose</p> 	<p data-bbox="520 472 639 501"><math>C_6H_{12}O_6</math></p>	<p data-bbox="767 472 1414 1384">Glucose is directly taken from the diet and, along with other monosaccharides, is transported across the intestinal wall to the hepatic portal vein and to liver cells and other tissues where it is converted to fatty acids, amino-acids and glycogen. Glucose crosses the plasma membrane and hexokinase converts it to glucoso-6-phosphate which enters the glycolytic pathway and produces ATP (adenosine triphosphate) and NADH (Nicotinamide adenine dinucleotide). D- glucose is the main carbohydrate given to a cell to produce energy in mammals <sup>[52]</sup>.</p> <p data-bbox="767 1451 1414 1630">Glucose in the blood is found in the ring form and can be found in two forms: <math>\alpha</math>-glucose and <math>\beta</math>-glucose <sup>[50]</sup>.</p>

### 3.3 Substrate Spectra

#### Ceramic Tile

The ceramic tile was purchased from a local B&Q store. It was white in colour with a gloss finish, 6mm thick, and advertised as a suitable tile for bathrooms and kitchens. Vibrational modes for substrates were taken from [53]. **Figure 19** shows the raw mean spectrum of ceramic tile. No components were identified for ceramic.

**Table 8:** The main Raman shifts and vibrational modes of ceramic tile.

Raman Shift/cm <sup>-1</sup>	Vibrational Mode
1008.0	$\nu(\text{C}=\text{S})$
2255.0	$\nu(\text{C}\equiv\text{N})$
2556.0	$\nu(\text{-S-H})$

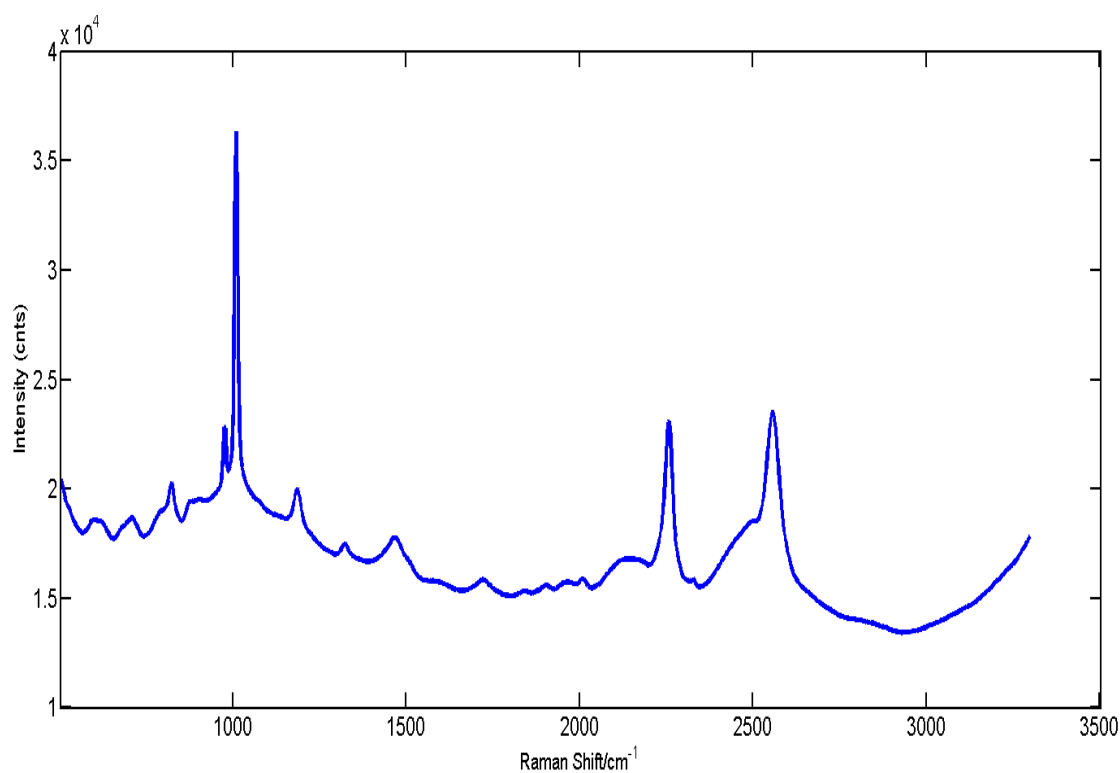


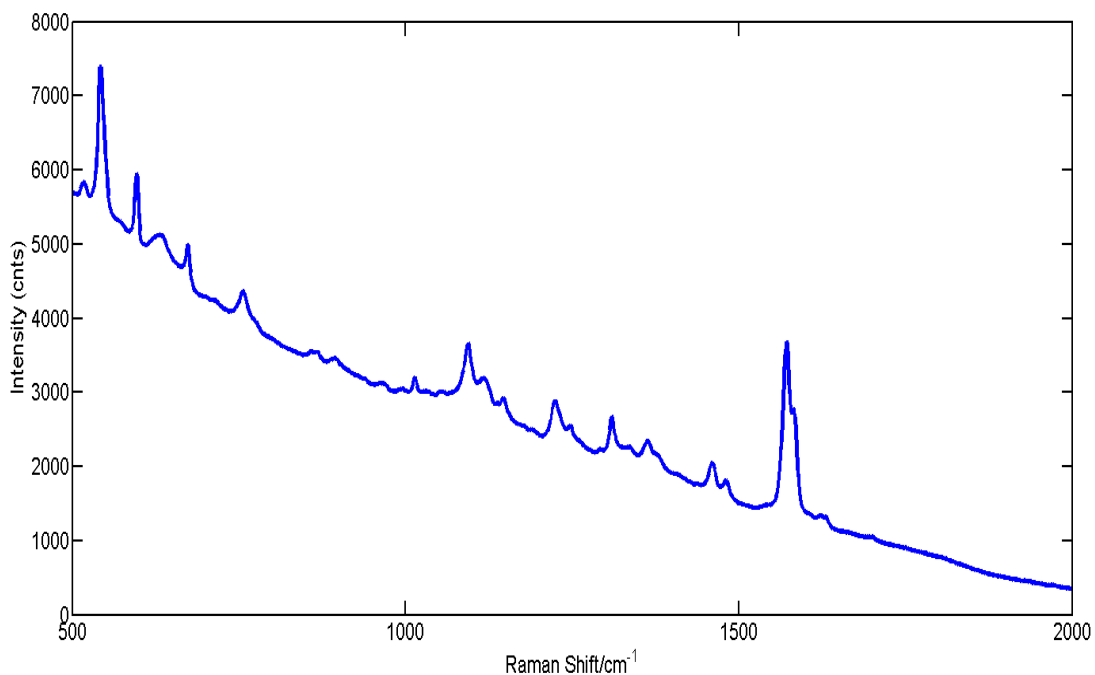
**Figure 19:** Raw mean Raman spectrum of ceramic tile.

## Blue Denim

Blue denim was purchased from a local textile shop. The tone of the denim was a light blue. For analysis purposes a small section of denim was attached to a glass microscope slide using tape to secure it in place. **Figure 20** shows the raw mean spectrum of blue denim.

**Table 9:** The Raman shifts, components and vibrational modes of blue denim.

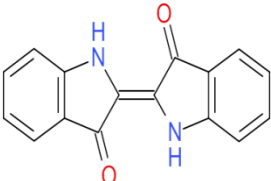
Raman Shift/cm <sup>-1</sup>	Component	Vibrational Mode
541.4	Indigo [54]	C—C-CO-C, C-N [54]
1092.0	Cellulose [55],[56]	C-O-C stretching ad deformation vibrations [55],[56]
1223.0		(CC) alicyclic, aliphatic chain vibrations
1572.0	Indigo Dye [55],[57],[54]	C-O and C-C stretching [55]



**Figure 20:** Raw mean Raman spectrum of blue denim.

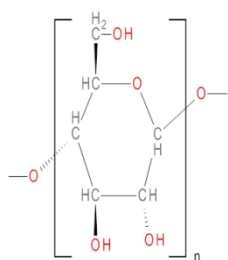
The main components identified from Raman analysis of blue denim were Indigo dye and cellulose (Tables 10, 11).

**Table 10:** Description of indigo dye.

Name	Molecular Formula	Description
Indigo Dye	<chem>C16H10N2O2</chem> 	Indigo, also known as indigotin, is the oldest dye and was originally found in the plants of the indigo-fera species, predominantly found in India <sup>[58]</sup> . Here it is present as a glucoside termed indicant which is extracted with water, is hydrolysed into indoxyl, then oxidised into indigo <sup>[58]</sup> . Indigo is a dye commonly used in jeans <sup>[59]</sup> .

**Table 11:** Description of cellulose.

Name	Molecular Formula	Description
Cellulose	C <sub>6</sub> H <sub>12</sub> O <sub>6</sub>	<p>Cellulose is found in the cell walls of terrestrial and aquatic plant life species with its function being to provide stiffness; it is one of the most abundant polymers on Earth. Animals, such as ruminants (e.g. sheep and cows) can digest cellulose and in native (natural) cotton the consisting units of cellulose number around 15,000 [60].</p> <p>Cellulose lacks significant acidic or basic properties and consists of linearly arranged biglucose units with either bridge linkages. The side groups of these units are primary and secondary alcoholic hydroxyl groups which makes the fibre hydrophilic. This property is responsible for the dyeing nature of cotton.</p>

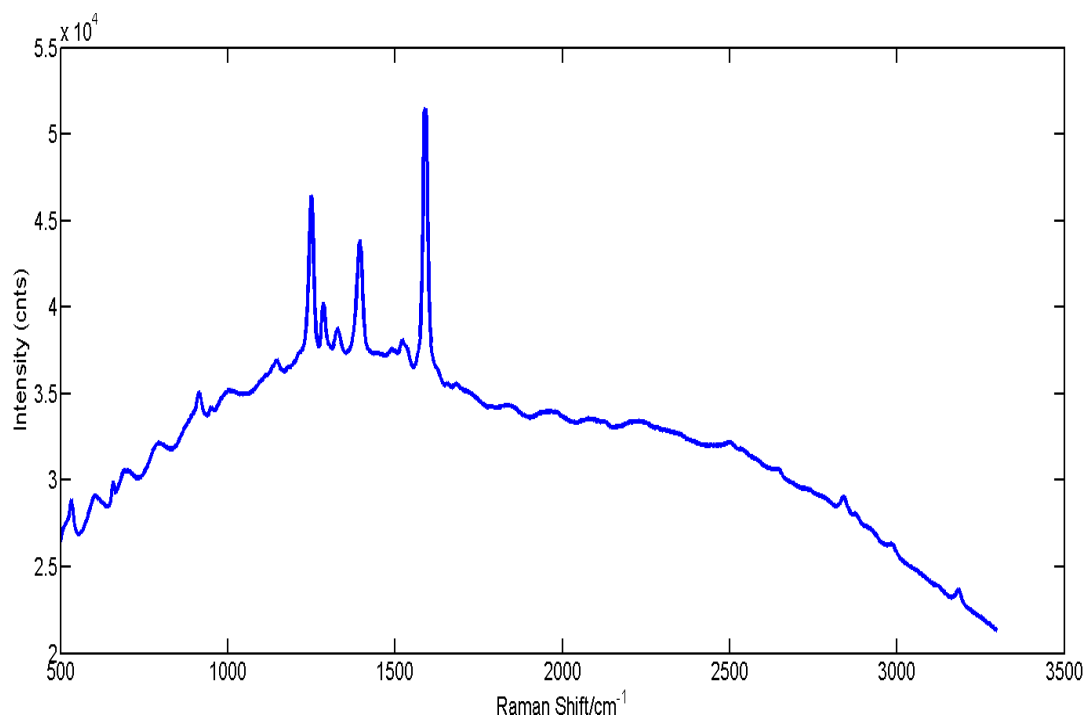


### Brown Leather

Pieces of brown leather material were purchased from a textile shop. For the purpose of analysis a section of brown leather was attached to a glass microscopic slide and secured in place with tape. **Figure 21** shows the raw mean Raman spectrum of brown leather.

**Table 12:** The Raman shifts, components and vibrational mode of brown leather.

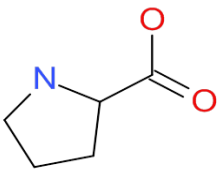
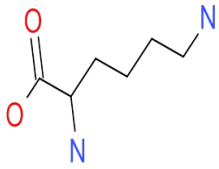
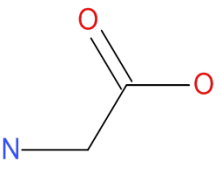
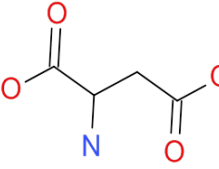
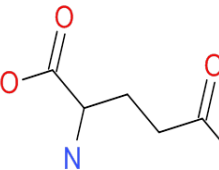
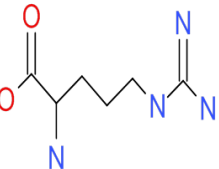
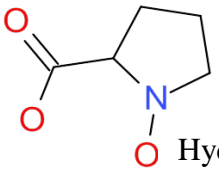
Raman Shift/cm <sup>-1</sup>	Component	Vibrational Mode
1249.0	Collagen (Amide III) [61]	(CC) alicyclic, aliphatic chain vibrations
1285.0		(CC) alicyclic, aliphatic chain vibrations
1395.0		(CH <sub>2</sub> )  (CH <sub>3</sub> ) asym
1590.0		C-(NO <sub>2</sub> ) asym



**Figure 21:** Raw mean Raman spectrum of brown leather.

The main component identified from Raman analysis of brown leather was collagen (Table 13).

**Table 13:** Description of collagen.

Name	Molecular Formula	Description
Collagen	Triple Helix Protein	<p>Collagen is a protein which makes up the fibres and fibre bundles which create most of the skin structures. The Collagen in skin exists as long unbranched, macromolecular chains formed from over 1000 amino acid residues. 30% of these are formed from the amino acid glycine and 10% are from proline and hydroxyproline. Also present are aspartic acid and glutamic acids and basic residues derived from arginine and lysine [62].</p> <p>The collagen molecule is a stable, rod like, triple helix with links between adjacent molecules within the fibrillar structure [62].</p> <p>The structure of collagen allows it to react readily with tanning agents (used in the tanning process) involving the addition of artificial cross-links to stabilise the skin fully and prevent bacterial putrefaction and decay [62].</p>
 Proline	 Lysine	
 Glycine	 Aspartic Acid	
 Glutamic Acid	 Arginine	
 Hydroxyproline		

## Condom

The condoms used for analysis were purchased from a local pharmacist. The brand of condom was chosen at random. These were Durex Thin Feel<sup>®</sup>. On contacting Durex, information was given including the addition of glycerol (glycerine) to their lubricants (which were water based) and that their condoms were made from Natural Latex Rubber. **Figure 22** shows the raw mean Raman spectrum of the condom.

**Table 14:** The Raman shifts, components and vibrational modes of Durex Thin Feel<sup>®</sup>

Raman Shift/cm <sup>-1</sup>	Component	Vibrational Mode
1450.0	Glycerine [63], [64]	(CH <sub>2</sub> ) [63], [64]
1663.0	Natural rubber (latex) [65], [66]	(C=C) [65] <i>cis</i> poly isoprene
2911.0	Natural rubber (latex) [65]	(C-H stretching) [65]

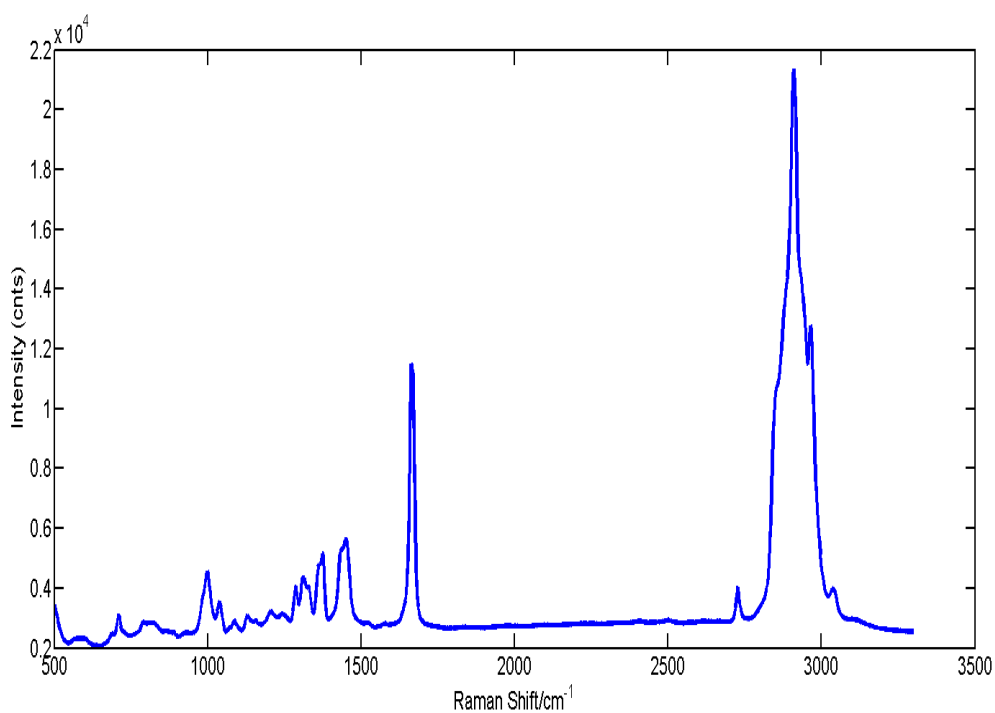
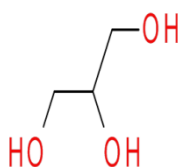


**Figure 22:** Raw mean Raman spectrum of Durex Thin Feel<sup>®</sup> Condoms.

The main components of Durex Thin Feel<sup>®</sup> condoms were latex and glycerine (**Table 15**).

**Table 15:** Description of latex and glycerine.

Name	Molecular Formula	Description
Latex		<p>Latexes are typically aqueous liquids in which microscopic polymers are dispersed <sup>[67]</sup>.</p> <p>Latex rubber can be natural (derived from the rubber tree), synthetic (emulsion polymerisation), or artificial (dispersion of a solid polymer in an aqueous medium <sup>[68]</sup>.</p>
Glycerine	C <sub>3</sub> H <sub>8</sub> O <sub>3</sub>	Used in a wide variety of pharmaceutical formulations, cosmetics and food additives <sup>[69]</sup> .



### Laminate Flooring

Sections of laminate flooring were purchased for analysis from a local DIY store. Laminate flooring consists of four main layers: a bottom layer of melamine plastic, a layer of core board (fibreboard or particle board), a decorative layer and finally a top

durable layer which may contain aluminium oxide as well as melamine resin <sup>[70]</sup>. **Figure 23** shows the raw mean Raman spectrum of laminate flooring. No components could be determined for laminate.

**Table 16:** The Raman shifts and vibrational modes of laminate flooring.

Raman Shift/cm <sup>-1</sup>	Vibrational Mode
635.2	(C-S) aliphatic
692.4	(CC) alicyclic, aliphatic chain vibrations

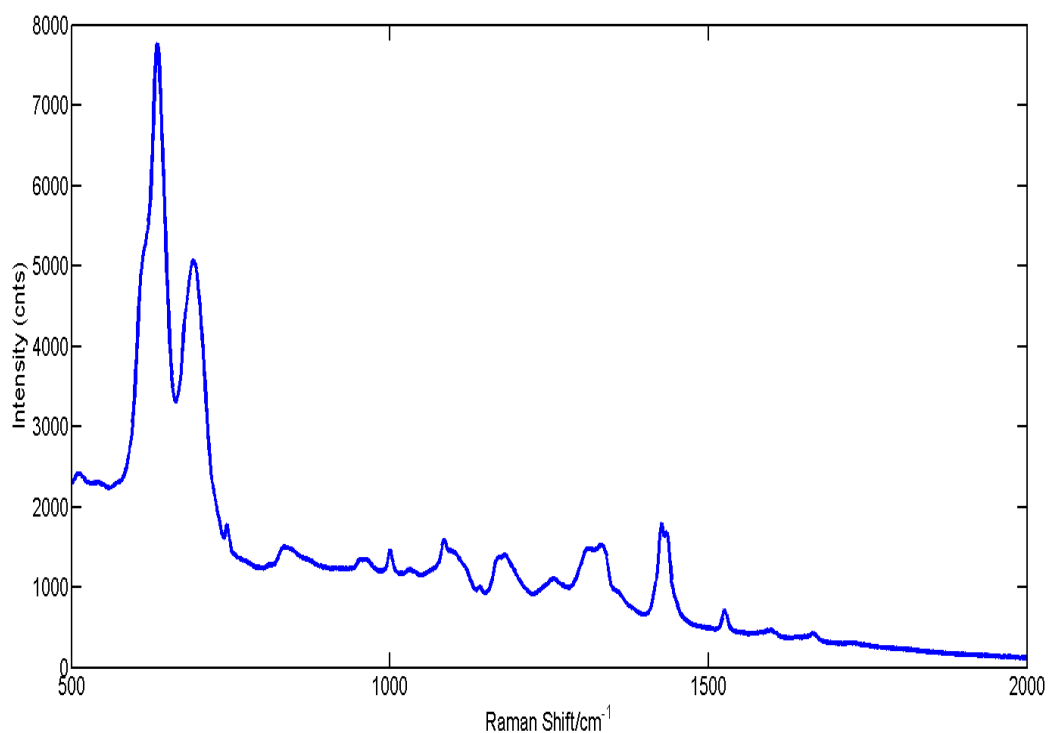


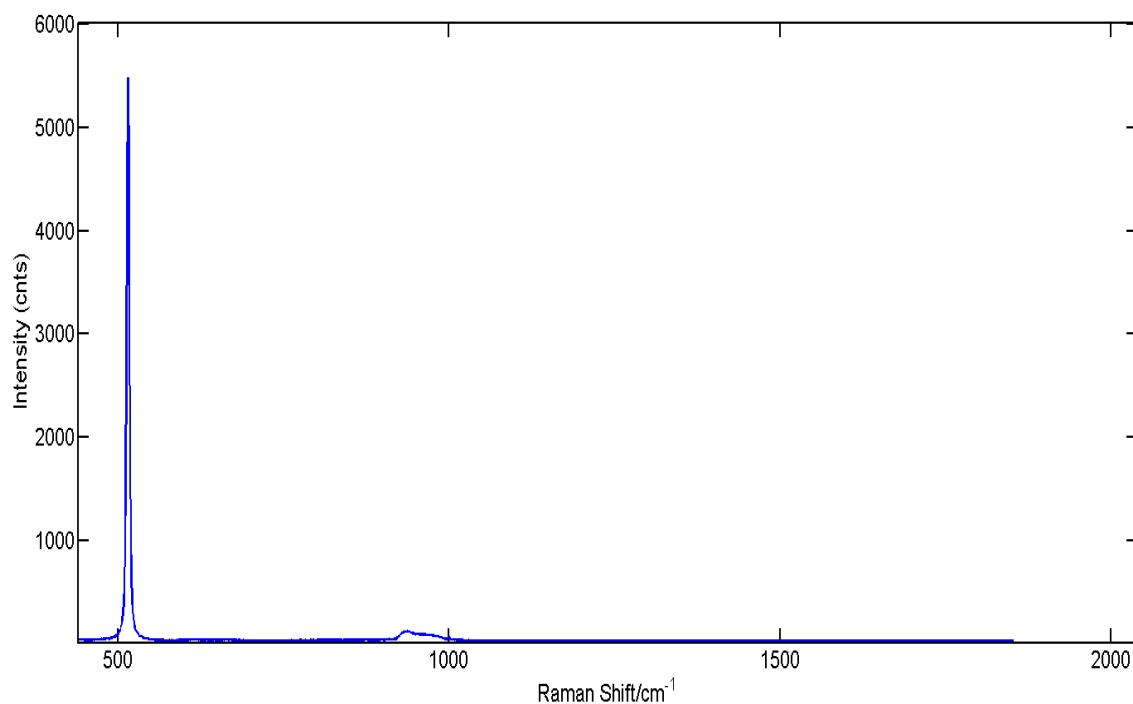
**Figure 23:** Raw mean Raman spectrum of laminate flooring.

## Crystalline Silicon

Crystalline silicon was made available in the laboratory. **Figure 24** shows the raw mean Raman spectrum of crystalline silicon.

**Table 17:** The Raman shifts, components and vibrational modes of crystalline silicon.

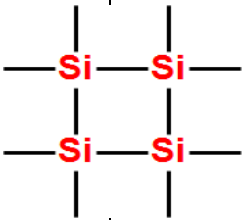
Raman Shift/cm <sup>-1</sup>	Component	Vibrational Mode
520	Crystalline silicon [71]	Si



**Figure 24:** Raw mean Raman spectrum of crystalline silicon.

The main component of crystalline silicon was silicon (**Table 18**).

**Table 18:** Description of crystalline silicon.

Name	Molecular Formula	Description
Silicon	Si 	<p>Crystalline silicon is a basic component of soil, sand and granite with quartz being the most common form of crystalline silicon <sup>[72]</sup>.</p> <p>Crystalline silicon exhibits silicon-silicon bonds which are symmetrical and cause strong Raman scattering resulting in a sharp, strong peak at <math>521\text{cm}^{-1}</math> <sup>[73]</sup>.</p>

### 3.4 Blood on Substrate

The raw spectra of blood on substrates were analysed for any apparent substrate peak interference based on the substrate standard scans. Condom was chosen to present here as this demonstrated the only significant substrate interference (**Figures 25, 26**).

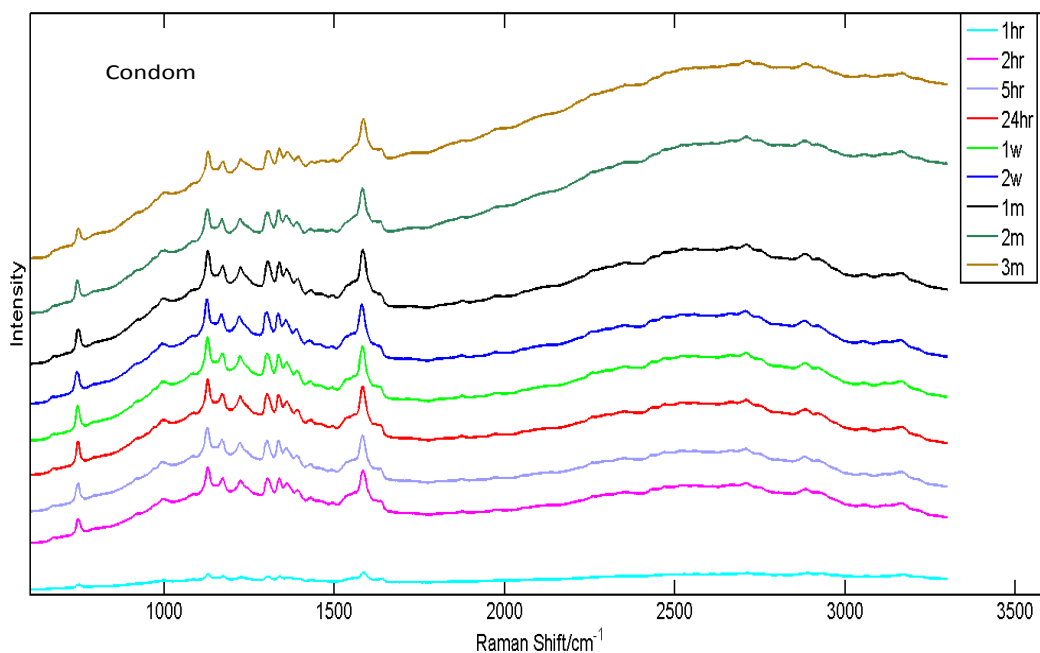


**Figure 25:** Mean raw spectra of blood on condom.

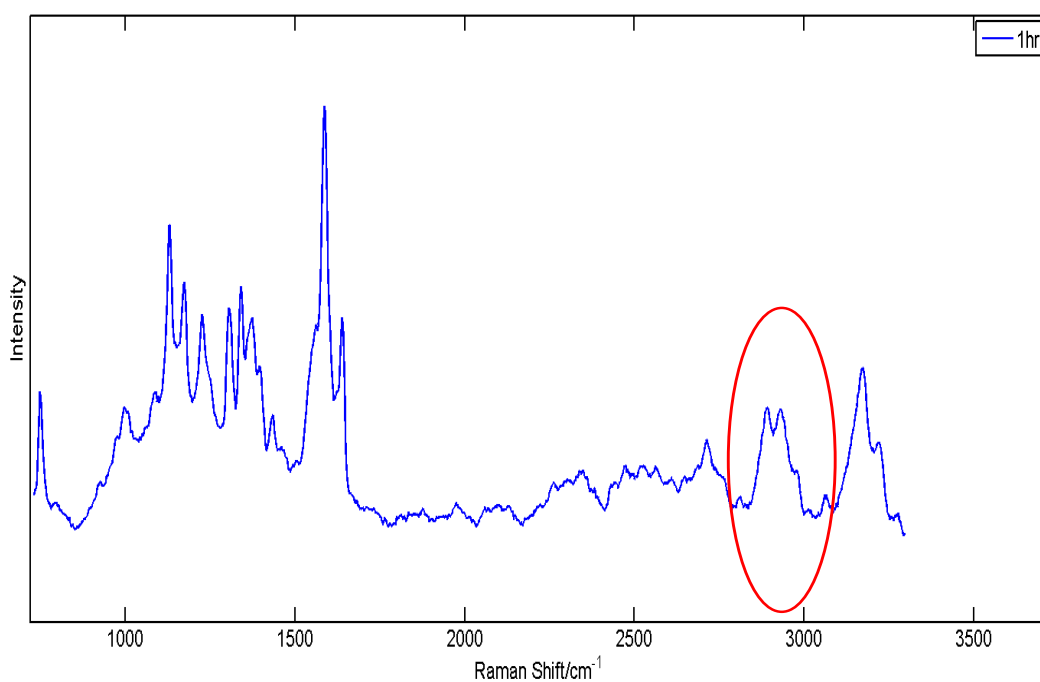


**Figure 26:** Spectrum of blood on condom after 5<sup>th</sup> order polynomial fit pre-processing technique.

The raw spectra of blood on condom (**Figure 25**) showed no visible substrate interference, this is due to the large amount of background fluorescence. Therefore 5<sup>th</sup> order polynomial fit was used to remove the background fluorescence. Pre-processed spectrum of blood on condom at  $\leq 1$ hr (**Figure 26**) showed substrate interference at  $2911\text{cm}^{-1}$  (**Highlighted**). This peak corresponds to interference from the latex rubber in the condom. However, although the substrate showed interference, this was only clear at  $\leq 1$ hr and later times showed no visible interference. Additionally, substrate interference was not seen around characteristic peaks for blood. Spectra from other substrates showed no visible interference.

### 3.5 Conclusions

Overall this chapter has successfully identified and described the components of blood and the main substrate components. This chapter has also demonstrated that substrate peaks can interfere on the Raman spectrum of blood although this interference does not impact on the main components of blood.

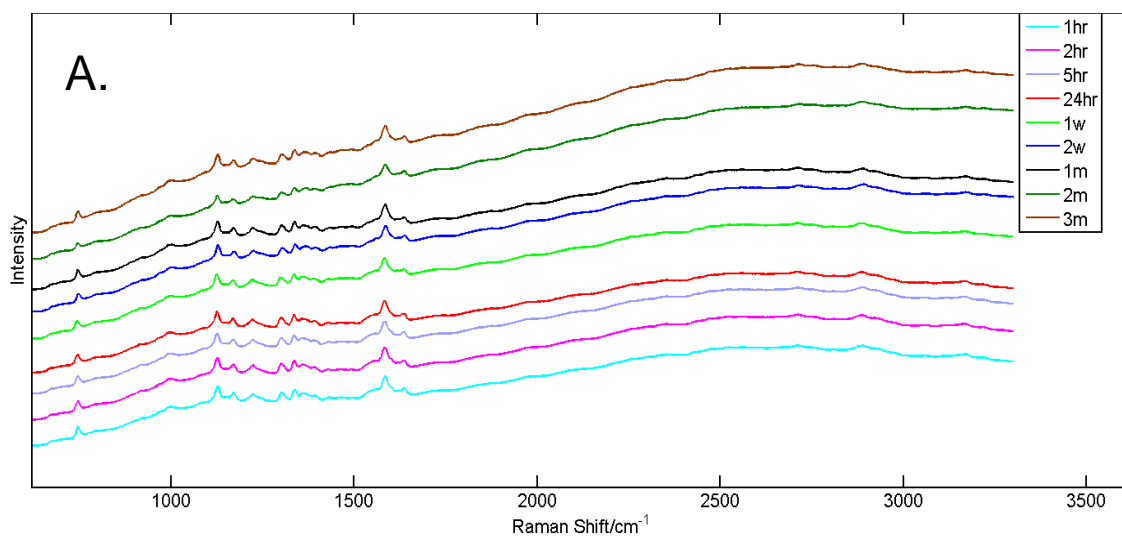
## CHAPTER 4

### INVESTIGATING THE EFFECT OF AGEING ON THE RAMAN SPECTRUM OF EQUINE BLOOD

Raman spectroscopy is typically utilized as a qualitative and quantitative, molecular fingerprinting analytical technique. This chapter investigates the use of Raman spectroscopy as a confirmatory technique for the identification of blood at different stages of ageing and the effect ageing has on the Raman spectrum of blood. Spectra used in this chapter were initially analysed as raw data to highlight the benefit of pre-processing techniques. Further spectra in this chapter were subject to pre-processing and MVA using MATLAB version 7.8.0.347 (R2009a) (The MathWorks, Inc., USA) before interpretation. Results from this chapter have been accepted and presented as a poster presentation at SciX 2014, Reno (**Appendix 1**).

#### 4.1 Raw Spectrum of Blood

The first stage of analysis involved the collection of blood spectra on each substrate surface, at time frames over a three month period. Spectra from three substrates were chosen to present in this study (**Figure 27: [A-C]**).



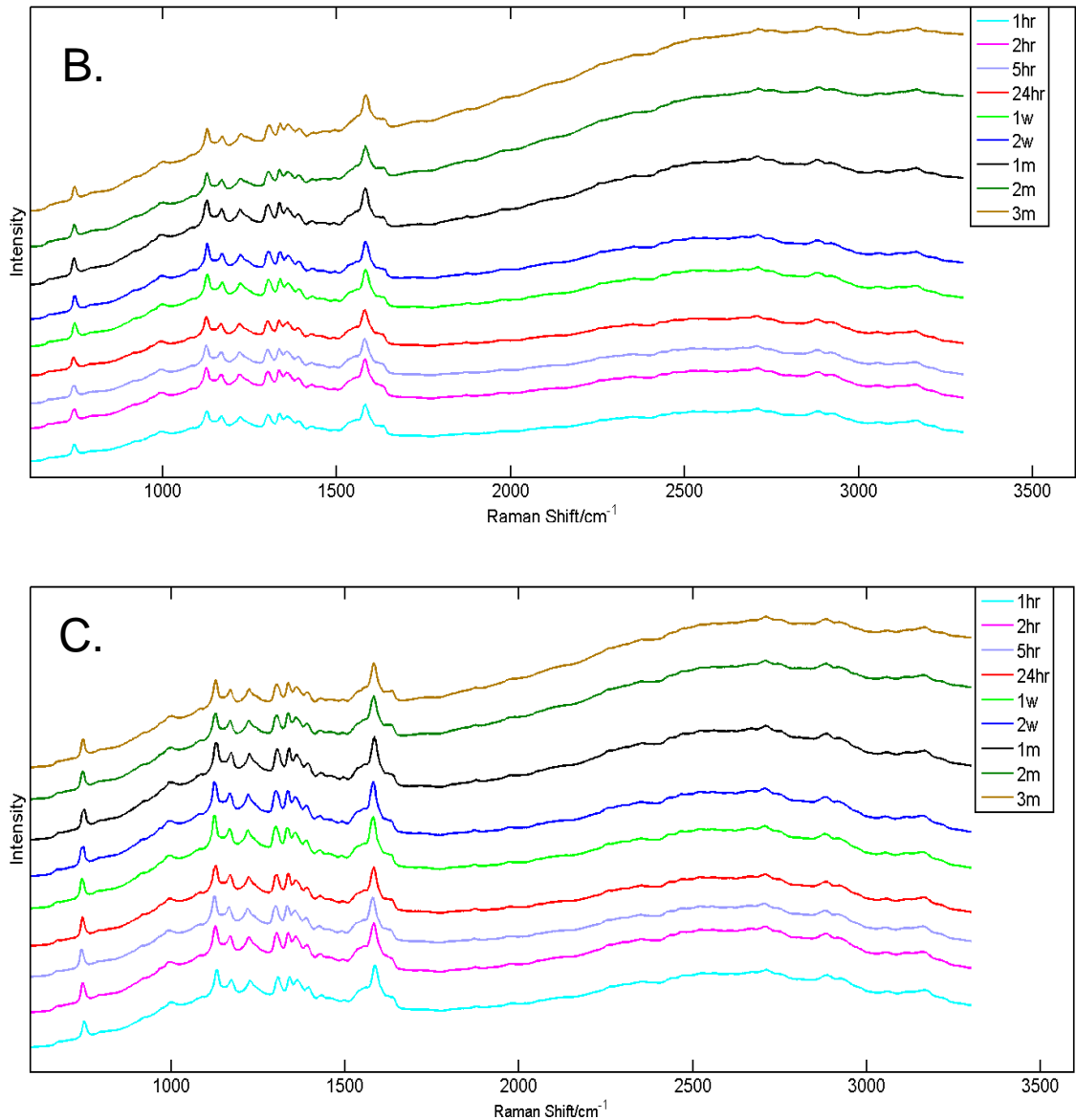


**Figure 27:** [A.] Mean raw Raman spectra of blood on denim. [B.] Mean raw Raman spectra of blood on leather. [C.] Mean raw Raman spectra of blood on laminate.

From these three spectra it is clear to see that substrates can affect the quality of the spectra produced due to some variation seen between them. For denim (**Figure 27: [A.]**) the intensities of the peaks corresponding to blood are lower than on the other substrates making them harder to identify. In **Figure 27: [C.]** the tryptophan and glucose peaks ( $747\text{cm}^{-1}$ ,  $1125\text{cm}^{-1}$ ) have a greater intensity than on the other substrates. Additionally in this figure, the peaks for haemoglobin ( $1363\text{cm}^{-1}$ ,  $1587\text{cm}^{-1}$ ) appear to decrease over time. Overall the peaks in each figure are difficult to see and compare. The reason for

the poor visual of the peaks is due to large background fluorescence caused by substrate fluorescence and fluorescence from the droplet itself.

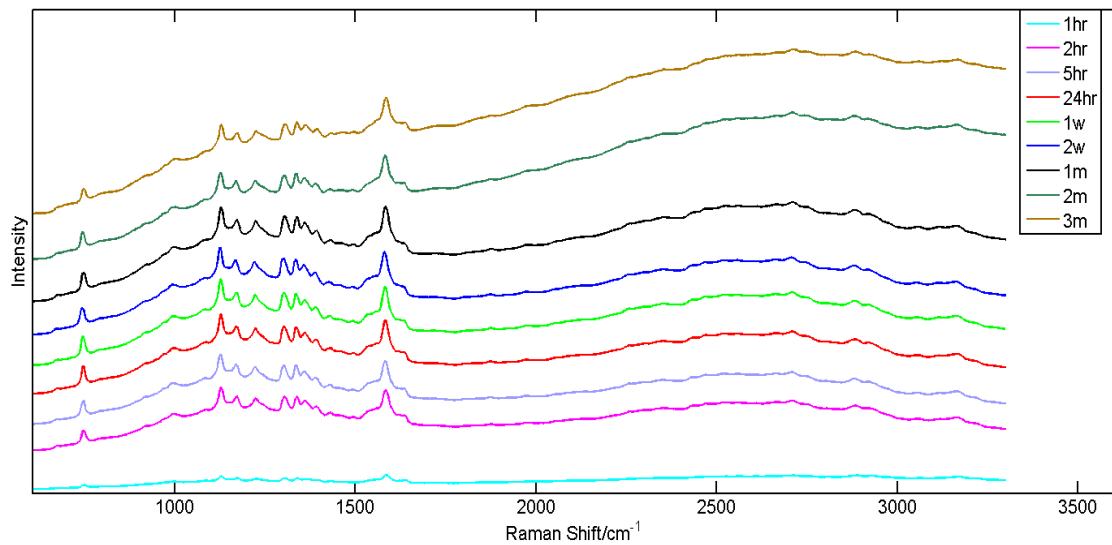


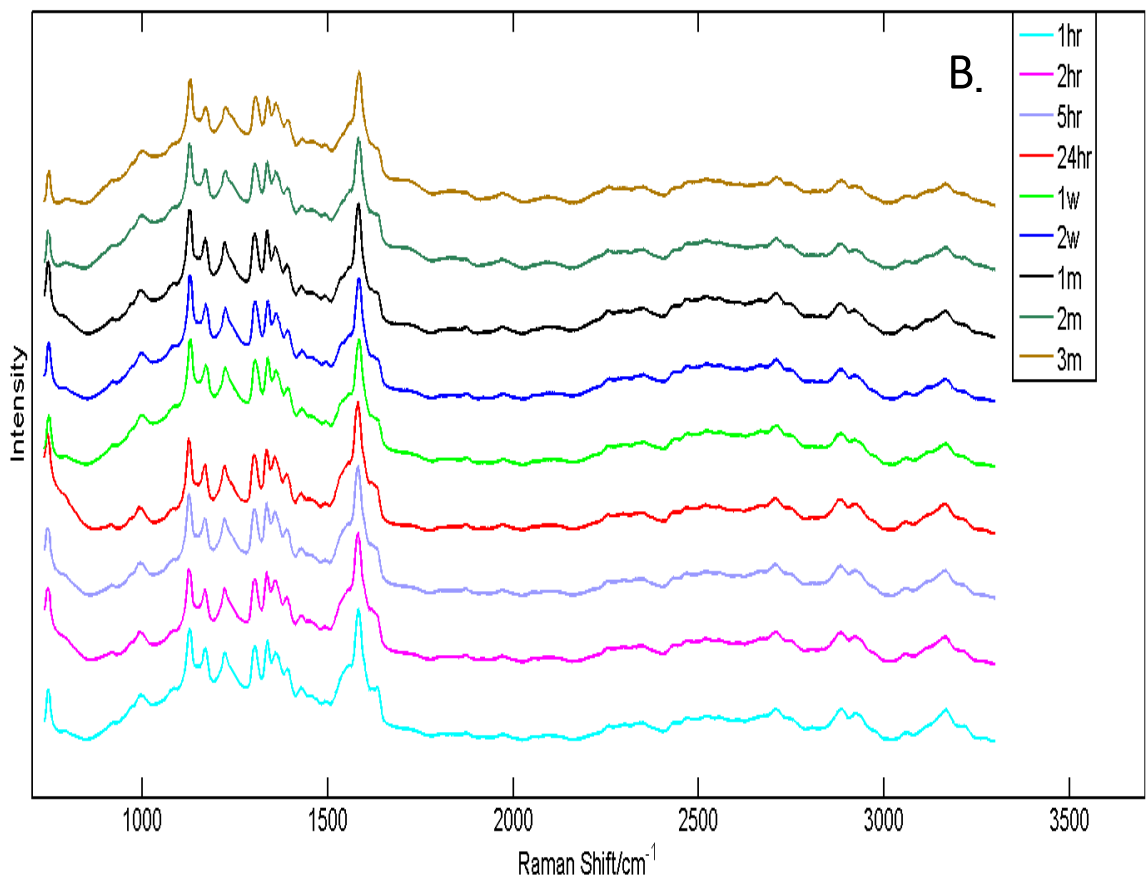
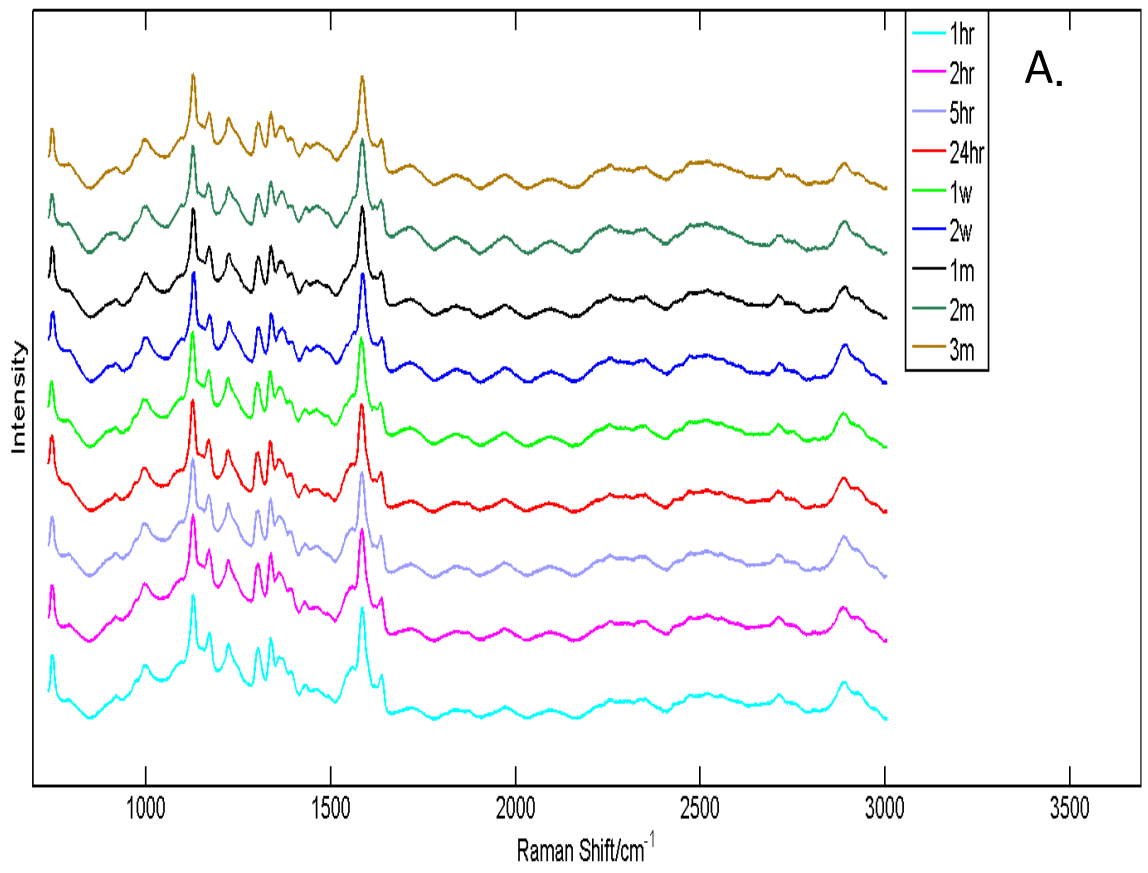
**Figure 28:** The mean raw Raman spectra of blood on condom.

The spectrum of blood on condom (**Figure 28**) was also included because it shows a very low intensity at  $\leq 1$ hr of ageing. At this time the droplet is still wet and analysis is difficult which explains this low intensity. This was also seen on crystalline silicon which suggests that for these substrates the drying of the droplet is longer than on the others.

At this point of the study good evidence can already be seen that substrate and ageing can interfere with the Raman spectrum of blood due to fluorescence and some peak intensity changes (although these are very difficult to see). Furthermore, when the droplet is still wet ( $\leq 1$ hr of ageing) the intensities of the peaks in the spectrum can be very low on some substrates and are hardly visible. Overall, because peaks corresponding to blood are difficult to analyse, further data processing is required.

#### 4.2 5<sup>th</sup> Order Polynomial Fit Pre-Processing

Pre-processing techniques were carried out to minimise the effect of the background fluorescence and therefore enhance the clarity of the characteristic blood peaks. One pre-processing technique carried out on the raw data was 5<sup>th</sup> order polynomial fit (described in Materials and Methods). Firstly, 5<sup>th</sup> order polynomial fit was applied to the spectra using Lab Spec 6 spectroscopy on the Raman instrument. Secondly, the pre-processed data was then imputed into MATLAB where part of the spectrum ( $\leq 735\text{cm}^{-1}$ ) was cut. This cutting was carried out to remove a section which did not have significance in the Raman spectrum of blood and would have only affected the intensity and clarity of characteristic peaks of blood and comparison of these peaks at different times. After cutting, spectra were then vector normalised. The next figures are after 5<sup>th</sup> order polynomial fit, cutting, and vector normalisation had been carried out (**Figure 29: [A-C]**).



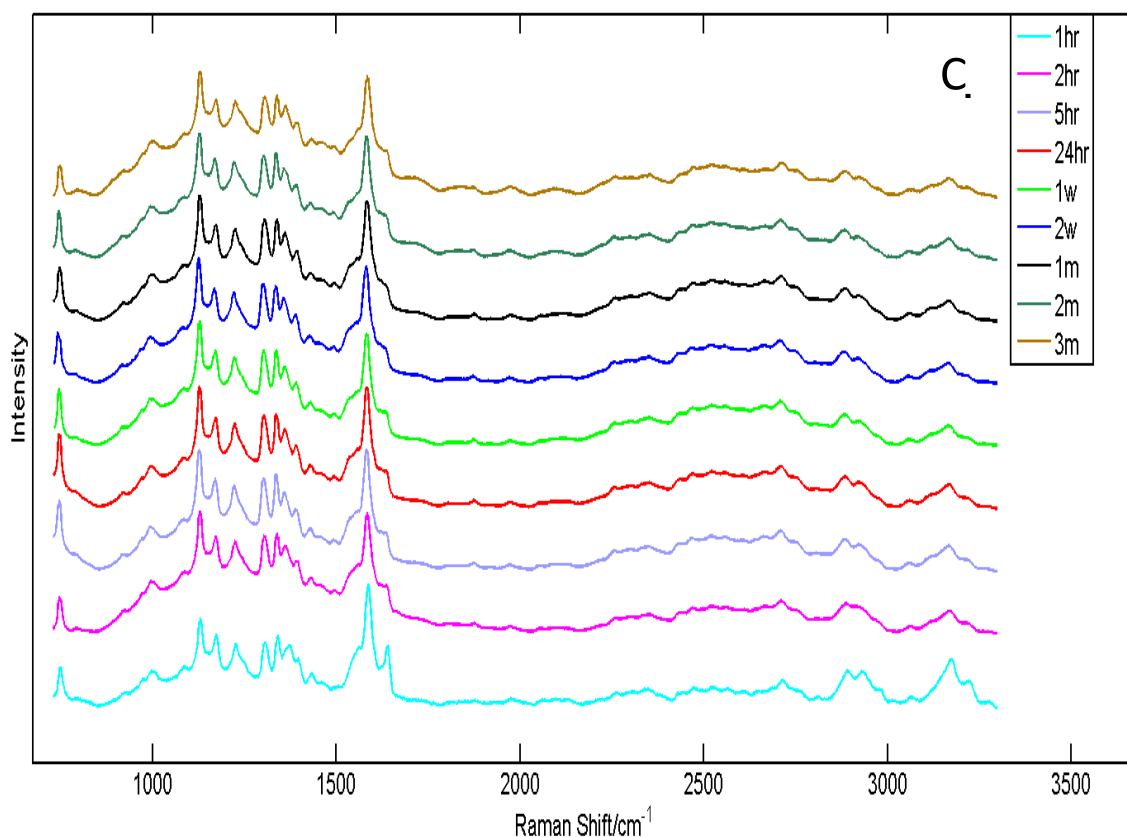


**Figure 29:** The mean 5<sup>th</sup> order polynomial fit pre-processed spectra of blood on: [A.] Denim [B.] Leather [C.] Condom.

The 5<sup>th</sup> order polynomial fit has removed the majority of background fluorescence from the substrate and droplet making the area with characteristic blood peaks clearer to see (particularly denim) (**Figure 29: [A-C]**). Additionally, vector normalisation has enabled a view of the spectrum of blood on condom at  $\leq 1$ hr and the ability to compare this spectrum to the other time frames. This would not have been possible to achieve from raw spectra.

On denim (**Figure 29: [A.]**) there is a small decrease in intensity of the tryptophan, glucose and haemoglobin peaks ( $747\text{cm}^{-1}$ ,  $1125\text{cm}^{-1}$ ,  $1587\text{cm}^{-1}$  and  $1640\text{cm}^{-1}$ ) from  $\leq 1$ hr to 3m. This could suggest that over time there is a degradation/depletion of tryptophan, glucose and haemoglobin in the blood droplet. Haemoglobin degradation

relates to the literature [8]. However, the fibrin peak ( $1225\text{cm}^{-1}$ ) appears unchanged in intensity over time.

These same decrease in intensity of the tryptophan, glucose and haemoglobin peaks ( $747\text{cm}^{-1}$ ,  $1125\text{cm}^{-1}$ ,  $1587\text{cm}^{-1}$  and  $1640\text{cm}^{-1}$ ) are also seen in both blood on leather (**Figure 29: [B.]**) and condom (**Figure 29: [C.]**) spectra. Suggesting there is a depletion of these components over time.

On leather (**Figure 29: [B.]**) there is also a decrease in the intensity of the peaks of haemoglobin, tryptophan and tryptophan ( $1587\text{cm}^{-1}$ ,  $1340\text{cm}^{-1}$  and  $1434\text{cm}^{-1}$ ) from  $\leq 1\text{hr}$  to  $3\text{m}$  which again suggests there is a depletion of tryptophan and haemoglobin over time. However, the fibrin peak ( $1225\text{cm}^{-1}$ ) appears unchanged in intensity over time. Additionally, the  $747.1\text{cm}^{-1}$  peak at  $24\text{hrs}$  and  $1\text{m}$  shows a shift in the peak compared to the other times. This could be due to fluorescence from the droplet at these times or the physical nature of the droplet. More research into this would have to be carried out.

On condom (**Figure 29: [C.]**) the haemoglobin peak at  $1640\text{cm}^{-1}$  shows a great decrease in intensity from  $\leq 1\text{hr}$  to  $2\text{hr}$ ; which is also seen in the spectra of blood on silicon. Additionally, the peak at  $1587\text{cm}^{-1}$  (haemoglobin) shows a slight decrease in intensity. These support haemoglobin degradation over time, especially after  $1\text{hr}$ . However, the fibrin peak ( $1225\text{cm}^{-1}$ ) appears unchanged in intensity over time.

Overall, after 5<sup>th</sup> order polynomial fit was carried out, changes in the corresponding blood peaks over time were clearly visible. The clearest changes were seen on denim, leather and condom. To distinguish these changes further, PCA analysis was also carried out. The non-change in intensity of the fibrin could be a result of the blood being defibrinated, although, this can only be speculated on as more research would have to be carried out comparing defibrinated to non-defibrinated blood.

### 4.3 5<sup>th</sup> Order Polynomial Fit PCA Plots

PCA plots were carried out to identify separation between mean, early ( $\leq 1$ hr to 5hr/24hr) and late (24hr/1w to 3m) times. Plots were carried out for all substrates, however, three which show the best separation and grouping were chosen to present here (Figures 30-32).

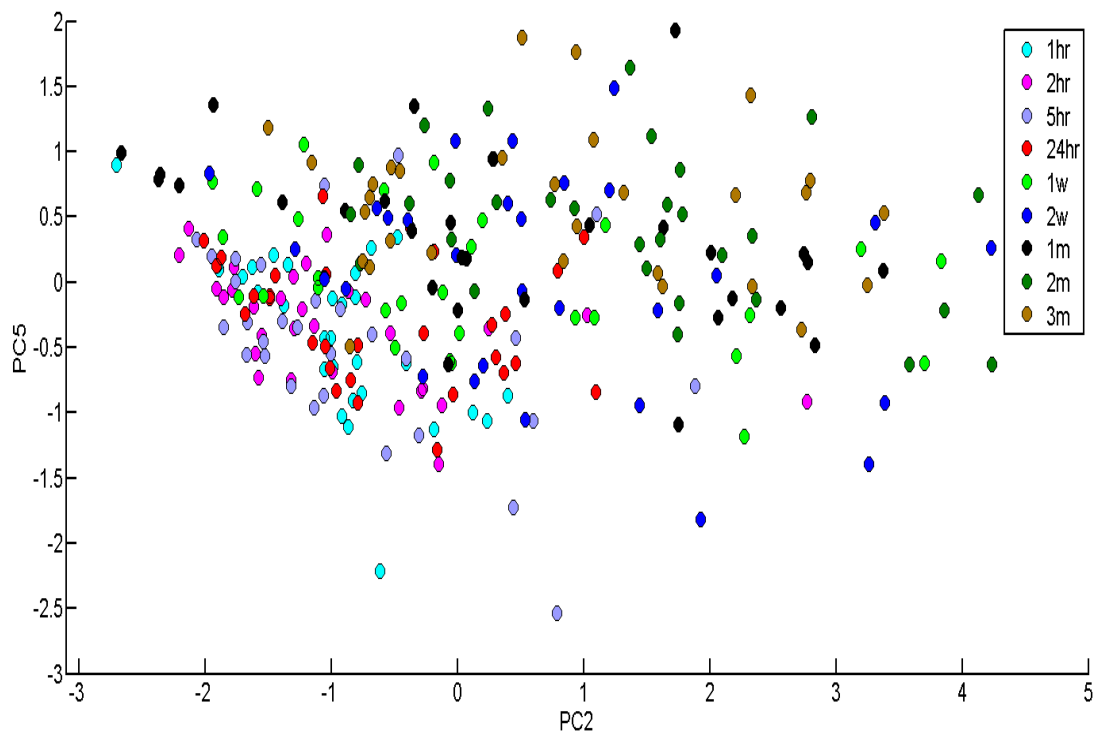


**Figure 30:** PCA plot of blood on denim.

Some grouping can be seen for early time points  $\leq 1$ hr to 24hr however later time points are scattered and show little grouping (Figure 30). There is also little separation between early and late times along the PC2 axis. This suggests PCA is not a suitable method of displaying separation of mean, early and late times.

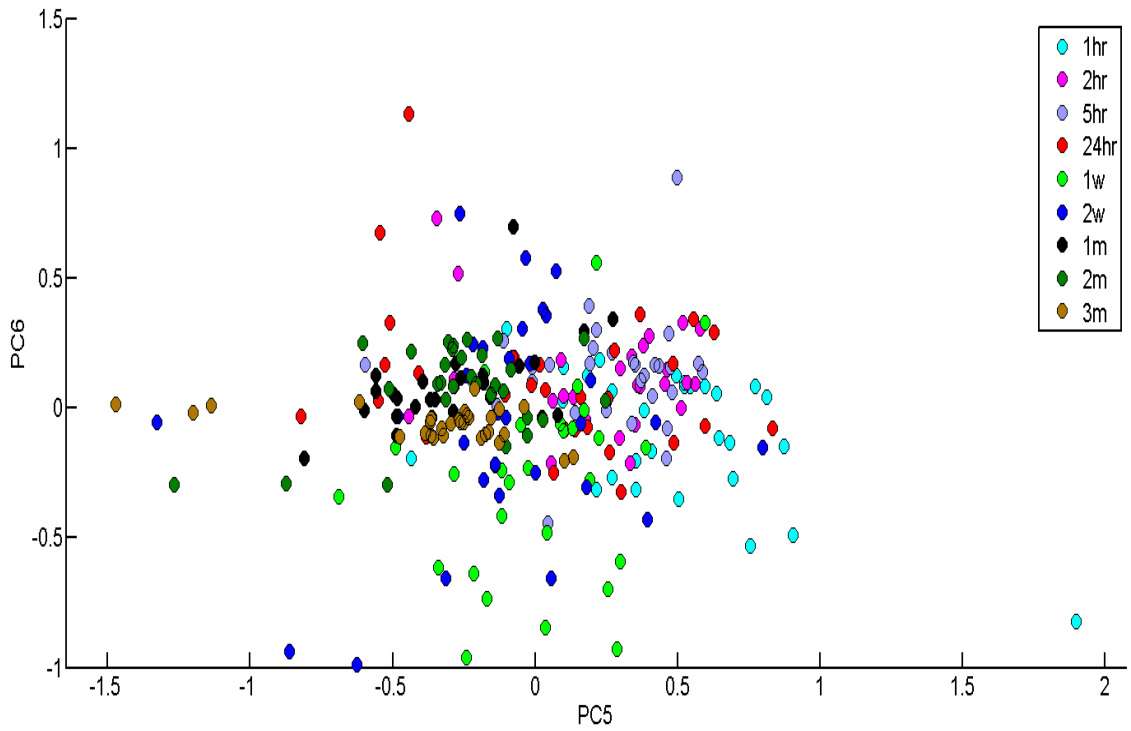


**Figure 31:** PCA plot of blood on leather.

There is some slight grouping of early and late times (**Figure 31**). However, there is no clear separation between early and late time points along the PC5 axis as they are scattered around each other.

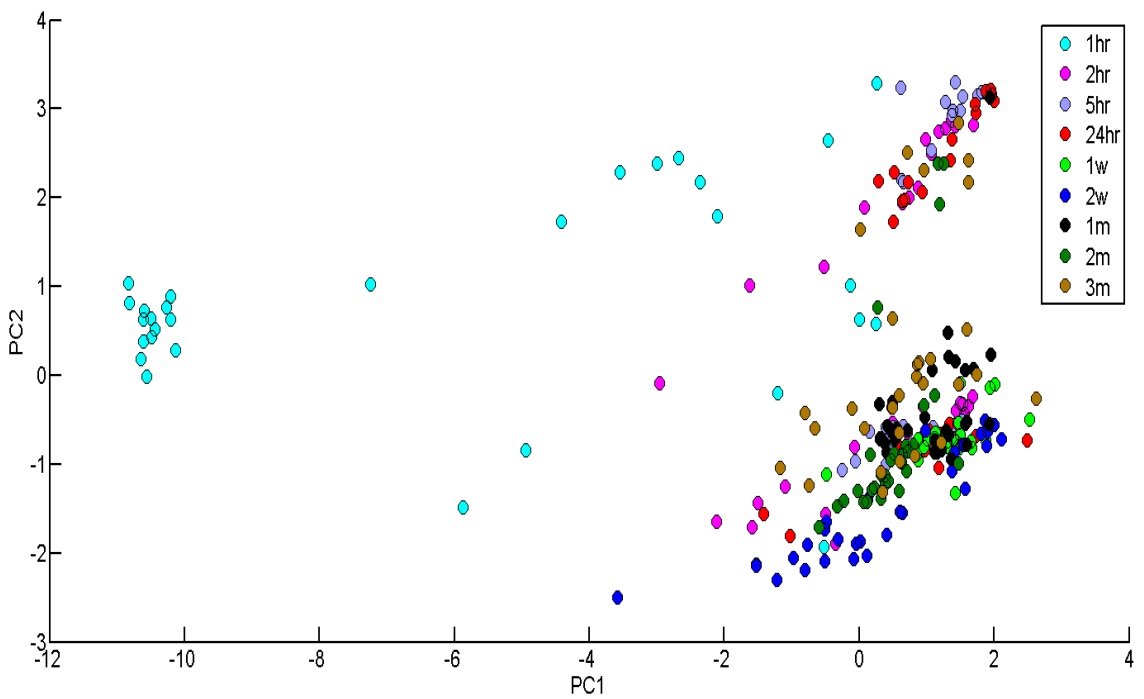


**Figure 32:** PCA plot of blood on crystalline silicon.

PCA plot of blood on silicon (**Figure 32**) shows some separation of  $\leq 1$ hr from the rest of the time plots along the PC1 axis. 2hr and 5hr show some grouping together and later time plots are grouped well together. However, 2hr and 5hr are interspersed within later time plots.

Overall, the PCA plots show no clear separation between early and late time periods along the PCA axis. PCA is not a useful method to show the separation between early and late time periods.

#### 4.4 5<sup>th</sup> Order Polynomial Fit DFA Plots

Firstly, the 5<sup>th</sup> order polynomial data was cut at the approximate Raman shift regions of  $\leq 735\text{cm}^{-1}$  and  $\geq 1650\text{cm}^{-1}$ . This was done to focus specifically on the region of peaks which correlate to blood. By doing this, any changes and separation visualised is therefore based on this region alone because there is less interference from background fluorescence. Vector normalisation was then carried out following cutting.

Finally, DFA was used to visualise separation between mean, early ( $\leq 1$ hr to 5hr/24hr) and late time points (24hr/1w to 3m). Three DFA plots which had the best separation between early and late time points are presented here (**Figures 33-35**).

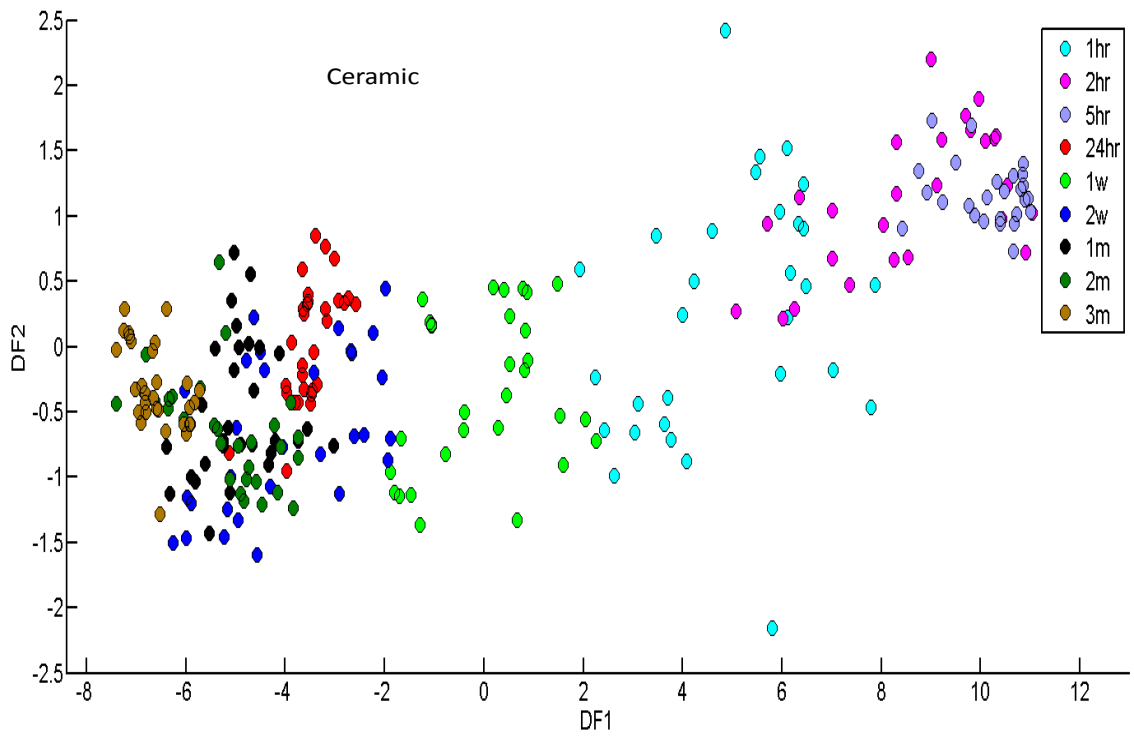


**Figure 33:** 5<sup>th</sup> order polynomial fit DFA plot of blood on ceramic.

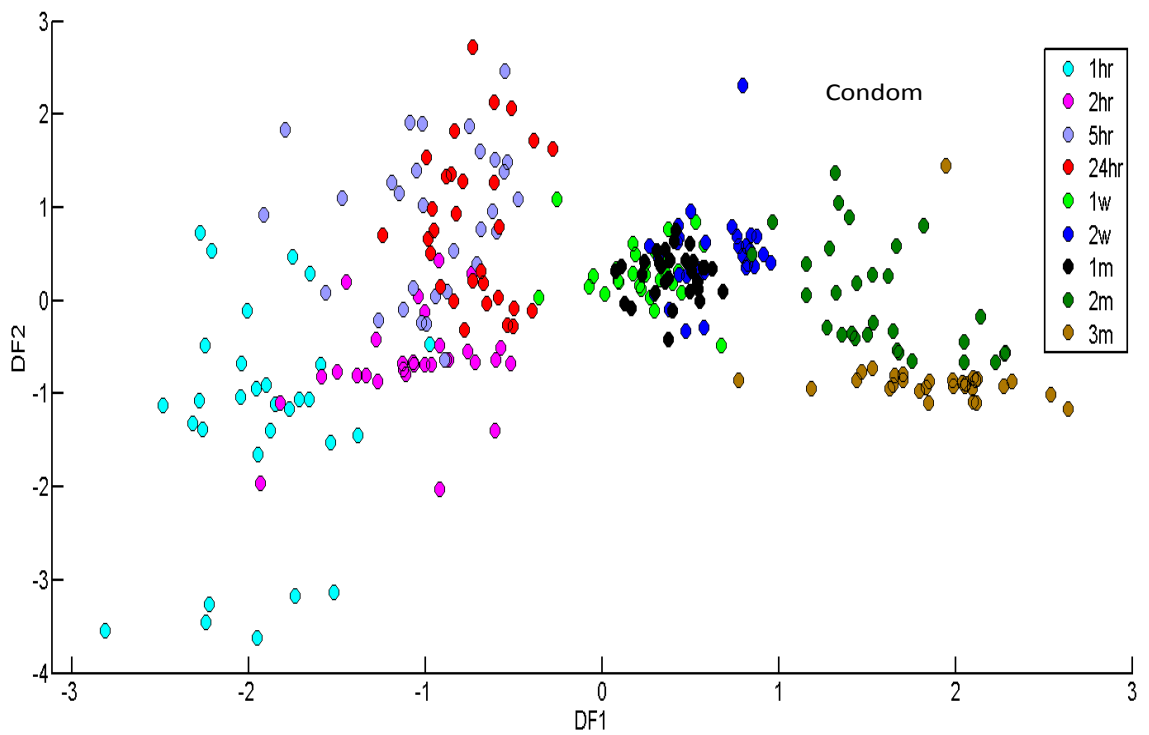


**Figure 34:** 5<sup>th</sup> order polynomial fit DFA plot of blood on condom.

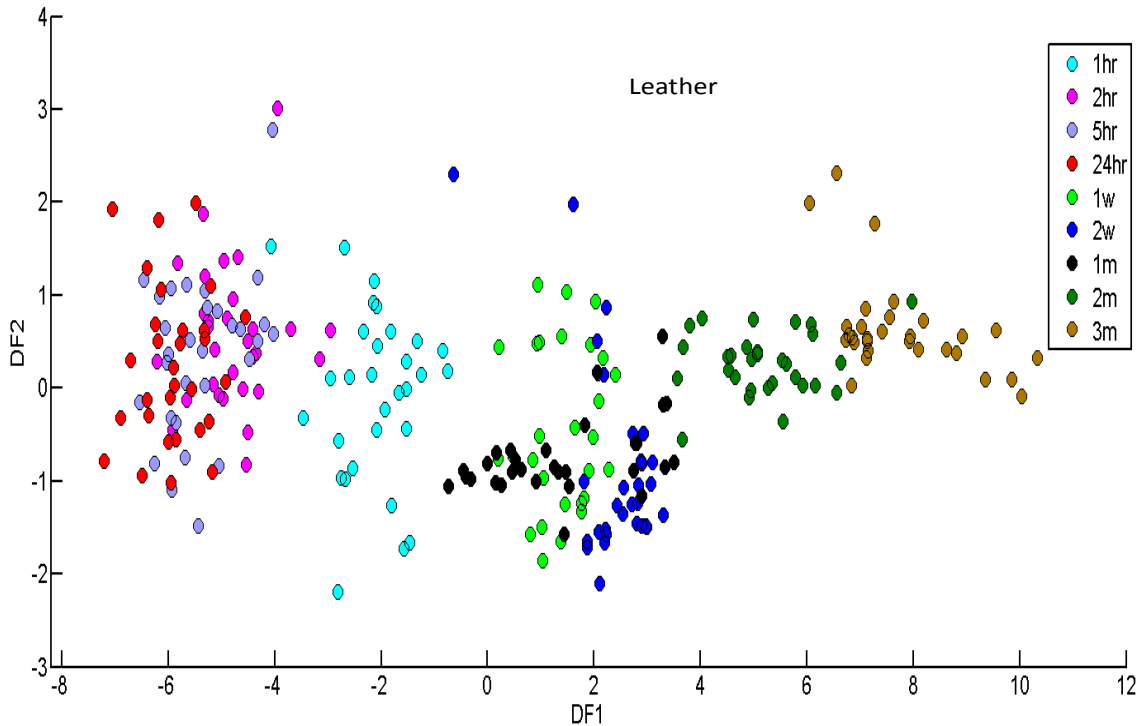


**Figure 35:** 5<sup>th</sup> order polynomial fit DFA plots of blood on leather.

There is very clear separation between early and late time plots in all three figures along the DF1 axis. In particular blood on condom and blood on leather (**Figures 34, 35**) demonstrate close grouping of plots within their own time frame and show a gradual shift of plots from left to right over time. Blood on ceramic (**Figure 33**) shows clear grouping of  $\leq 1$ hr to 5hr. However, 24hr is grouped with later time points which may be due to the substrate properties. This suggests blood on ceramic ages faster than on condom and leather.

Denim also showed very clear separation between early and late time plots, clear grouping within time frames, and a shift from left to right with increasing time. Blood on laminate had clear grouping of plots within their own time frame and separation between early and late times. However 24hr was grouped with later time plots. This suggests that blood dries quicker on laminate similarly to ceramic. Crystalline silicon demonstrated clear separation between early and late, however, all other time points

were interspersed within each other and showed little grouping in relation to one another over time.

Overall, DFA has proven to be an effective method of displaying separation between early and late time plots. This appears to be the more suitable method over PCA for this study.

The following step after DFA was to present the spectra on all substrates against the DFA spectrum separation. The reason to present the data in this way would be to highlight the major areas of peak intensity differences. **Figures 36-38** were chosen to demonstrate the DFA spectrum of separation.

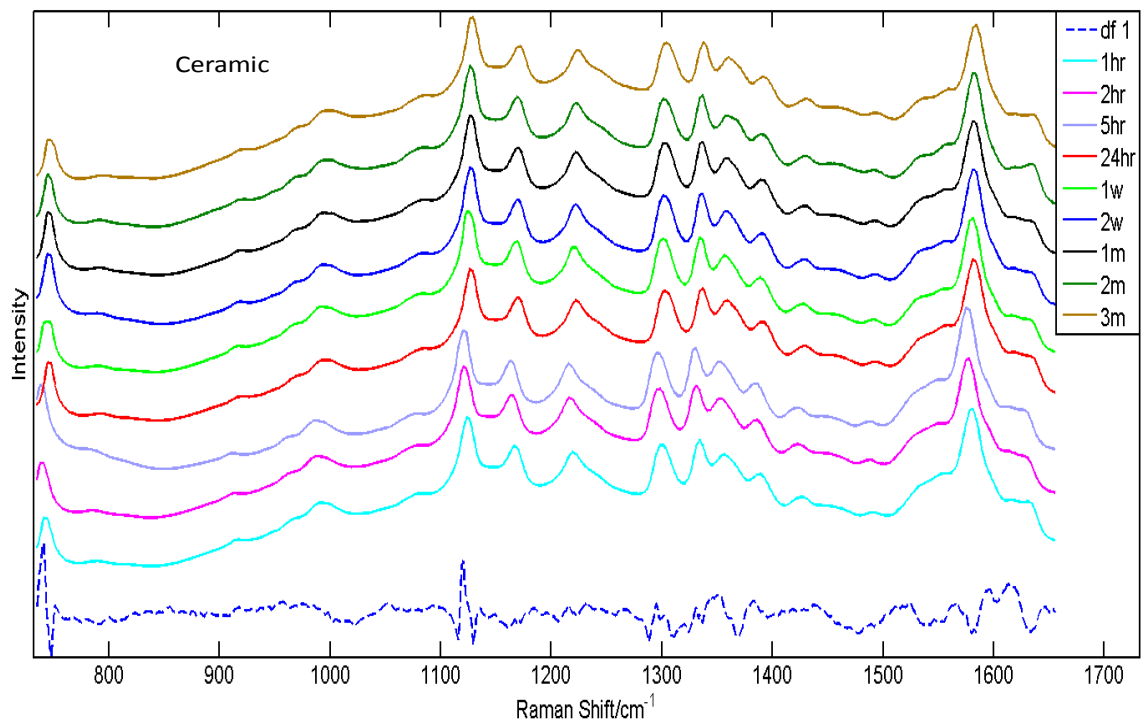


**Figure 36:** The mean 5<sup>th</sup> order polynomial spectra of blood on ceramic against DFA spectrum.

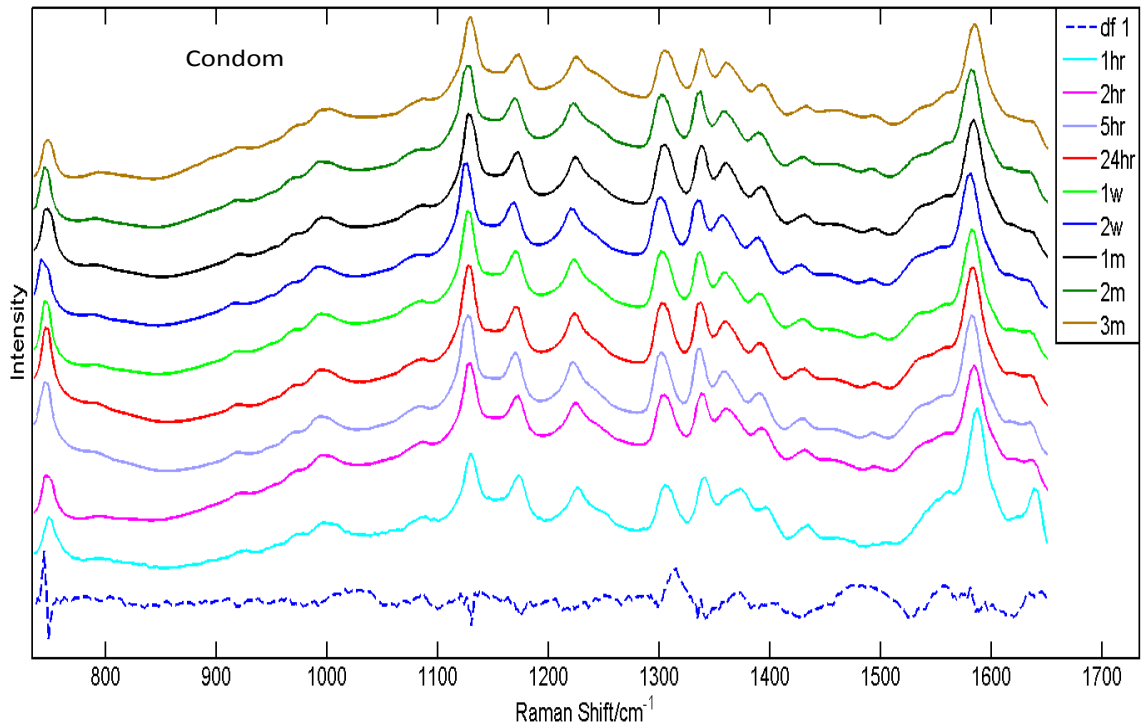


**Figure 37:** The mean 5<sup>th</sup> order polynomial spectra of blood on condom against DFA spectrum.

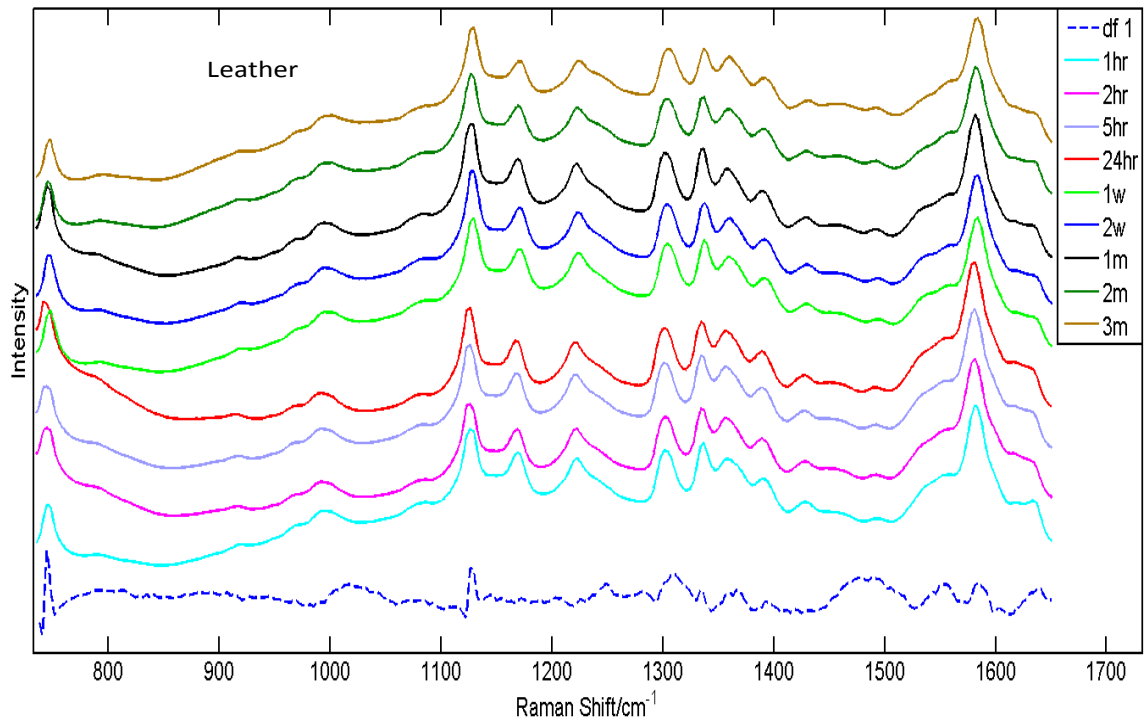


**Figure 38:** The mean 5<sup>th</sup> order polynomial spectra of blood on leather against DFA spectrum.

The large peak in the DFA spectrum at  $740\text{cm}^{-1}$  (tryptophan) indicates that the levels of tryptophan in the blood droplet vary over time. Additionally in Figures 36, 37 and 38 at 5hrs, 5hrs and 24hrs, and 24hrs respectively the  $740\text{cm}^{-1}$  peak shows a shift in the intensity. This could be explained by a chemical change which is happening to the tryptophan in the droplet or a greater fluorescence affecting the peak at these times. This shift could be and additional reason a large peak is apparent at  $740\text{cm}^{-1}$  in the DFA spectrum. There is also a DFA peak at  $1129\text{cm}^{-1}$  (glucose) which indicates that the levels of glucose in the blood droplets vary over time. There are also smaller peaks that can be seen in the DFA spectrum in all figures at  $1340\text{cm}^{-1}$ ,  $1587\text{cm}^{-1}$  and  $1640\text{cm}^{-1}$ . These peaks relate to tryptophan, haemoglobin and haemoglobin respectively and suggest that the levels of these components vary over time. Although the DFA spectrum shows the peaks where changes in the spectrum of blood occur, these changes are still not 100% clear to see. Additionally, there are shifts in the peaks at these positions at different times and (although this study is not analysing the changes in peak shifts) it is interesting to note that these could be producing the peaks in the DFA spectrum. Therefore further analysis to see the changes between early and late spectra is required.

#### **4.5 5<sup>th</sup> Order Polynomial Fit Early Against Late Spectra**

To visualise these changes in the blood spectrum over time mean early and late times for each substrate were then compared against the DFA spectrum. Three substrates were chosen to present here which demonstrate the best and clearest separation between early and late times (**Figures 39-41**).

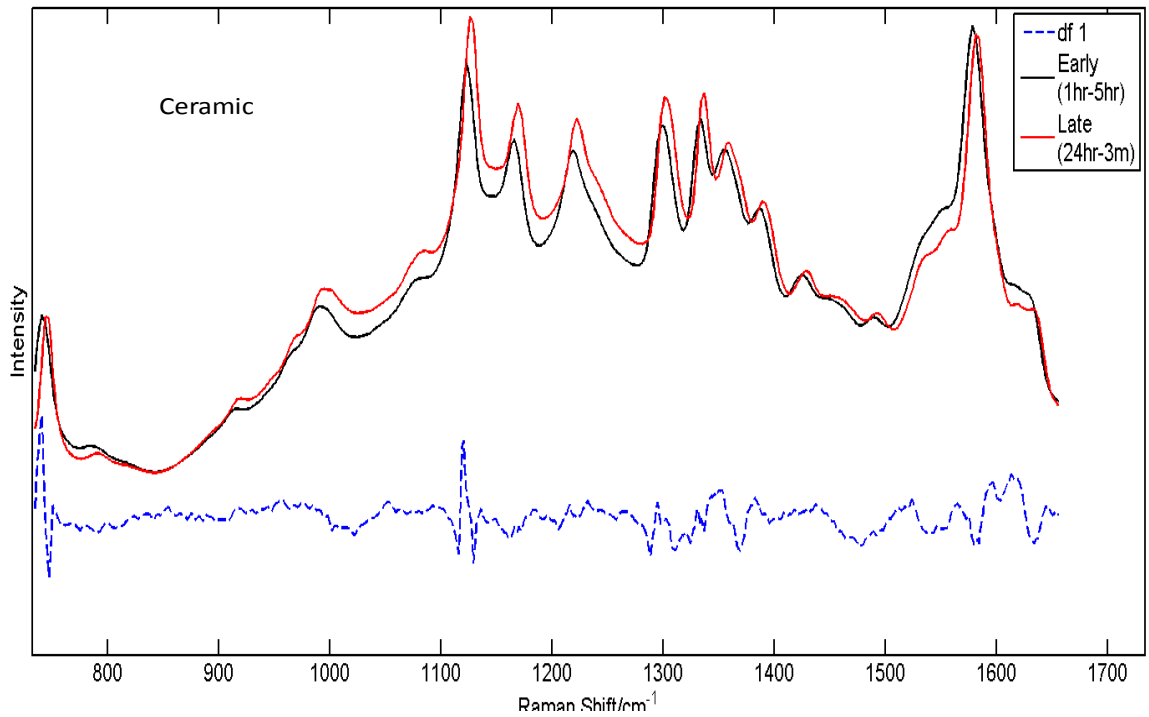


**Figure 39:** The mean early and late spectra of blood on ceramic against DFA spectrum.

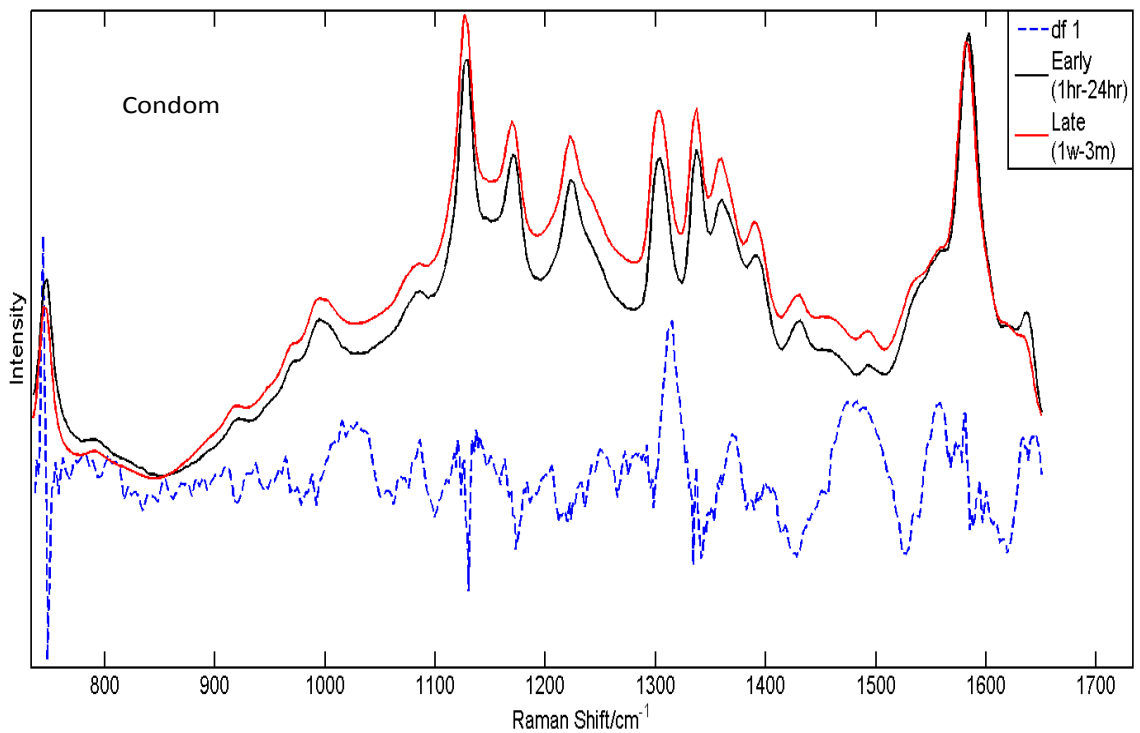


**Figure 40:** The mean early and late spectra of blood on condom against DFA spectrum.

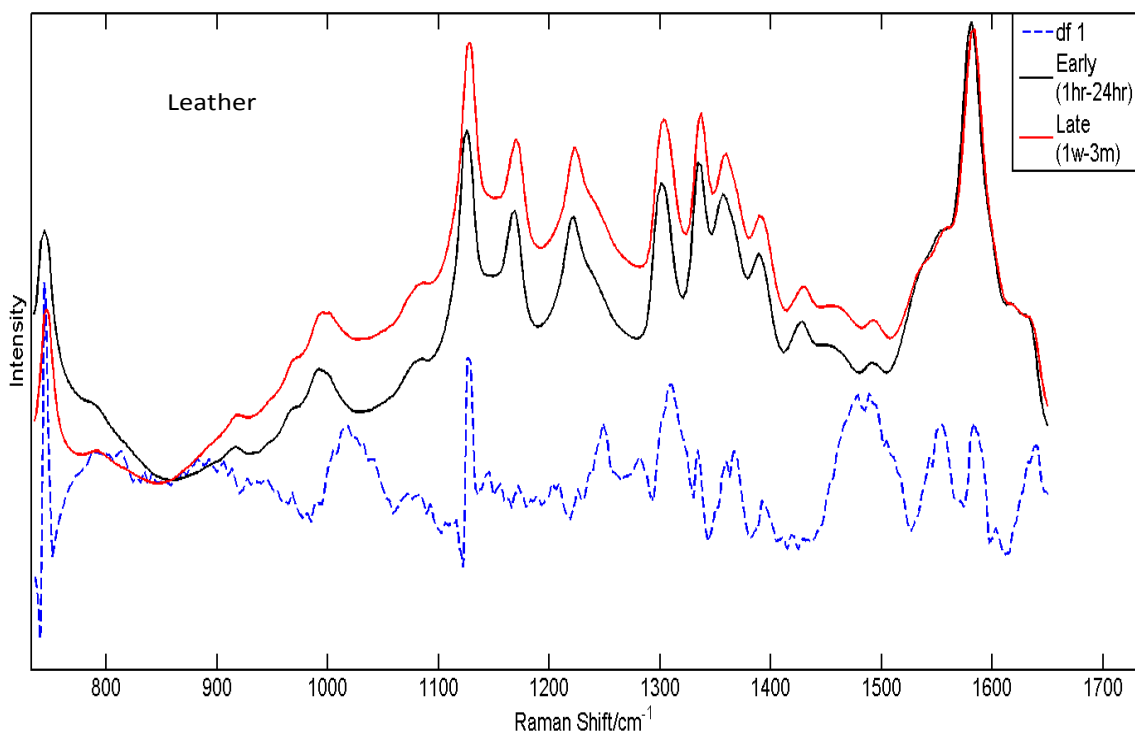


**Figure 41:** The mean early and late spectra of blood on leather against DFA spectrum.

The DFA peak at  $740\text{cm}^{-1}$  could correspond to the early spectrum having a higher intensity of tryptophan over the late spectrum. This decrease in intensity suggests that after 24hrs there is a decrease in the tryptophan present in the blood droplet. This trend was seen on all substrates except silicon which showed an increase in intensity for the late spectrum. **Figure 41** (leather) has the greatest decrease in tryptophan from early to late time points out of all the substrates. This exception for silicon suggests a substrate effect. However, this DFA peak could have also been caused by a shift in the  $740\text{cm}^{-1}$  peak (particularly Figure 39). Therefore, further research would have to be carried out.

The DFA peak at  $1129\text{cm}^{-1}$  could correspond to the late spectrum having a greater intensity of glucose over the early spectrum on ceramic, condom and leather. This suggests that there is an increase of glucose in the blood droplet after 24hr. This trend was replicated on laminate and silicon however on denim early times had a higher intensity than late time points. This exception of denim suggests a substrate effect.

However a shift in the  $1125\text{cm}^{-1}$  peak in Figure 39 could also contribute to the DFA peak.

The DFA peak at  $1362\text{cm}^{-1}$  could correspond to a change in haemoglobin. In **Figure 39** (ceramic) the early spectrum has a higher intensity than the late spectrum which relates to haemoglobin degradation over time. This is replicated on denim and laminate substrates. However, in **Figure 40, 41** (condom and leather), the late spectrum has a higher intensity than the early spectrum which does not relate to haemoglobin degradation over time. This is replicated on silicon. There is a shift in the  $1362\text{cm}^{-1}$  peak in Figure 39 which could contribute to the DFA peak.

The DFA peaks at  $1587\text{cm}^{-1}$  and  $1640\text{cm}^{-1}$  could also correspond to a change in haemoglobin. The early spectrum had a higher intensity than the late spectrum on ceramic and condom substrates (**Figures 39, 40**). This was replicated by silicon and denim substrates. However, the late spectrum had a greater intensity than the early spectrum at  $1640\text{cm}^{-1}$  on leather substrate (**Figure 41**). Additionally, the late spectrum had a greater intensity than the early spectrum at  $1587\text{cm}^{-1}$  on laminate substrate. Again there is a shift in the  $1587\text{cm}^{-1}$  peak in Figure 39 which could contribute to the DFA peak.

Overall, these results demonstrate that for the majority of peaks late spectra has a greater intensity than early spectra. However, peaks at  $1587\text{cm}^{-1}$  and  $1640\text{cm}^{-1}$  are the exceptions as early spectra has a higher intensity than late for the majority. These results prove that ageing does have an effect on the Raman spectrum of blood. They also prove that haemoglobin degradation does occur over time. However, peak shifts occur in **Figure 39** which could contribute to the peaks seen in the DFA spectrum. Therefore, analysis would have to be carried out to determine whether the DFA peaks are caused

by peak intensities alone. Finally, in practice this provides good evidence that a rough time frame can be determined for blood found at the crime scene.

#### 4.6 2<sup>nd</sup> Order Derivative DFA Plots

2<sup>nd</sup> order derivative was performed on the raw data as a second pre-processing technique to be compared with 5<sup>th</sup> order polynomial fit. Firstly the raw data was cut ( $\leq 735\text{cm}^{-1}$  and  $\geq 1650\text{cm}^{-1}$ ) leaving the region corresponding to blood. 2<sup>nd</sup> order derivative and vector normalisation were then carried out after cutting. **Figures 42-44** have been selected here to represent the 2<sup>nd</sup> order pre-processing technique. Additionally the leather and ceramic substrates have been selected again so the results from the two pre-processing techniques can be compared against each other.

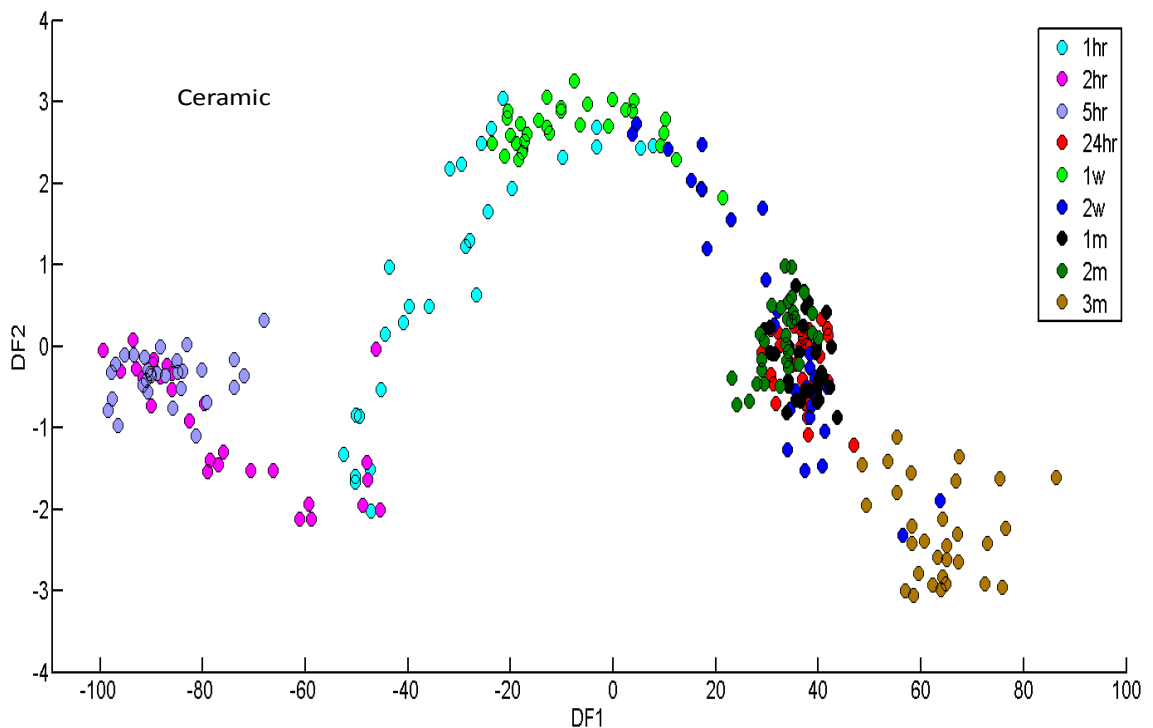


**Figure 42:** 2<sup>nd</sup> order derivative DFA plot of blood on ceramic.

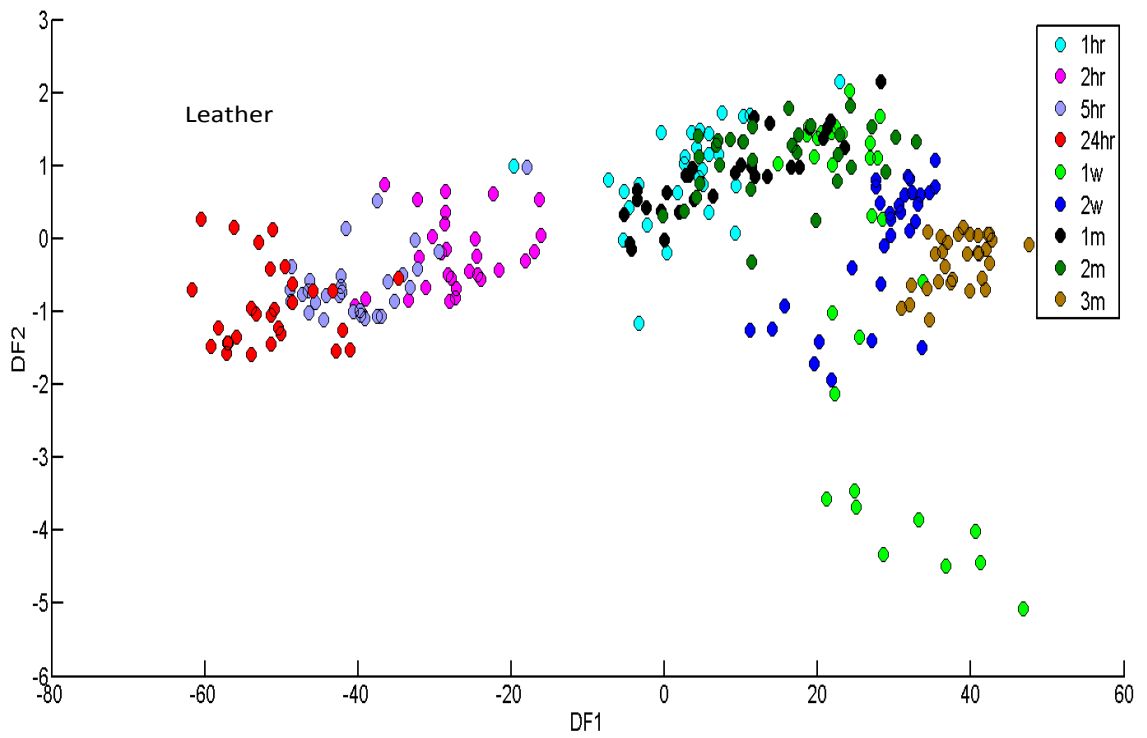


**Figure 43:** 2<sup>nd</sup> order derivative DFA plot of blood on leather.

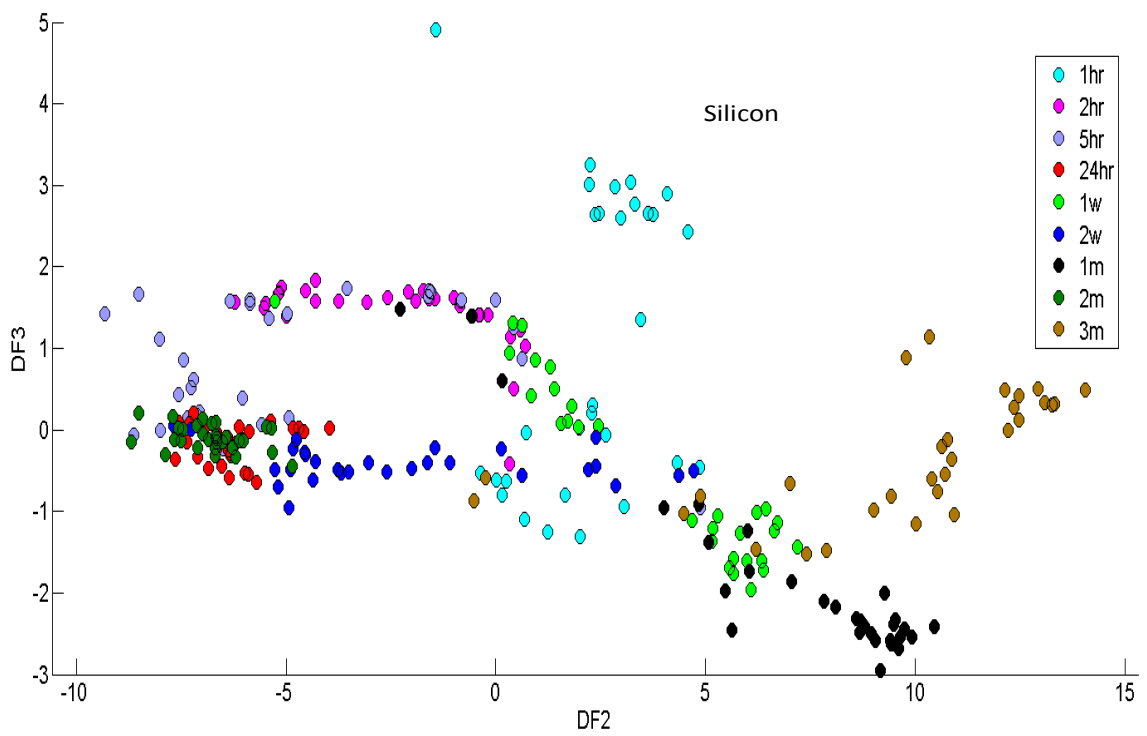


**Figure 44:** 2<sup>nd</sup> order derivative DFA plot of blood on crystalline silicon.

On ceramic (**Figure 42**) there is some clear grouping of time points and there is a slight shift pattern of early to late time points from left to right. However, 1hr time points are interspersed within late times and 24hr is grouped fully with late time points.

On leather substrate (**Figure 43**) there is clear separation of early time points (excluding 1hr) from late time points along DF1 axis, however, 1hr is grouped with late time points.

On silicon substrate (**Figure 44**) there is no clear separation between early and late time points along the DF2 axis. There is also no clear shift pattern over time and points within their own time frame are widely spread out.

Overall, the 2<sup>nd</sup> order derivative DFA scatter plots on ceramic, leather and silicon have unclear separation between early and late time points. This is also replicated on denim, condom and laminate with denim showing no separation between early and late time points. At this stage, 5<sup>th</sup> order polynomial fit is the better pre-processing technique when analysing the separation between early and late time points. Mean 2<sup>nd</sup> derivative spectra of blood on substrates were plotted against DFA separation spectrum (**Figure 45-47**).

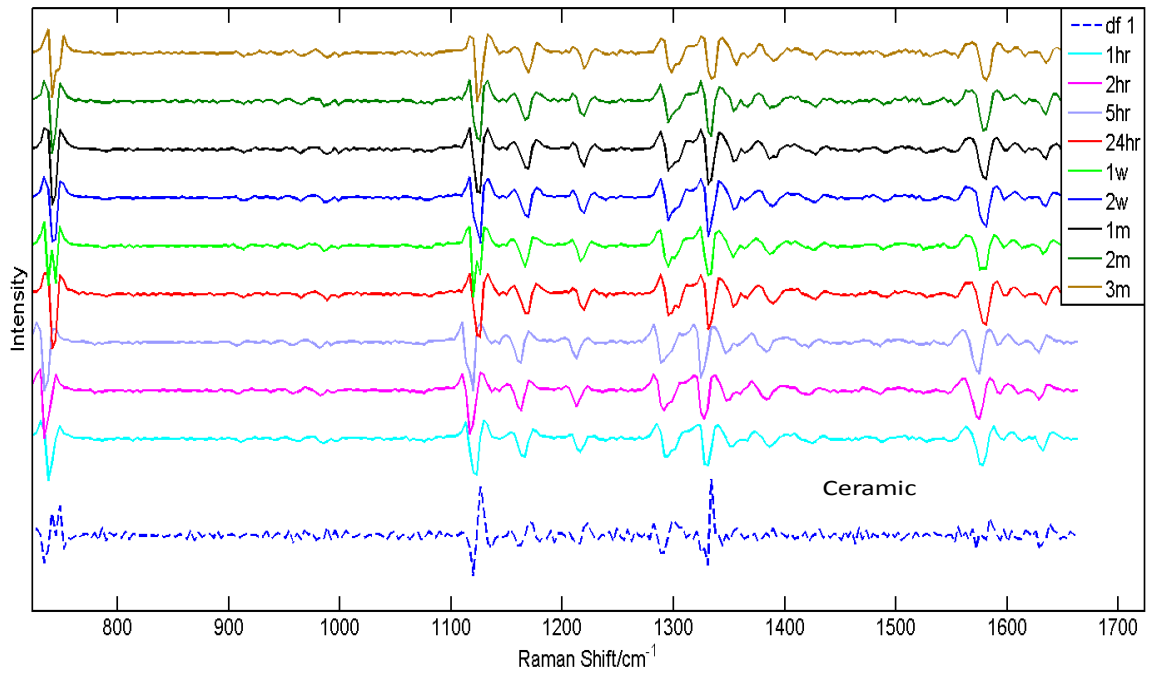


**Figure 45:** Mean 2<sup>nd</sup> order derivative spectra of blood on ceramic against DFA spectrum.

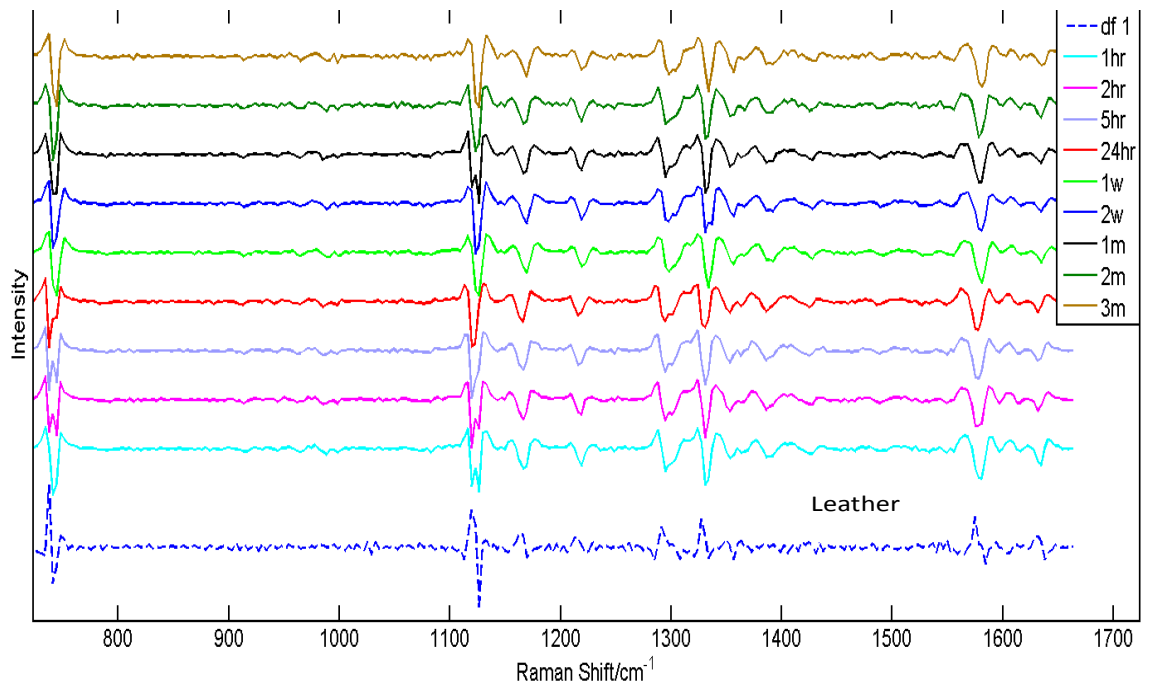


**Figure 46:** Mean 2<sup>nd</sup> order derivative spectra of blood on leather against DFA spectrum.

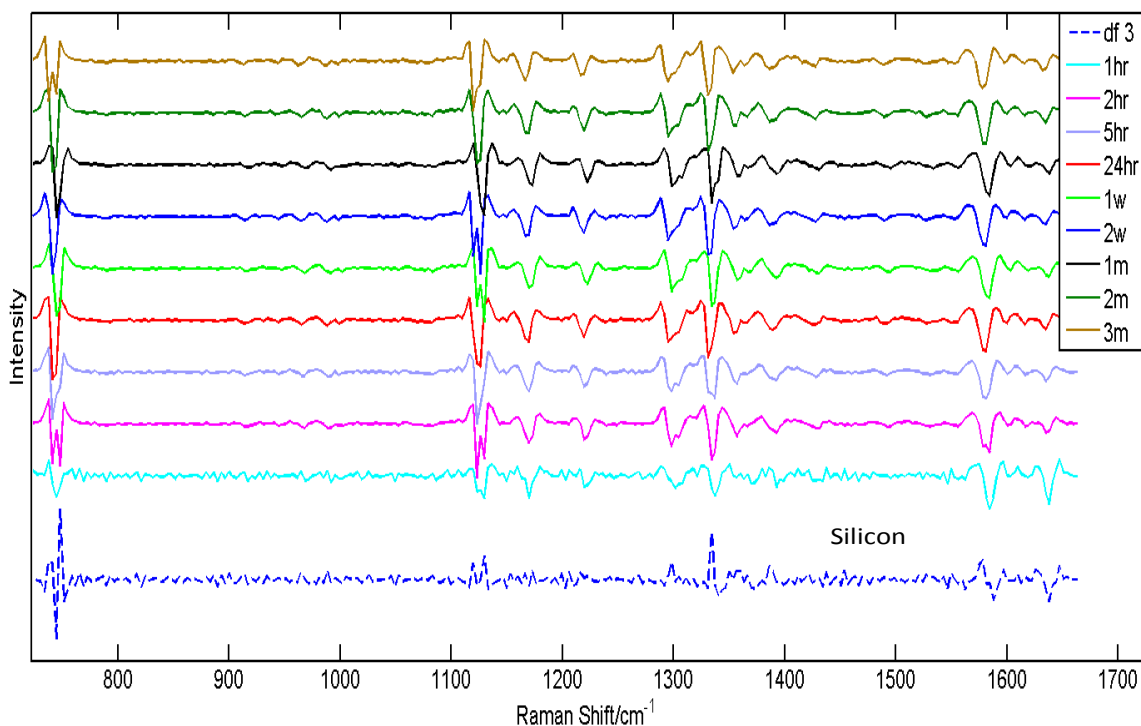


**Figure 47:** Mean 2<sup>nd</sup> order derivative spectra of blood on silicon against DFA spectrum.

The peaks in the DFA spectrum correspond to changes in the mean spectra over time. The DFA spectrum on ceramic (**Figure 45**) shows clear peaks at 740cm<sup>-1</sup> (tryptophan), 1125cm<sup>-1</sup> (glucose) and 1340cm<sup>-1</sup> (tryptophan). DFA peaks at these points could suggest that there is a variation in the amount of the component related to that peak. There are clear changes at these peaks, however, there appears to be no clear pattern from ≤1hr-3m. Additionally, a shift at these points can be seen after 5hrs which could contribute to the corresponding DFA peaks.

The DFA spectrum on leather (**Figure 46**) shows clear peaks at 740cm<sup>-1</sup> (tryptophan), 1125cm<sup>-1</sup> (glucose) and 1587cm<sup>-1</sup> (haemoglobin). DFA peaks at these points suggest that there is a variation in the amount of the component related to that peak. There are clear intensity changes in these peaks however there appears to be no clear pattern from

≤1hr-3m. Additionally, a shift at these points can be seen after 24hrs which could contribute to the corresponding DFA peaks.

The DFA spectrum on silicon (**Figure 47**) shows clear peaks at  $740\text{cm}^{-1}$  (tryptophan),  $1125\text{cm}^{-1}$  (glucose),  $1340\text{cm}^{-1}$  (tryptophan),  $1587\text{cm}^{-1}$  (haemoglobin) and  $1640\text{cm}^{-1}$  (haemoglobin). DFA peaks at these points suggest that there is a variation in the amount of the component related to that peak. There are clear intensity changes in these peaks, however, there appears to be no clear pattern from ≤1hr-3m. Again, a shift at these points can be seen after 24hrs which could contribute to the corresponding DFA peaks.

Similar DFA peaks as seen for ceramic were also seen on laminate and condom. Denim also showed similar peaks however they were unclear.

Overall, intensity changes can be seen in the spectra at different time points. Also, the 2<sup>nd</sup> order derivative DFA spectrum shows clearer peaks than the 5<sup>th</sup> order polynomial DFA spectrum. However, the changes seen in the spectra do not fit a pattern overtime whereas a clear decrease in intensity could be seen over time in the 5<sup>th</sup> order polynomial spectra. At this point, 5<sup>th</sup> order polynomial appears to be the better pre-processing technique. Shifts at main peaks can also be seen after 5hrs/24hrs which could have also contributed to the DFA peaks or fully contributed to these peaks. However further analysis of whether intensity or shifts have caused the DFA peaks.

#### **4.7 2<sup>nd</sup> Order Derivative Early Against Late Spectra**

The early and late time spectra were plotted against DFA spectra to compare the separation between the two (**Figures 48-50**). Three substrates demonstrated here show the clearest separation between the early and late spectra at the main blood peaks.

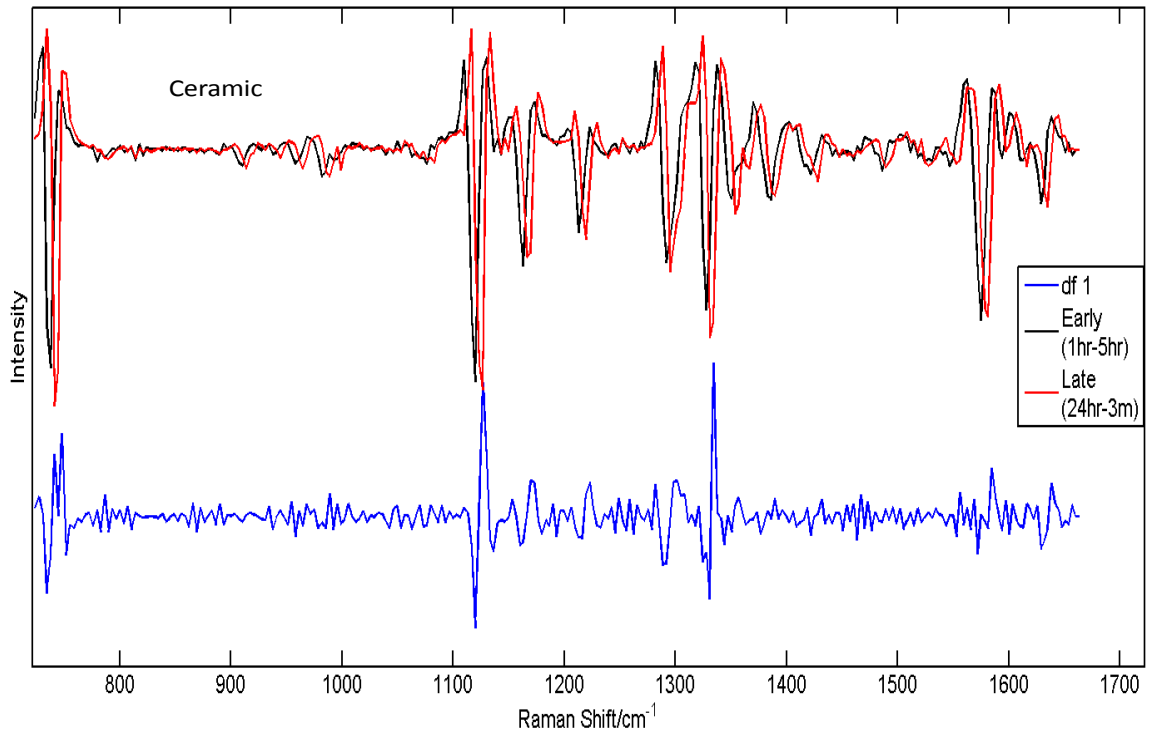


**Figure 48:** The mean early and late spectra of blood on ceramic against DFA spectrum.

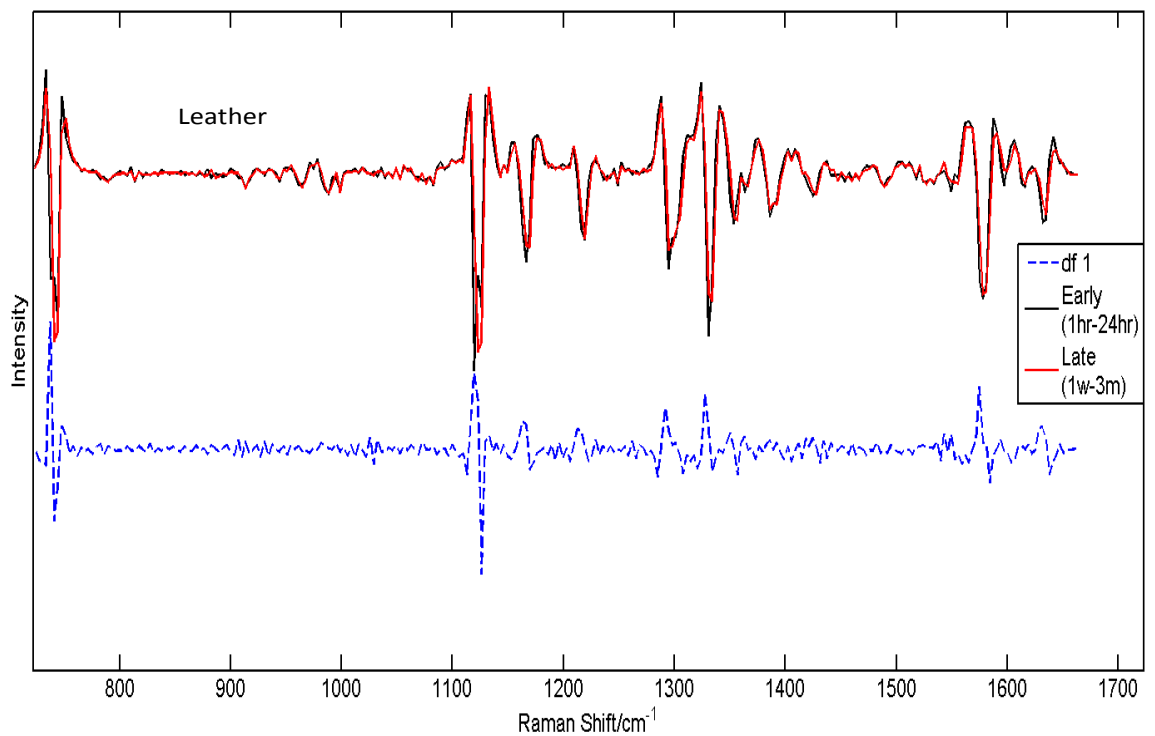


**Figure 49:** The mean early and late spectra of blood on leather against DFA spectrum.

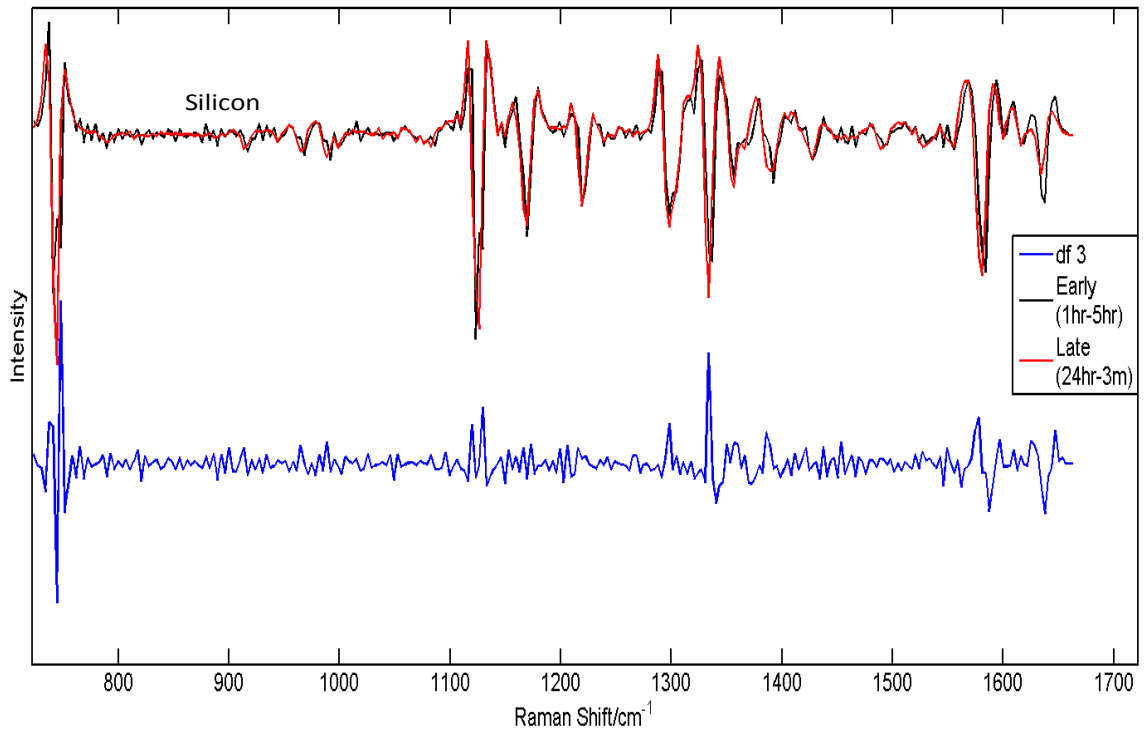


**Figure 50:** The mean early and late spectra of blood on silicon against DFA spectrum.

For ceramic substrate (**Figure 48**) the DFA peaks at  $735\text{cm}^{-1}$ ,  $1125\text{cm}^{-1}$ ,  $1340\text{cm}^{-1}$  could correspond to the late spectrum having a greater intensity than the early spectrum. The small DFA peak at  $1587\text{cm}^{-1}$  could correspond to the early spectrum having a slightly greater intensity than the late spectrum. The small peak at  $1640\text{cm}^{-1}$  could correspond to the late spectrum having a slightly greater intensity than the early spectrum. Overall, the mean 2<sup>nd</sup> order derivative spectra of early and late times of blood on ceramic do not comply with the degradation of a blood droplet over time. Additionally, there is a great shift of spectrum from early to late. This correlates with the shifts seen at the peaks after 5hrs (Figure 45). This shift could contribute to the DFA peaks.

For leather substrate (**Figure 49**) the DFA peak at  $735\text{cm}^{-1}$  could correspond to the late spectrum having a greater intensity than the early spectrum. The DFA peaks at  $1125\text{cm}^{-1}$ ,  $1340\text{cm}^{-1}$ ,  $1587\text{cm}^{-1}$  and  $1640\text{cm}^{-1}$  could correspond to the early spectrum having a greater intensity than the late spectrum. Overall, the mean 2<sup>nd</sup> order derivative spectra of

early and late times of blood on leather do comply with the degradation of a blood droplet over time.

For silicon substrate (**Figure 50**) the DFA peaks at  $735\text{cm}^{-1}$ ,  $1340\text{cm}^{-1}$ ,  $1587\text{cm}^{-1}$  could correspond to a greater intensity of the late spectrum than the early spectrum. DFA peaks at  $1125\text{cm}^{-1}$ ,  $1640\text{cm}^{-1}$  could correspond to a greater intensity of the early spectrum than the late spectrum. In particular, the peak at  $1640\text{cm}^{-1}$  shows a great difference in intensity between the two spectra. Overall, the mean 2<sup>nd</sup> order derivative spectra of early and late times of blood on silicon do not comply with the degradation of a blood droplet over time.

Of the other substrates, early spectrum showed greater intensity than late spectrum for the majority of DFA peaks on denim and condom which comply with the degradation of a blood droplet over time. However, the late spectrum showed greater intensity than early spectrum for the majority of DFA peaks on laminate which does not comply with the degradation of a blood droplet over time.

Overall, 2<sup>nd</sup> order derivative DFA data of early against late spectra show that late spectra has a greater intensity than early spectra for the majority of blood peaks. However, early spectra do have a greater intensity than late spectra for peaks at  $1587\text{cm}^{-1}$  and  $1640\text{cm}^{-1}$ . This supports haemoglobin degradation. Additionally, a shift can be seen from early to late spectra which could contribute to the DFA peaks as well as a change in intensity. These results show that ageing does have an effect on the Raman spectrum of blood.

## 4.8 Conclusions

In summary, the spectrum of blood on six substrates has been analysed over a period of time from  $\leq 1$ hr to 3m. Two different pre-processing techniques have been carried out to enhance visualisation and comparison of the spectra. The results demonstrate that for the majority of main peaks which correspond to blood there is a general increase in intensity and some peak shifts from early to late times. This does not fit with the prediction before analysis that the intensity of the main peaks would decrease over time due to blood degradation. However, focusing specifically on the  $1587\text{cm}^{-1}$  and  $1640\text{cm}^{-1}$  peaks, these are the exception to this and therefore do correspond to blood degradation overtime. Specifically, haemoglobin degradation.

Additionally, 2<sup>nd</sup> order derivative does allow some visualisation of the differences between the early and late spectra of blood on substrates. However, these differences are not always clear. Additionally, the 2<sup>nd</sup> order derivative spectra are quite noisy and this makes visualisation of the blood peaks difficult. Comparing the two pre-processing techniques, 2<sup>nd</sup> order derivative is a less suitable technique for visualising and comparing the spectrum of blood on substrates over time in comparison to 5<sup>th</sup> order polynomial fit. In practice using 2<sup>nd</sup> order derivative may result in a difficulty to clearly visualise the spectrum in a forensic context when analysing blood found at the crime scene. Additionally, the worst outcome that using 2<sup>nd</sup> order derivative would be to effect the characteristic blood peaks in a way that reduces the intensity of the peaks or creates a noisier spectrum.

Overall, this chapter has successfully demonstrated that changes in intensity do occur in the Raman spectrum of blood overtime. Additionally, shifts also occur in the Raman spectrum of blood overtime, the majority of these main shifts occur after 24hrs. These

shifts could also account for the DFA spectrum peaks which are seen as well as the changes in intensity. To identify the major contributor to the DFA peaks (shifts or intensity) further research would have to be carried out.

## CHAPTER 5

### INVESTIGATING THE EFFECT OF SUBSTRATE VARIATION ON THE RAMAN SPECTRUM OF EQUINE BLOOD

Raman spectroscopy is typically utilized as a qualitative and quantitative, molecular fingerprinting analytical technique. This chapter investigates Raman spectroscopy as a confirmatory technique for the identification of blood on different substrates and the effect substrate variation has on the Raman spectrum of blood. As prior use of PCA was ineffective at demonstrating clearly the separation between the time frames it was not used in this chapter of research. Therefore the first stage of analysis was DFA followed by comparing the spectra collected from each substrate at the different time frames. Additionally, 5<sup>th</sup> order polynomial fit was the only pre-processing technique used as this was preferred over 2<sup>nd</sup> order derivative when analysing and comparing the spectra.

#### 5.1 5<sup>th</sup> Order Polynomial Fit DFA Plots

The next figures demonstrate DFA plots (of blood on substrates) at three time frames presented along with the corresponding spectra (of blood on substrates) against the DFA spectrum (**Figures 51-56**). Three times showing the best separation and grouping of the substrates were chosen to present here. Additionally, the clearest spectra were chosen to present also.

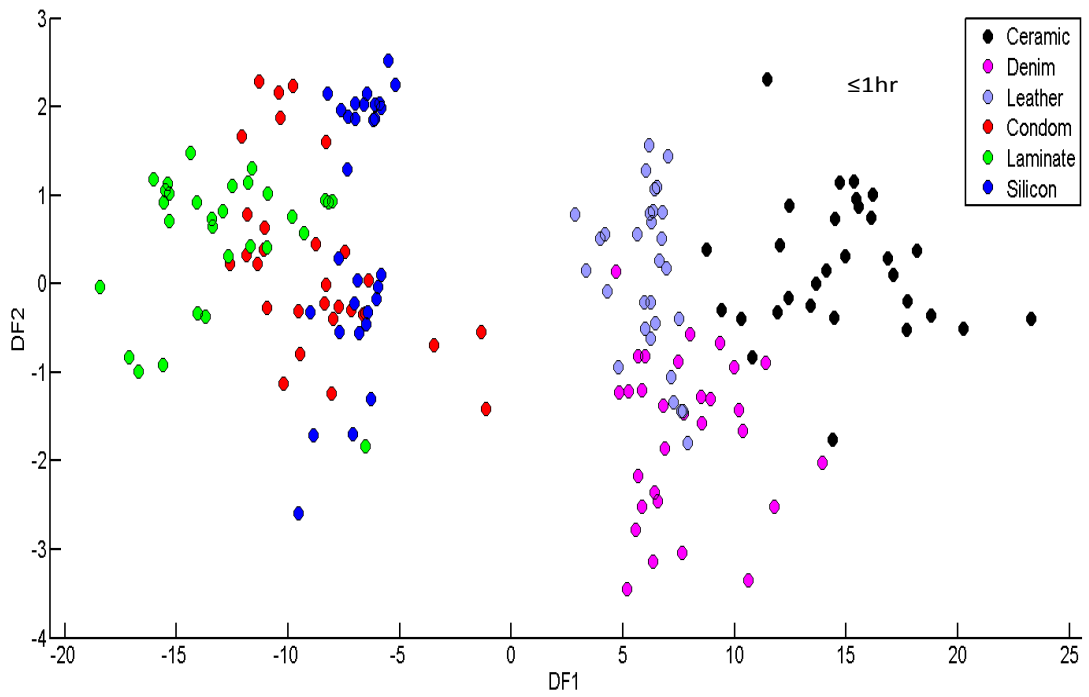


**Figure 51:** DFA plot of blood on substrates at  $\leq 1$ hr.

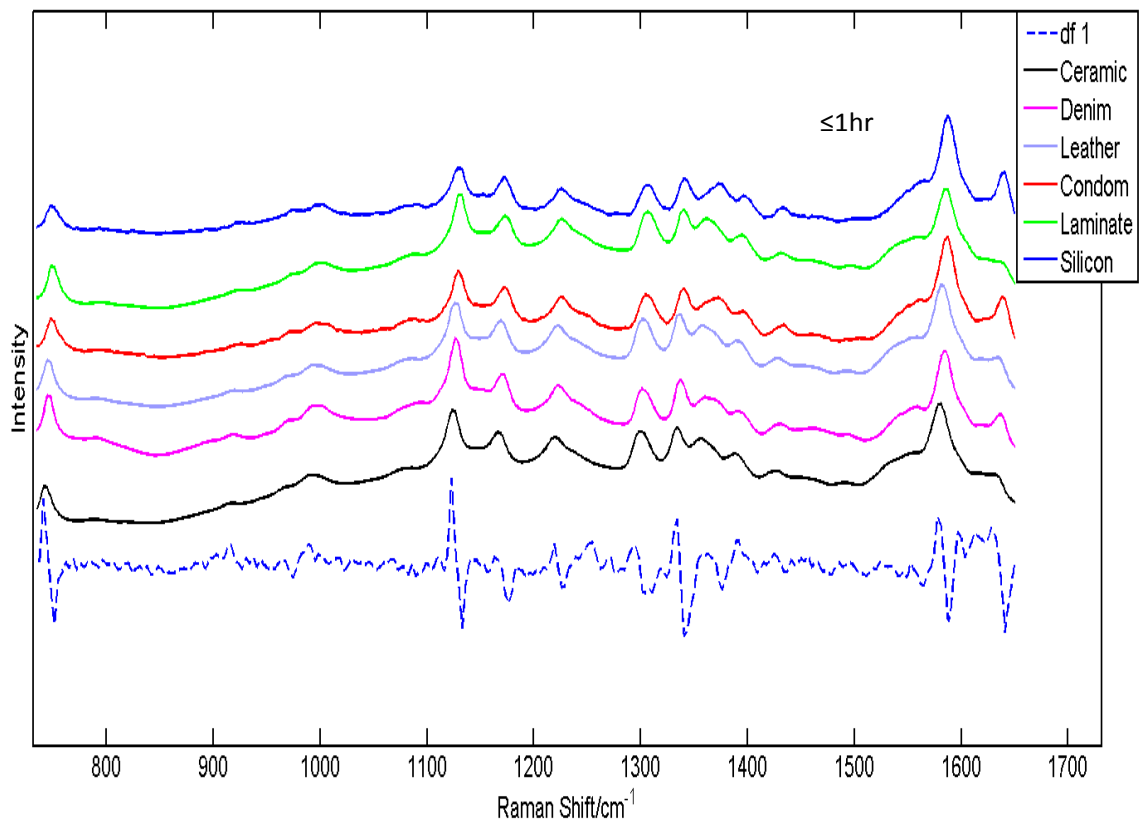


**Figure 52:** Mean 5<sup>th</sup> order polynomial Raman spectra of blood on substrates at  $\leq 1$ hr against DFA spectrum.

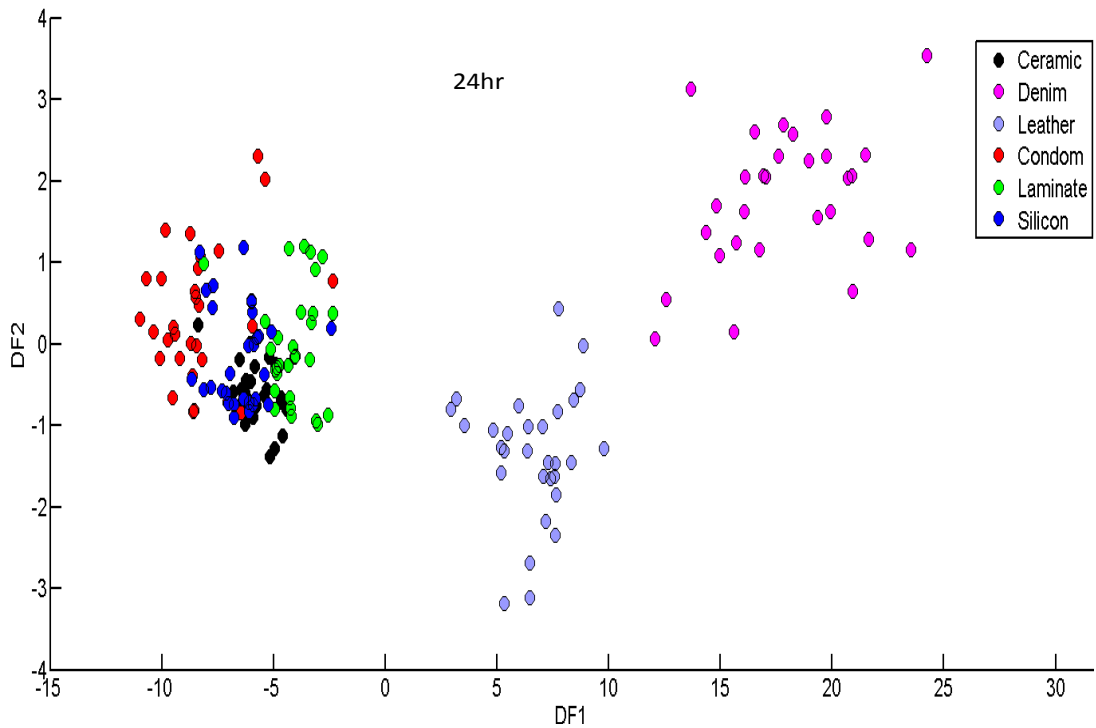


**Figure 53:** DFA plot of blood on substrates at 24hr.

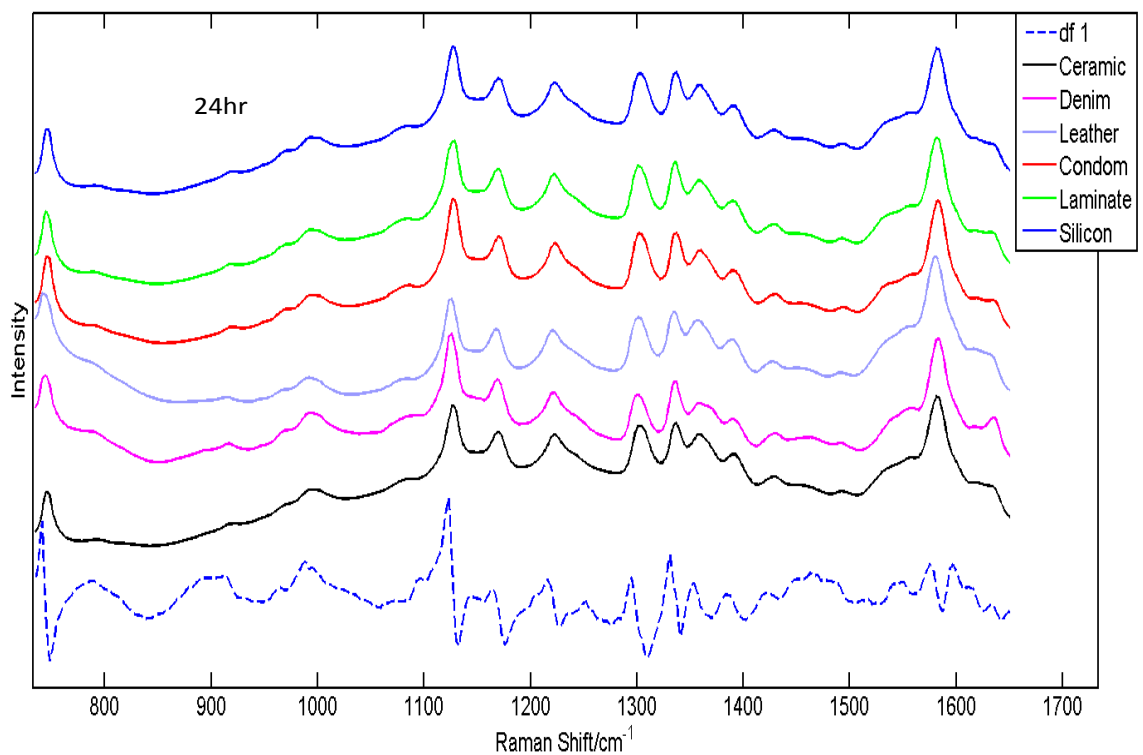


**Figure 54:** Mean 5<sup>th</sup> order polynomial Raman spectra of blood on substrates at 24hr against DFA spectrum.

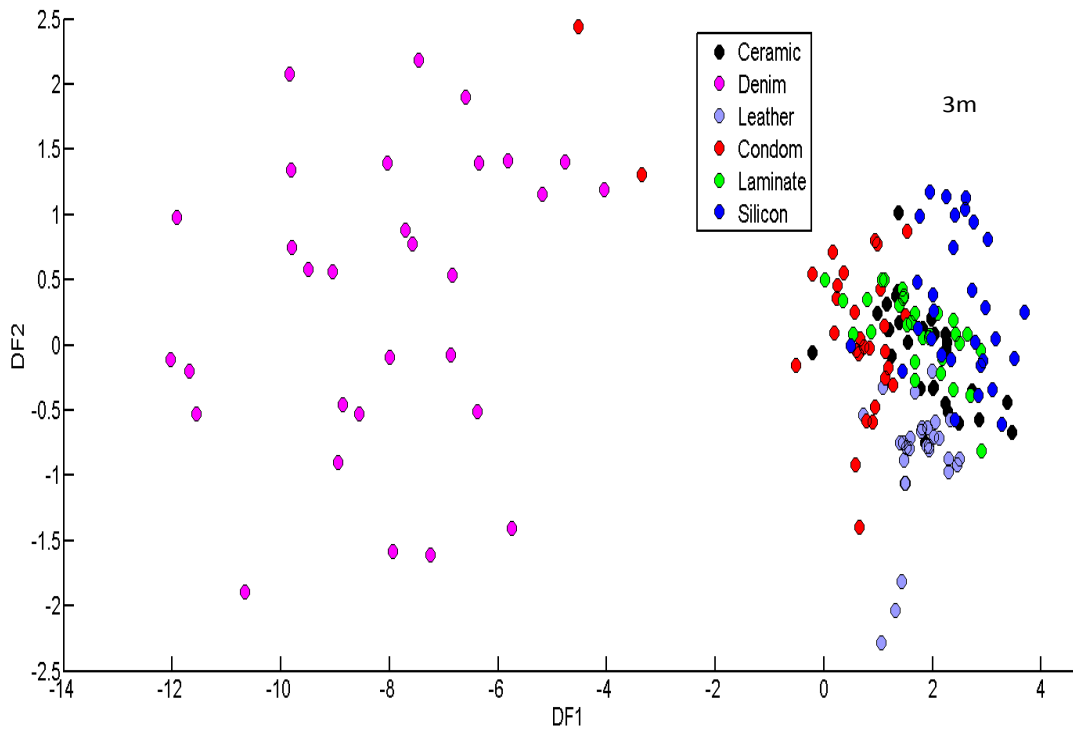


**Figure 55:** DFA plot of blood on substrates at 3m.

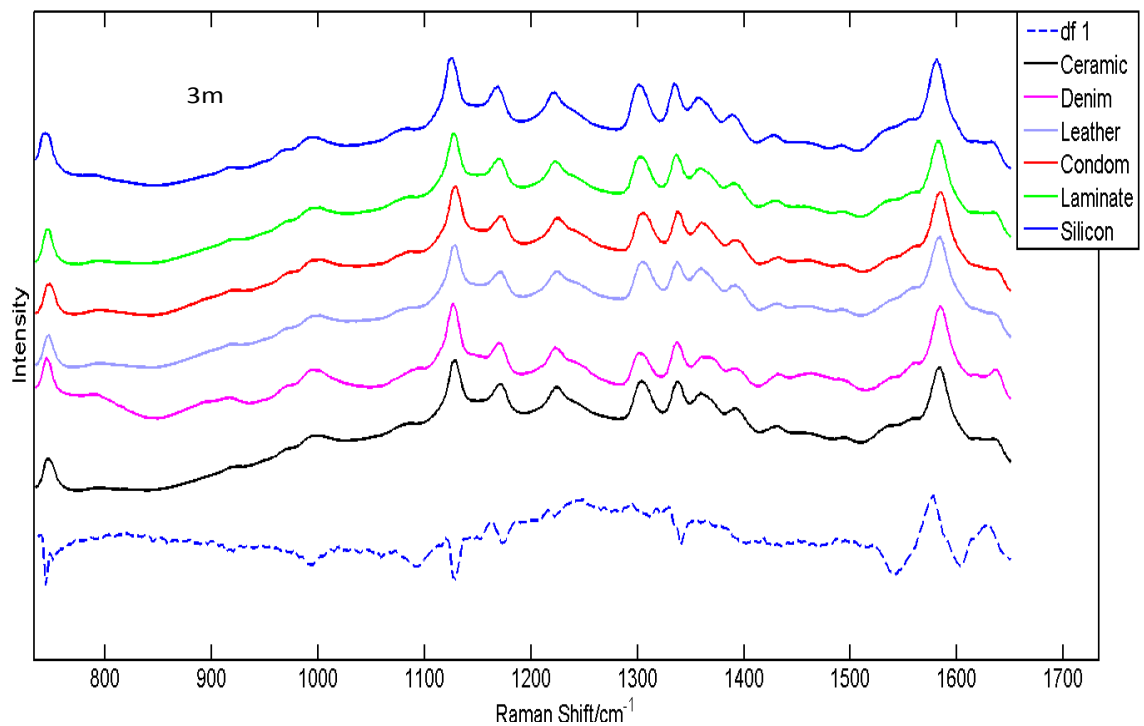


**Figure 56:** Mean Raman 5<sup>th</sup> order polynomial spectra of blood on substrates at 3m against DFA spectrum.

Grouping of ceramic, denim and leather and grouping of condom, laminate and silicon can be seen of blood at  $\leq 1$ hr (**Figure 51**). This suggests that these grouped substrates act on the blood droplet in the same way. DFA spectrum against substrate spectra at  $\leq 1$ hr (**Figure 52**) shows peaks at  $785\text{cm}^{-1}$ ,  $1125\text{cm}^{-1}$ ,  $1340\text{cm}^{-1}$ ,  $1587\text{cm}^{-1}$  and  $1640\text{cm}^{-1}$  which relate to tryptophan, glucose, tryptophan, haemoglobin and haemoglobin respectively.

These peaks at  $785\text{cm}^{-1}$ ,  $1125\text{cm}^{-1}$ ,  $1340\text{cm}^{-1}$  and  $1587\text{cm}^{-1}$  show some minor intensity changes across the different substrates although they are not major and are not visually clear. However, denim, condom and silicon have a greater intensity for the peak at  $1640\text{cm}^{-1}$  than ceramic, leather and laminate. The change in intensity of this peak is quite evident which suggests that haemoglobin decay is more rapid on ceramic, leather and laminate. Overall this does suggest that substrate variation does have an effect on the Raman spectrum of blood.

DFA plot of blood at 24hr (**Figure 53**) shows grouping of ceramic, condom, laminate and silicon. Denim and leather are separated from the rest of the substrates and each other. These plots suggest that at this time frame there is a similarity between the blood droplets on ceramic, condom, laminate and silicon. Additionally, it suggests that denim and leather have different effects on the blood droplets than the other substrates.

The peaks at  $785\text{cm}^{-1}$ ,  $1125\text{cm}^{-1}$ ,  $1340\text{cm}^{-1}$  and  $1587\text{cm}^{-1}$  show some minor intensity changes and shifts across the substrates at 24hr (**Figure 54**). However, similarly to the spectra of blood on substrates at  $\leq 1$ hr they are not major. The main visual change in the spectra is at peak  $1640\text{cm}^{-1}$  where denim shows a greater intensity in this peak than the other substrates. The change in intensity of this peak is quite evident and suggests that haemoglobin decay is more rapid on ceramic, leather, condom, laminate and silicon

than on denim. This could be due to the nature of denim as it absorbs the blood which may delay the decay of the droplet. There is obvious peak shifts particularly at  $747\text{cm}^{-1}$  for both Denim and Leather. The peak at  $747\text{cm}^{-1}$  is shifted higher up which could contribute to the DFA peak and the separation of these two substrates from the others seen in **Figure 53**. Additionally at this point the spectra appear to increase in intensity generally from  $\leq 1\text{hr}$ - $24\text{hr}$  which can be explained by an increase in fluorescence from the droplet and the substrates. Overall these findings suggest that substrate variation does have an effect on the Raman spectrum of blood.

DFA plot of blood at 3m (**Figure 55**) shows grouping of all substrates together excluding denim. These plots suggest that at this time frame there is a similarity between the blood droplets on ceramic, leather, condom, laminate and silicon. Additionally, it suggests that denim has a different effect on the blood droplets than the other substrates which again is more likely due to its retentive properties.

Peaks at  $785\text{cm}^{-1}$ ,  $1125\text{cm}^{-1}$ ,  $1340\text{cm}^{-1}$  and  $1587\text{cm}^{-1}$  now show little to no visual intensity changes in the spectra of blood across different substrates at 3m (**Figure 56**). The only clear visual intensity change which can be seen is at  $1640\text{cm}^{-1}$  where denim shows a greater intensity in comparison to the other substrates. This suggests that the haemoglobin degradation is more rapid on ceramic, leather, condom, laminate and silicon than denim. However, in comparison to 24hr the intensity of this peak on denim does decrease slightly. Again a clear shift in the peak  $747\text{cm}^{-1}$  can be seen for the Denim spectrum which could contribute to the peak in the DFA spectrum at this point and could also be the reason that Denim is separate from the others substrates in **Figure 55**. Overall this suggests that substrate variation does have an effect on the Raman spectrum of blood. Additionally, the general intensity of the spectra has increased again from 24hr which is caused by fluorescence from the droplet and the substrate.

Spectra of blood on substrates at other time frames show similar results. Early time points show more variation of the Raman spectrum of blood across different substrates and the peak at  $1640\text{cm}^{-1}$  is the most prominent. Late time points however show less to no variation of the Raman spectrum of blood across different substrates excluding  $1640\text{cm}^{-1}$  where Denim has a greater intensity than the other substrates.

## 5.2 Conclusions

In summary, using 5<sup>th</sup> order polynomial fit it is possible to see the variation of the spectrum across the substrates. Slight intensity changes can be seen at the peak positions  $785\text{cm}^{-1}$ ,  $1125\text{cm}^{-1}$ ,  $1340\text{cm}^{-1}$  and  $1587\text{cm}^{-1}$ . However the main differences across substrates are clearly noticeable at the peak position  $1640\text{cm}^{-1}$ . Notably, denim appears to reduce the degradation rate of haemoglobin compared to the other substrates. This could be due to the soaking effect of the denim material which shields the blood from the environment. Additionally, the background fluorescence of the spectra increases over time which is due to fluorescence from the droplet and the substrate. Finally, evident peak shifts (particularly at  $747\text{cm}^{-1}$ ) could contribute to the DFA peaks and why separation of the substrates is seen in the plots. Further research would have to be carried out to identify the contribution of both intensity and peaks shifts on the results. These results demonstrate that substrate variation does have an effect on the Raman spectrum of blood and suggests the more retentive the substance/material then the slower the degradation and therefore the greater the intensity of peaks overtime.

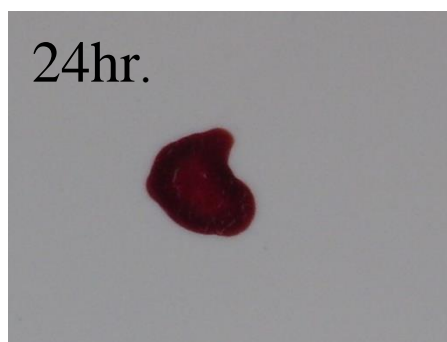
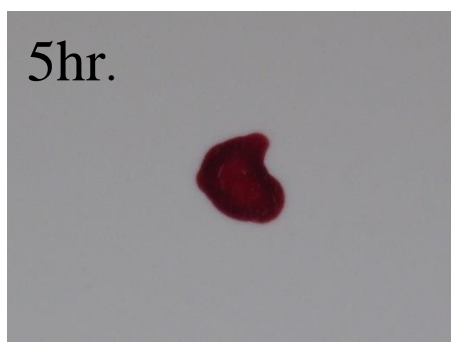
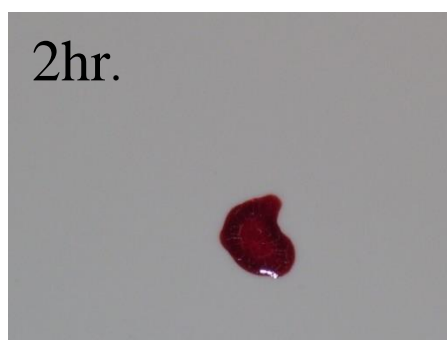
In practice, the spectrum corresponding to blood can be clearly and confidently visualised when using Raman spectroscopy to identify blood on a number of substrates. Denim substrate appears to allow for the best blood spectrum to be produced due to its compositional properties. Therefore in a crime scene situation, this is a significant result

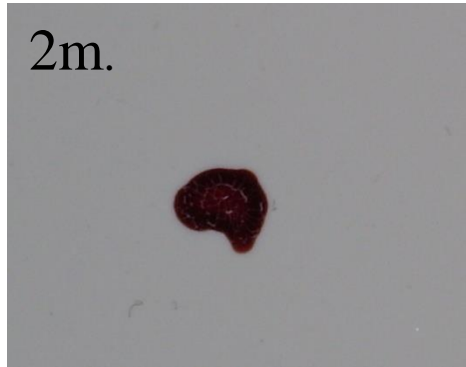
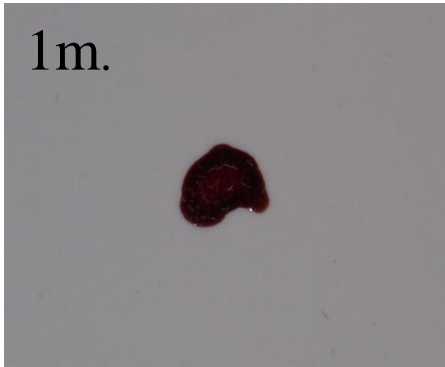
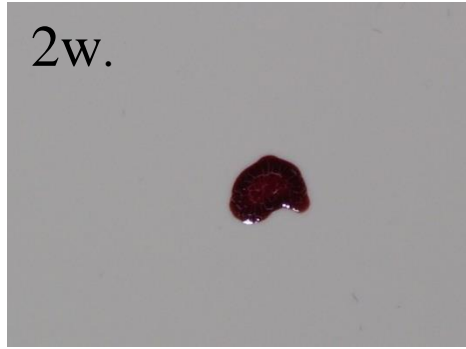
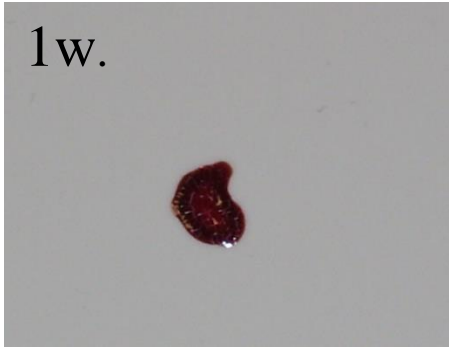
when denim jeans and other absorbent materials such as cotton and wool are involved in the crime.

## CHAPTER 6

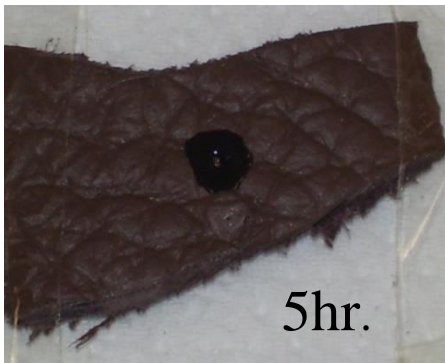
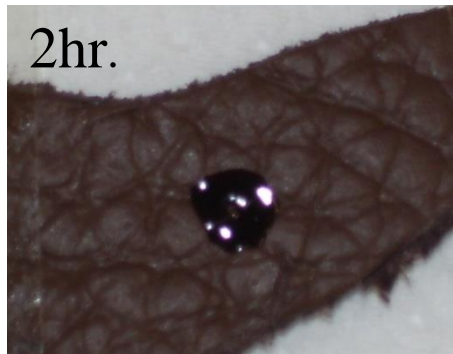
### INVESTIGATING THE EFFECT OF AGEING AND SUBSTRATE VARIATION ON THE RAMAN SPECTRUM OF BLOOD (PHOTO TIMELINE)

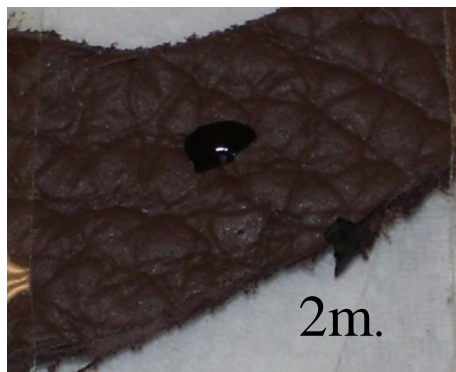
During the ageing and substrate studies of blood using Raman spectroscopy, photos were taken of the different stages of ageing on all substrates to provide a timeline of the blood droplets and to demonstrate the physical and visual changes that occurred. Three substrates which demonstrated the clearest changes were chosen to present here (**Figure 57-59**). Photos were taken on a Kodak EasyShare C433 digital camera (4.0 mega pixels), on an auto setting, in lab conditions under artificial lighting. Pictures were taken at a distance of ~150mm using the zoom lens in an attempt to produce clear photos.



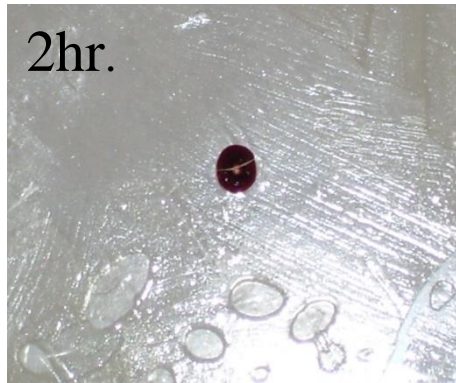
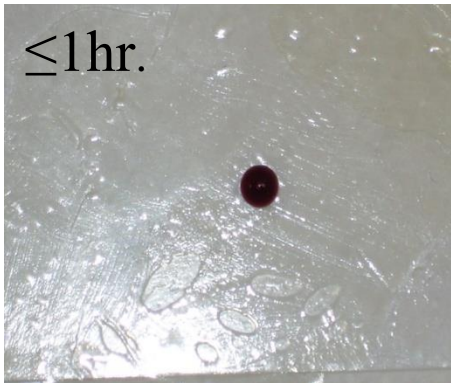


**Figure 57:** Photo timeline of blood on ceramic tile from  $\leq 1$ hr to 2m.





**Figure 58:** Photo timeline of blood on brown leather from  $\leq 1$  hr to 2m.



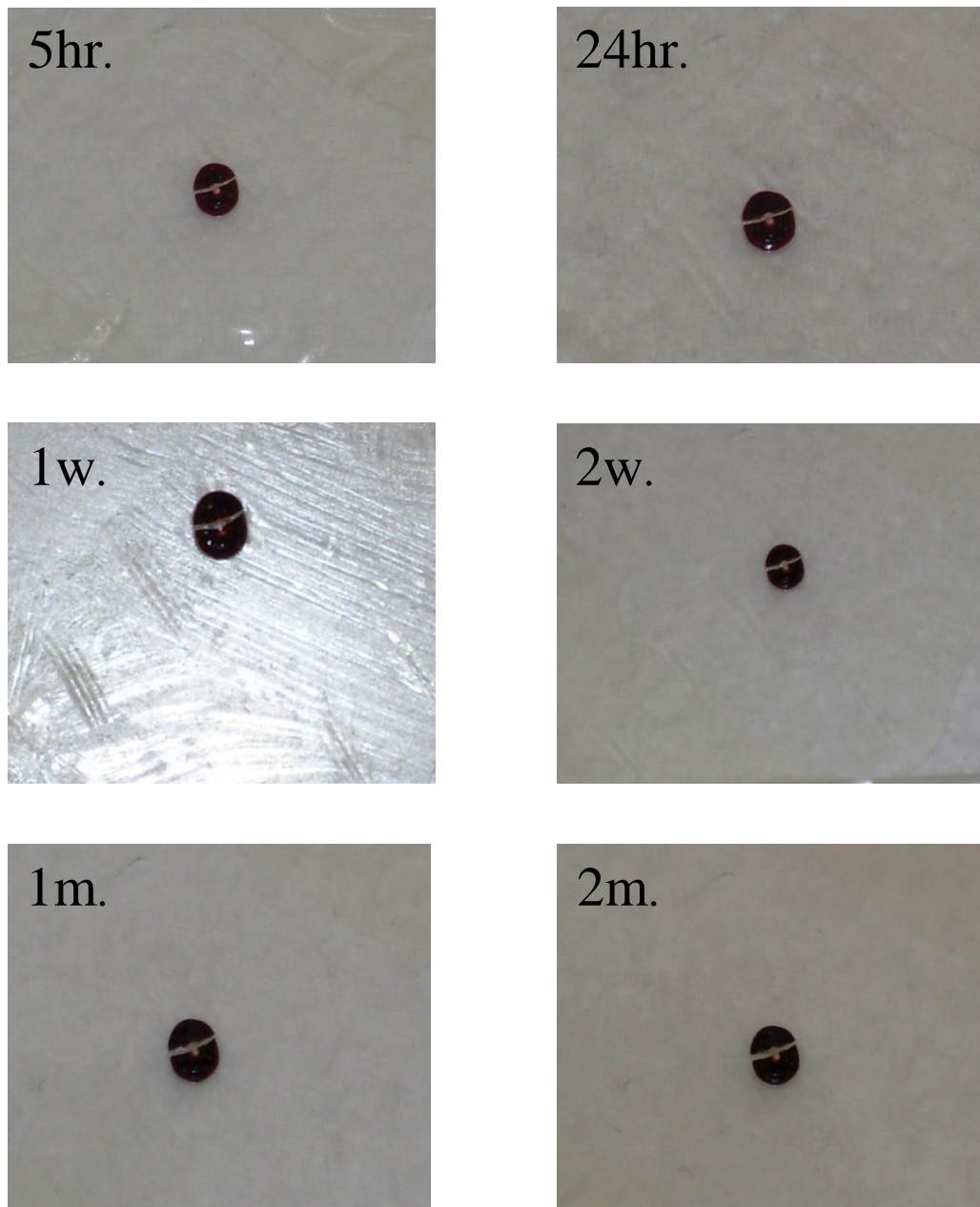


**Figure 59:** Photo timeline of blood on condom from  $\leq 1$ hr to 2m.

The blood droplet on ceramic (**Figure 57**) at  $\leq 1$ hr of ageing shows a vibrant red colour with an obvious wet composition. The droplet shape is convex with a contained boundary and does not soak readily into the ceramic substrate which would explain its shape. Additionally, the convex and bulbous shape of the droplet with a contained boundary demonstrates also the height at which the droplet was deposited (less than 5mm above the substrate surface). At 2hr there is an immediate drying of the droplet which can be seen. Although the vibrant red colour remains on the majority of the

droplet, there is now a darker red rim around the outer edge of the droplet which suggests this area is drying more rapidly than the rest. The shape of the droplet is slightly less bulbous but the boundary is still well contained. These characteristics are also seen at 5hr and 24hr of ageing and at these stages the droplet becomes drier, the vibrant red colour becomes darker (along with the rim around the edge), and the shape becomes less bulbous.

After 24hr the droplet becomes even darker in colour (more brown than red) and the rim around the edge becomes almost black. The shape is still well contained but the bulbous shape has reduced dramatically. The most notable change is that the droplet now shows very apparent cracks which suggests there is little to no moisture remaining. These cracks continue to become more apparent, and the droplet becomes darker to the point where parts are almost black (1w to 2m). Additionally, comparing  $\leq 1$ hr to 2m, the droplet has remained the same shape, however, the width and length has slightly increased which would explain the decrease in the bulbous shape of the droplet. 3m was not included because no apparent changes could be seen from 2m to 3m.

Overall, the droplet on ceramic has demonstrated clear physical and visual changes over time from  $\leq 1$ hr to 2m. These include a darkening in colour, increasing drying and cracking and a decrease in the bulbous shape. Additionally, a dramatic change in the droplet can be seen after 24hr which provides a separation between early and late time frames. These results suggest: that ageing does have an effect on the droplet and corresponds with the results demonstrated from the Raman spectra in particular the separation seen in the DFA plots and the separation between early and late spectra.

The blood droplet on leather (**Figure 58**) at  $\leq 1$ hr of ageing does not show the vibrant red colour which is seen on ceramic but is black and does demonstrate an apparent wet

composition. The shape however is again quite convex and bulbous with a contained, circular boundary. This again demonstrates that the leather substrate, like ceramic, does not readily absorb the blood. At 2hr and 5hr the droplet has become dry and the shape and colour have remained the same as at  $\leq 1$ hr. At 24hr the most notable change can be seen the droplet has begun to flake away from the substrate which suggests that at this point there is little to no moisture remaining in the droplet. This level of drying occurs earlier than on leather and suggests that the rate of drying has increased on the leather substrate. From 1w to 2m there is little change in the physical and visual appearance of the droplet, although a section of the droplet has been completely separated from the leather. 3m was not included because no apparent change could be seen between 2m and 3m.

Overall, the droplet on leather demonstrated clear visual and physical changes over time from  $\leq 1$ hr to 2m. These include an increase in drying and flaking in particular between 5hr and 24hr. These changes provide a separation between early and late time frames. These results suggest that ageing does have an effect on the droplet which corresponds with the results demonstrated from the Raman spectra. In particular the separation seen in the DFA plots and the separation between early and late spectra.

The blood droplet on condom (**Figure 59**) at  $\leq 1$ hr of ageing shows a dark red colour with a wet composition. The shape is also convex and bulbous with a well contained circular boundary. Between 2hr and 24hr the droplet dries and is separated down the middle with a crack. The droplet also becomes slightly darker and less bulbous in shape however the circular and contained shape remains. One of the biggest changes occurs after 24hr where the droplet becomes dark brown to black in colour and begins to flake away from the surface. This can be seen by the increase in margin of the gap between

the two halves. Between 1w and 2m there is little apparent change of the droplet. 3m was not included as there was no apparent change of the droplet between 2m and 3m.

Overall the droplet on condom demonstrated clear visual and physical changes overtime from  $\leq 1$ hr and 2m. These include a darkening of the droplet, a cracking, and a drying seen particularly between 24hr and 1w. These changes explain the separation between early and late time frames. These all suggest that ageing does have an effect on the droplet and corresponds with the results demonstrated from the Raman spectra. In particular the separation seen in the DFA plots and the separation between early and late spectra.

### 6.1 Blood on Denim-Photo Timeline

In this section, timeline photos of denim at  $\leq 1$ hr and 2m are included (**Figure 60**) to demonstrate the absorbent properties of denim.



**Figure 60:** Blood on blue denim at  $\leq 1$ hr and 2m.

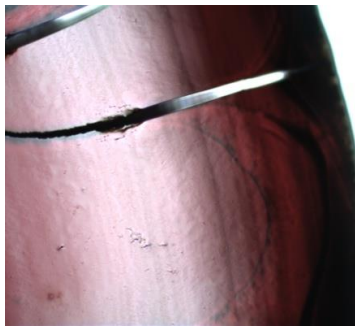
It is clear to see that blood is readily absorbed into the denim material (**Figure 60**). It is also clear to see that there is very little apparent difference between blood at  $\leq 1$ hr and 2m which suggests that the degradation rate of the blood droplet is dramatically reduced due to the denim substrate. This corresponds with the separation of denim DFA plots

from the other substrate DFA plots. This also corresponds to the larger intensity seen at the peak  $1640\text{cm}^{-1}$  (haemoglobin) for denim at 3m.

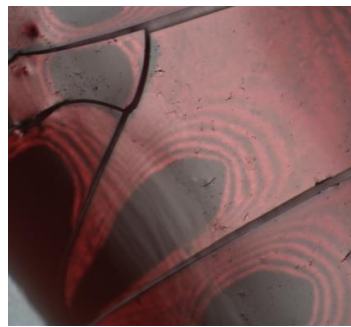
Blood on laminate showed very similar (physical and visual) changes to blood on leather and blood on silicon showed very similar (physical and visual) changes to blood on ceramic.

## 6.2 Raman Microscopic Images

This section presents images taken of blood on the substrates using the Raman microscope. These demonstrate the ability to locate and analyse the blood and the difference in substrate composition.



**Silicon**



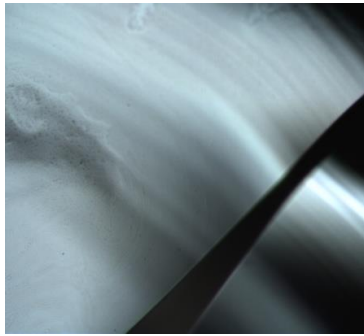
**Ceramic**



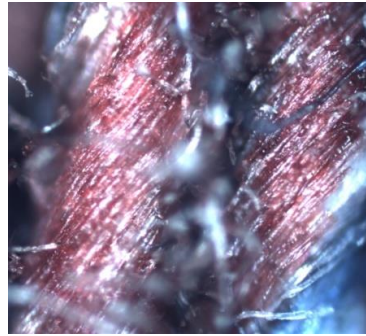
**Laminate**



**Condom**



**Leather**



**Denim**

**Figure 61:** Microscopic images of blood on substrates at 10x magnification.

Microscopic images (**Figure 61**) were taken at 10x magnification to show a greater area of blood and substrate. The images show how substrates can affect the blood droplet in size, shape and appearance. Notable, denim shows the greatest effect as blood is soaked into the cotton fibres. Additionally, the droplet and red colour can be easily distinguished on silicon, ceramic and laminate. However, the droplet is darker and harder to distinguish on condom and leather. Scans carried out on denim were difficult as the blood surface was hard to locate due to the intricacy of the fibres. Fluorescence from the fibres in denim was also a factor.

### 6.3 Conclusions

Overall the photo timeline of blood on the substrates from  $\leq 1$ hr to 2m has demonstrated that visual and physical changes do occur over time. This corresponds with changes seen in the Raman spectrum of blood across the time frames. The photo timeline also demonstrates clearly how blood can act differently on different substrates, in particular denim which soaks the blood into the fabric. This also corresponds to changes seen in the Raman spectrum of blood across the different substrates. Finally, microscopic images show how the substrate can affect the droplet and how the clarity of the blood droplet can vary across the substrates.

In practice, the visual and physical changes of the blood droplet (over time and across the different substrates) demonstrate how it is difficult to identify blood when it is found at the crime scene. For instance, over time blood colour becomes darker and therefore does not characteristically look like blood. Additionally, the photos demonstrate how blood can start to flake at around 24hr and later, which in practice, causes issues in forensic science as most blood on substrates will therefore be lost if not found early enough. Although, the photos demonstrate clearly that one of the best substrates for blood retention is denim due to its fibrous composition which is useful in practice.

## CHAPTER 7

### CONCLUSIONS

This research profiles Equine blood using Raman spectroscopy, identifying spectral differences between blood at different time stages and on different substrates. It is noted that Raman spectroscopy is an effective technique for the confirmatory identification of blood in the area of forensic examination and crime scene analysis. Spectral profiling of blood identifies peaks at the regions of  $747.1\text{cm}^{-1}$ ,  $1001\text{cm}^{-1}$ ,  $1129\text{cm}^{-1}$ ,  $1225\text{cm}^{-1}$ ,  $1340\text{cm}^{-1}$ ,  $1362\text{cm}^{-1}$ ,  $1434\text{cm}^{-1}$ ,  $1587\text{cm}^{-1}$  and  $1640\text{cm}^{-1}$  which correspond to tryptophan, phenylalanine, glucose, fibrin, tryptophan, haemoglobin, tryptophan, haemoglobin and haemoglobin respectively (**CHAPTER 3**). Using these characteristic peaks it is possible to identify blood with certain surety and the recent development of handheld Raman spectrometer means that this identification can be carried out rapidly and *in vitro* at the crime scene (**CHAPTER 1.8**).

The analysis of blood at different time stages has shown a general increase in intensity of the main peaks of blood over time. However haemoglobin peaks ( $1587\text{cm}^{-1}$ ,  $1640\text{cm}^{-1}$ ) have shown a general decrease. The decrease in intensity at these two peaks relates to haemoglobin degradation (**CHAPTER 4**). The MVA has also shown separation between early and late time points. These results demonstrate that between the times of  $\leq 1\text{hr}$  and  $3\text{m}$  the blood droplet undergoes physical and visual changes and although these changes occur, the spectrum of blood is still clearly recognisable at each time stage (**CHAPTER 4.7**). Finally, in some spectra, shifts are evident which could have resulted from the droplet composition or fluorescence from the droplet or background. These shifts could have contributed to the DFA peaks however further research, to identify whether intensity or shifts effect the spectrum more, has to be carried out. In

relation to forensic science this data proves that Raman spectroscopy is a reliable and effective tool for the identification of blood up to 3m. Additionally, it proves that time can have an effect on the Raman spectrum of blood and allows for further investigation into later time periods than 3m.

The analysis of blood on different substrate materials has shown changes in the main peaks of blood across the substrates (**CHAPTER 5**). In particular variation in intensity at the peak position  $1640\text{cm}^{-1}$  can be seen across the substrates. At early time points this variation is frequent between the different substrates and at later time points this variation is only clearly visual between denim and the rest of the substrates (**CHAPTER 5**). Finally, shifts are seen again and could contribute to the DFA peaks and substrate separations in the plots. These results prove that substrate variation does affect the Raman spectrum of blood. However, the characteristic peaks can still be clearly seen across all substrates. These results allow for further research on other substrates which may affect the Raman spectrum of blood. Again, further research must be carried out to determine what affects the spectrum more (shifts or intensity)

Overall, this research provides evidence for the use of Raman spectroscopy as a confirmatory technique for the identification of blood at time stages of up to 3m and across a variety of substrates.

## CHAPTER 8

### FUTURE WORK

This research has provided evidence for: the investigation of the effect of ageing and substrate variation on the Raman spectrum of Equine blood. Further research needs to be carried out investigating, the effect of ageing and substrate variation on the Raman spectrum of blood, over longer periods of time and on more substrates. Further research could be carried out on different types and brands of condom (e.g. non latex condoms) and lubricants also used in these condoms and how this affects results. Investigation into human blood at different stages of ageing and on different substrates should also be carried out to demonstrate whether results would correlate to results in this study. Further research also needs to be carried out to address the effect shifts in the spectrum may have on results. Shifts may contribute to DFA peaks and substrate separations seen in the plots (**Figures 51, 53, 55**). This future research also needs to highlight the major contributor to results; shifts or intensity. Additionally, a blind test could be carried out in order to determine the time since the blood droplet was deposited. It could also be possible to create a spectral library of blood on various substrates at various time points. This would be beneficial to forensic science when blood is found at the scene of the crime. Also, in this study blood was deposited at a height of <5mm above the substrate. Therefore the effect (on the Raman spectrum of blood) of depositing blood from different heights onto substrates should also be investigated.

## BIBLIOGRAPHY

- [1] Wonder, A.Y. 2001. *Blood Dynamics*. Academic Press. London. Pg. 8-14,101-111
- [2] McLaughlin, G; Sikirzhytski, V; Lednev, I.K. 2013. *Circumventing Substrate Interference in the Raman Spectroscopic Identification of Blood Stains*. Forensic Science International, Vol. 231, Iss. 1-3, Pg. 157-166
- [3] Bremmer, R.H; de Bruin, K.G; van Gemert, M.J.C; van Leeuwen, T.G; Aalders, M.C.G. 2012. *Forensic Quest for Age Determination of Bloodstains*. Forensic Science International, Vol. 216, Iss. 1-3, Pg. 1-11
- [4] Dorling, K.M; Baker, M.J. 2013. *Highlighting Attenuated Total Reflection Fourier Transform Infrared Spectroscopy for Rapid Serum Analysis*. Trends in Biotechnology, Vol. 31, Iss. 6, Pg. 327-328
- [5] Hands, J.R; Dorling, K.M; Abel, P; Ashton, K.M; Brodbelt, A; Davis, C; Dawson, T; Jenkinson, M.D; Lea, R.W; Walker, C; Baker, M.J. 2014. *Attenuated Total Reflection Fourier Transform Infrared (ATR-FTIR) Spectral Discrimination of Brain Tumour Severity from Serum Samples*. Journal of Biophotonics. Vol. 7, Iss. 3-4, Pg. 189-199
- [6] Sikirzhytski, V; Sikirzhytskaya, A; Lednev, I.K. 2012. *Advanced Statistical Analysis of Raman Spectroscopic Data for the Identification of Body Fluid Traces: Semen and Blood Mixtures*. Forensic Science International, Vol. 222, Iss. 1-3, Pg. 259-265

- [7] Sikirzhyskaya, A; Sikirzhyski, V; McLaughlin, G; Lednev, I.K. 2013. *Forensic Identification of Contaminations Using Raman Microspectroscopy Coupled with Advanced Statistics: Effect of Sand, Dust and Soil*. Journal of Forensic Sciences, Vol.58, Iss. 5, Pg. 1141-1148
- [8] Lemler, P; Premasiri, W.R; DelMonaco, A; Ziegler, L.D. 2014. *NIR Raman Spectra of Whole Human Blood: Effects of Laser-Induced and in Vitro Hemoglobin Denaturation*. Analytical and Bioanalytical Chemistry, Vol. 406, Iss. 1, Pg. 193-200
- [9] Bremmer, R; Aalders, M. 2011. *Reflectance Spectroscopy for Recognition and Age Determination of Bloodstains*. <http://www.slideshare.net/rolfok/ageing-bloodstains>. Accessed: 13/02/2014
- [10] Botonjic-Sehic, E; Brown, C.W; Lamontagne, M; Tsaparikos, M. 2009. Forensic Application of Near-Infrared Spectroscopy: Aging of Bloodstains. Url Address: <http://www.spectroscopyonline.com/spectroscopy/Near-IR+Spectroscopy/Forensic-Application-of-Near-Infrared-Spectroscopy/ArticleStandard/Article/detail/583780?contextCategoryId=36822> Accessed: 21/07/2014
- [11] Houck, M.M; Siegel, J.A. 2006. *Fundamentals of Forensic Science*. Elsevier Science and Technology. Burlington, USA. Pg. 244, 245, 246
- [12] Bevel, T; Gardner, R.M. 2001. *Bloodstain Pattern Analysis: With an Introduction to Crime Scene Reconstruction, 2<sup>nd</sup> Edition*. CRC Press. London. Pg. 134

- [13] Virkler, K; Lednev, I.K. 2009. *Analysis of Body Fluids for Forensic Purposes: From Laboratory Testing to Non-destructive Rapid Confirmatory Identification at a Crime Scene*. Forensic Science International, Vol. 188, Iss. 1-3, Pg. 1-17
- [14] Lin, A.C.-Y; Hsieh, H.-M; Tsai, L.-C; Linacre, A; Lee, J.C.-I. 2007. *Forensic Applications of Infrared Imaging for the Detection and Recording of Latent Evidence*. Journal of Forensic Sciences, Vol. 52, Iss. 2, Pg. 1148-1150
- [15] Virkler, K; Lednev, I.K. 2008. *Raman Spectroscopy Offers Great Potential for the Nondestructive Confirmatory Identification of Body Fluids*. Forensic Science International, Vol. 181, Iss. 1-3, Pg. e1-e5
- [16] Koenig, J.L. 2001. *Infrared and Raman Spectroscopy of Polymers*. Smithers Rapra. Shrewsbury. Pg. 5, 11
- [17] Ferraro, J.R; Nakamoto, K; Brown, C.W. 2003. *Introductory Raman Spectroscopy*. Academic Press. San Diego. USA. Pg. 14, 15, 16, 22, 23, 24, 25, 26, 27
- [18] Nakamoto K. 2009. *Infrared and Raman Spectra of Inorganic and Coordinatrion Compounds, Theory and Applications in Inorganic Chemistry*. Wiley. New Jersey. USA. Pg. 5, 9
- [19] National University of Singapore. *Energy Level Diagram to Explain Raman Scattering*. Url address:  
<http://vhosts.science.nus.edu.sg/organicelectronics/?p=1376>. Accessed:  
 10/02/2014
- [20] McLaughlin, G. 2013. *RamanSpectroscopic Analysis of Bodily Fluids: Species Differentiation and the Effect of Substrate Interference and Laser Power*.

ProQuest Dissertations and Thesis. Url Address:

<http://search.proquest.com/docview/1468679357/previewPDF?accountid=17233>

Accessed: 24/02/2014

- [21] Rana, V; Cañamares, M.V; Kubic, T; Leona, M; Lombardi, J.R. 2011. *Surface Enhanced Raman Spectroscopy for Trace Identification of Controlled Substances: Morphine, Codeine and Hydrocodone*. Journal of Forensic Sciences, Vol. 56, Iss. 1, Pg. 200-207
- [22] Geiman, I; Leona, M; Lombardi, J.R. 2009. *Application of Raman Spectroscopy and Surface-Enhanced Raman Scattering to the Analysis of Synthetic Dyes Found in Ballpoint Pen Inks*. Journal of Forensic Sciences, Vol. 54, Iss. 4, Pg. 947-942
- [23] Zięba-Palus, J; Trzcińska, B.M. 2013. *Application of Infrared and Raman Spectroscopy in Paint Trace Examination*. Journal of Forensic Sciences, Vol. 58, Iss. 5, Pg. 1359-1363
- [24] Izake, E.L. 2010. *Forensic and Homeland Security Applications of Modern Portable Raman Spectroscopy*. Forensic Science International, Vol.202, Iss. 1-3, Pg. 1-8
- [25] Messina, G; Santangelo, S. 2002. *GNSR 2001: State of Art and Future Development in Raman Spectroscopy and Related Techniques*. IOS Press. Amsterdam. Pg. 41
- [26] Boyd, S; Bertino, M.F; Ye, D; White, L.S; Seashols, S.J. 2013. *Highly Sensitive Detection of Blood by Surface Enhanced Raman Scattering*. Journal of Forensic Sciences, Vol. 58, Iss. 3, Pg. 753-756

- [27] Harvey, S.D; Vucelick, M.E; Lee, R.N; Wright, B.W. 2002. *Blind Field Test Evaluation of Raman Spectroscopy as a Forensic Tool*. Forensic Science International, Vol. 125, Iss. 1, Pg. 12-21
- [28] Vandenabeele, P; Edwards, H.G.M; Jehlicka, J. 2014. *The Role of Mobile Instrumentation in Novel Applications of Raman Spectroscopy: Archaeometry, Geosciences and Forensics*. Chemical Society Reviews, Vol. 43, Iss. 8, Pg. 2628-2649
- [29] Zhang, X; Young, M.A; Lyandres, O; Van Duyne, R.P. 2005. *Rapid Detection of Anthrax Biomarker by Surface Enhanced Raman Spectroscopy*. Journal of American Chemical Society, Vol. 127, Iss. 12, Pg. 4484-4489
- [30] Virkler, K; Lednev, I.K. 2010. *Raman Spectroscopic Signature of Blood and its Potential Application to Forensic Body Fluid Identification*. Analytical and Bioanalytical Chemistry, Vol. 396, Iss. 1, Pg. 525-534
- [31] Boyd, S; Bertino, M.F; Seashols, S.J. 2011. *Raman Spectroscopy of Blood Samples for Forensic Applications*. Forensic Science International, Vol. 208, Iss. 1-3, Pg. 124-128
- [32] Edelman, G; Manti, V; Van Ruth, S.M; Van Leeuwen, T; Aalders, M. 2012. *Identification and Age Estimation of Blood Stains on Coloured Backgrounds by Near Infrared Spectroscopy*. Forensic Science International, Vol. 220, Iss. 1-3, Pg. 239-244
- [33] Lieber, C.A; Mahadevan-Jansen, A. 2003. *Automated Method for Substraction of Fluorescence from Biological Raman Spectra*. Applied Spectroscopy, Vol. 57, Iss. 11, Pg. 1363-1367.

- [34] Bocklitz, T; Walter, A; Hartmann, K; Rösch, P; Popp, J. 2011. *How to Pre-process Raman Spectra for Reliable and Stable Models?* *Analytica Chimica Acta*, Vol. 704, Iss. 1-2, Pg. 47-56
- [35] Heraud, P; Wood, B.R; Beardall, J; McNaughton, D. 2006. *Effects of Pre-processing of Raman Spectra on in vivo classification of Nutrient Status of Microalgal Cells.* *Journal of Chemometrics*, Vol. 20, Iss. 5, Pg. 183-197
- [36] Virkler, K; Lednev, I.K. 2009. *Blood Species Identification for Forensic Purposes Using Raman Spectroscopy Combined with Advanced Statistical Analysis.* *Analytical Chemistry*, Vol. 81, Iss. 18, Pg. 7773-7777
- [37] Sikirzhyskaya, A; Sikirzhyski, V; Lednev, I.K. 2012. *Raman Spectroscopic Signature of Vaginal Fluid and Its Potential Application in Forensic Body Fluid Identification.* *Forensic Science International*, Vol. 216, Iss. 1-3, Pg. 44-48
- [38] Sikirzhyski, V; Virkler, K; Lednev, I.K. 2010. *Discriminant Analysis of Raman Spectra for Body Fluid Identification for Forensic Purposes.* *Sensors*, Vol. 10, Iss. 4, Pg. 2869-2884
- [39] Li, X; Yang, T; Lib, S; Yu, T. 2011. *Surface-enhanced Raman Spectroscopy Differences of Saliva Between Lung Cancer Patients and Normal People.* *European Conference on Biomedical Optics.* DOI: <http://dx.doi.org/10.1364/ECBO.2011.808722>
- [40] Weng, X; Cloutier, G; Pibarot, P; Durand, L.G. 1996. *Comparison and Simulation of Different Levels of Erythrocyte Aggregation With Pig, Horse, Sheep, Calf and Normal Human Blood.* *Biorheology*. Vol. 33, Iss. 4, Pg. 365-377

- [41] Baskurt, O.J; Farley, R.A; Meiselman, H.J. 1997. *Erythrocyte Aggregation Tendancy and Cellular Properties In Horse, Human, and Rat: A Comparative Study*. The American Journal of Physiology. Vol. 273, Pg. H2604-2612
- [42] E&O Laboratories Ltd. *Defibrinated Horse Blood-DHB*. Url Address: <http://www.eolabs.com/defibrinated-horse-blood-dhb.html>. Accessed: 09/04/2015
- [43] Yeh, E; Pinsky, B.A; Banaei, N; Baron, E.J. 2009. *Hair Sheep Blood, Citrated or Defibrinated, Fulfills all Requirements of Blood Agar for Diagnostic Microbiology Laboratory Tests*. PloS One. Vol. 4, Iss. 7, e6141
- [44] Colorado Serum Company. Url Address: <http://www.colorado-serum.com/reagent/sheep.html>. Accessed: 09/04/2015
- [45] McLaughlin, G; Doty, K.C; Lednev, I.K. 2014. *Discrimination of Human and Animal Blood Traces Via Raman Spectroscopy*. Forensic Science International. Vol. 238, Pg. 91-95
- [46] *Chemical and Component Structures*. Symyx Draw 3.3. Accessed: 28/08/14
- [47] Sikirzhytskaya, A; Sikirzhytski, V; Lednev, I.K. 2014. *Raman Spectroscopy Coupled with Advanced Statistics for Differentating Menstrual and Peripheral Blood*. Journal of Biophotonics, Vol. 7, Iss. 1-2, Pg. 59-67
- [48] Okusaga, O; Muravitskaja, O; Fuchs, D; Ashraf, A; Hinman, S; Giegling, I; Hartmann, A.M; Konte, B; Friedl, M; Schiffman, J; Hong E; Reeves, G; Groer, M; Dantzer, R; Rujescu, D; Postolache, T.T. 2014. *Elevated Levels of Plasma Phenylalanine in Schizophrenia: A Guanosine Triphosphate Cyclohydrolase-1 Metabolic Pathway Abnormality?* PloS ONE, Vol. 9, Iss. 1, Pg. 1-5

- [49] Wiley and Sons. 2009. *Novartis Foundation Symposia: Aromatic Amino Acids in the Brain*. John Wiley and Sons. Somerset. New Jersey. Pg. 1
- [50] Srivastava, H.S. 2010. *Elements of Biochemistry*. Global Media. Meerut, India. Pg. 161-162, 280-281
- [51] Nova Science Publishers, Inc. 2013. *Macromolecular Chemistry: New Research*. Nova Science Publishers, Inc. Hauppauge. New York. Pg. 84-85
- [52] Szablewski, L. 2011. *Glucose Homeostasis and Insulin Resistance*. Bentham Science Publishers. Sharjah, UAE. Pg. 1
- [53] Horiba Jobin Yvon Raman Spectroscopy for Analysis and Monitoring. Url Address:  
<http://www.horiba.com/fileadmin/uploads/Scientific/Documents/Raman/bands.pdf>  
df Accessed: 29/07/2014
- [54] Doménech, A; Doménech-Carbó, M.T; Edwards, H.G.M. 2011. *On the Interpretation of the Raman Spectra of Maya Blue: A Review on the Literature Data*. Journal of Raman Spectroscopy, Vol. 42, Iss. 1, Pg. 86-96
- [55] Fiedler, A; Baranska, M; Schulz, H. 2011. *Ft-Raman Spectroscopy- a Rapid and Reliable Quantification Protocol for the Determination of Natural Indigo Dye in Polygonum Tinctorium*. Journal of Raman Spectroscopy, Vol. 42, Iss. 3, Pg. 551-557
- [56] Schrader, B; Klump, H.H; Schenzel, K; Schulz, H. 1999. *Non-Destructive NIR-FT Raman Analysis of Plants*. Journal of Molecular Structure, Vol. 509, Iss. 1-3, Pg. 201-212

- [57] Coupry, C; Sagon, G; Gorguet-Ballesteros, P. 1997. *Raman Spectroscopic Investigation of Blue Contemporary Textiles*. Journal of Raman Spectroscopy. Vol, 28, Iss. 2-3, Pg. 85-89
- [58] Chatwal, G.R; Arora, M. 2009. *Synthetic Dyes*. Global Media. Mumbai, India. Pg. 9, 225
- [59] Smith, J.L. 2009. *Textile Processing*. Global Media. Chandigarh, India. Pg. 55
- [60] Dufresne, A. 2012. *Nanocellulose: From Nature to High Performance Tailored Materials*. Walter de Gruyter. Munchen. DEU. Pg. 17-21
- [61] Cárcamo, J.J; Aliaga, A.E; Clavijo, R.E; Brañes, M.R; Compos-Vallette, M.M. 2012. *Raman Study of the Shockwave Effect on Collagens*. Spectrochimica Acta Part A: Molecular and Biomolecular Spectroscopy, Vol. 86, Pg. 360-365
- [62] May, E; Jones, M; Barker, B.D. 2006. *Conservation Science: Heritage Materials*. Royal Society of Chemistry. Cambridge. GBR. Pg. 96-98
- [63] Mendelovici, E; Frost, R.L; Kloprogge, T. 2000. *Cryogenic Raman Spectroscopy of Glycerol*. Journal of Raman Spectroscopy, Vol. 31, Iss. 12, Pg. 1121-1126
- [64] Coyle, T; Anwar, N. 2009. *A Novel Approach to Condom Lubricant Analysis: In-situ Analysis of Swabs by FT-Raman Spectroscopy and its Effects on DNA Analysis*. Science and Justice, Vol. 49, Iss. 1, Pg. 32-40
- [65] Simoes, R.D; Job, A.E; Chinaglia, D.L; Zucolotto, V; Carmargo-Filho, J.C; Alves, N; Giacometti, J.A; Oliveira Jr, O.N; Constantino, C.J.L. 2005.

*Structural Characterization of Blends Containing Both PVDF and Natural Rubber Latex.* Journal of Raman Spectroscopy, Vol. 36, Iss. 12, Pg. 1118-1124

- [66] Job, A.E; Constantino, C.J.L; Mendes, T.S.G; Teruya, M.Y; Alves, N; Mattoso, L.H.C. 2003. *Effect of Natural Rubber Latex on the Conducting State of Polyaniline Blends Determined by Raman Spectroscopy.* Journal of Raman Spectroscopy, Vol. 34, Iss. 10, Pg. 831-836
- [67] Anderson, C.D; Daniels. 2003. *Emulsion Polymerisation and Latex Applications.* Smithers Rapra. Shrewsbury. GBR. Pg. 3
- [68] Simpson, R. 2002. *Rubber Basics.* Smithers Rapra. Shrewsbury. GBR. Pg. 28-29
- [69] Saraf, S; Saraf, S. 2008. *Cosmetics: A Practical Manual.* Pharmamed Press, Hyderabad. IND. Pg. 23
- [70] Great Floors. *Laminate How It's Made.* Url Address: <http://www.greatfloors.com/contentpage.aspx?Id=10618>. Accessed: 07/07/2014
- [71] Semrock. *Green Photonics Raman Spectroscopy.* Url Address: <http://www.semrock.com/green-photonics-raman-spectroscopy.aspx> Accessed: 28/07/2014
- [72] Occupational Safety and Health Administration. *Crystalline Silica Exposure Health Hazard Information.* Url Address: [https://www.osha.gov/OshDoc/data\\_General\\_Facts/crystalline-factsheet.pdf](https://www.osha.gov/OshDoc/data_General_Facts/crystalline-factsheet.pdf) Accessed: 04/07/2014
- [73] Deschaines, T; Hodkiewicz, J; Henson, P. Thermo Scientific. *Characterization of Amorphous and Microcrystalline Silicon using Raman Spectroscopy.* Url

Address:

[http://www.thermoscientific.de/eThermo/CMA/PDFs/Product/productPDF\\_568](http://www.thermoscientific.de/eThermo/CMA/PDFs/Product/productPDF_568)

86.PDF Accessed: 04/07/2014

# APPENDICES

## Appendix 1- A poster presented at SciX 2014, Reno. Entitled “The Effect of Ageing and Substrate Variation on the Raman Spectrum of Equine Blood.”

### Investigating the Effect of Ageing and Substrate Variation on the Raman Spectrum of Equine Blood

Christopher J. Wassell<sup>1</sup>, Matthew J. Baker<sup>1,2</sup>, Graeme Clemens<sup>1</sup>  
<sup>1</sup>Centre for Materials Science, Division of Chemistry, University of Central Lancashire, PR1 2HE, UK  
<sup>2</sup>WestCHEM, Department of Pure and Applied Chemistry, University of Strathclyde, 295 Cathedral Street, Glasgow, G1 1XL  
 \*email: [c.wassell@uclan.ac.uk](mailto:c.wassell@uclan.ac.uk), [mjbaker@uclan.ac.uk](mailto:mjbaker@uclan.ac.uk), and [g.clemens@uclan.ac.uk](mailto:g.clemens@uclan.ac.uk)

---

#### Introduction

- Blood pattern analysis (BPA) involves the study of blood found at the crime scene from discovery through to identification and further analysis. Blood is one of the most common types of evidence found at the crime scene in particular involving cases such as; murder, assaults and accidents [1].
- BPA can provide essential information about the crime scene including; the sequence of events, identifying the number of individuals involved, the weapon used and linking suspects and victims to the crime scene.
- Raman spectroscopy can be used to identify bodily fluids including blood [2] and recent advances in Raman spectroscopy has enabled the production of handheld spectrometers to be used in the field to enable analysis of unknown substances *in vitro* [3]. However, the time since blood was deposited at the scene and the surfaces and materials blood will come into contact with will vary and this may have an effect on the Raman spectrum.
- The purpose of this study was to determine whether Raman spectroscopy could be used as a reliable confirmatory technique for blood in conditions similar to those found at the crime scene.

#### Method

- Six substrates were used for analysis; ceramic tile, brown leather, blue denim, laminate tile, condom and a single crystal silicon standard.
- Three drops of 2µl of equine blood was pipetted onto each substrate and scans were taken at time stages of 51hr, 2hrs, 5hrs, 24hrs, 1week, 2weeks, 1month, 2months and 3months.
- 10 scans per drop were taken totalling 30 scans for each time frame on each substrate. A line scan of a blood droplet was also carried out to determine the point of the droplet which would produce the best spectrum. Scans were carried out using a Horiba Jobin-Yvon LabRam HR800 spectrometer over a wavelength of 500cm<sup>-1</sup> – 3500cm<sup>-1</sup>.
- A 532nm, 1% laser power produced major peaks at 747cm<sup>-1</sup>, 1001cm<sup>-1</sup>, 1129cm<sup>-1</sup>, 1225cm<sup>-1</sup>, 1340cm<sup>-1</sup>, 1362<sup>-1</sup>, 1434cm<sup>-1</sup>, 1587cm<sup>-1</sup> and 1640cm<sup>-1</sup> for Tryptophan, Phenylalanine, Glucose, Fibrin, Typtophan, Heme, Typtophan, Heme and Heme respectively.

---

#### Study Results

- The line scan of the droplet (Figure 4) showed no significant differences in the raw Raman spectrum at the four different points. Also on denim and leather substrates the blood soaked into the material and blood parameters were difficult to locate. Therefore spectrum were taken from wherever blood could be found on the substrates.
- Baseline correction was carried out using 5<sup>th</sup> order polynomial on LabRam and 2<sup>nd</sup> order derivative was also carried out using Matlab software. Vector normalisation was carried out after both.
- 5<sup>th</sup> order polynomial spectra (Figure 5) shows changes in the spectra over time at regions of ~1640cm<sup>-1</sup> and ~1362 which are Heme regions.
- 2<sup>nd</sup> order derivative spectra showed changes in peaks relating to Heme at ~1635cm<sup>-1</sup> and Fibrin at ~1225cm<sup>-1</sup>.

#### Conclusions

- Spectrum collected at 51hr (Figure 5, cyan colour) shows low intensities, possibly due to the droplet still being wet and therefore the droplet surface is difficult to focus on using the Raman microscope. Spectrum at 2hr and after, when drying has occurred, the intensities are greater.
- Condon spectra results show that changes do occur in the Raman spectra of blood over time and Heme and Fibrin degradation observed supports previous literature results [14]. PCA analysis (Figure 6), carried out after 2<sup>nd</sup> order derivative and vector normalisation, showed separation of spectra between 1hr and 3 months of ageing.
- Study results demonstrate that Raman spectroscopy can be used as a confirmatory technique for the identification of blood in conditions similar to those found at the crime scene.

---

#### Figure 1

Figure 1: Blood droplet on ceramic tile at time stages of 51 hour (top left), 2 hours, 5 hours, 24 hours, 1 week, 2 weeks and 3 months (far right). Drying, spreading and deformation in droplet can be visualised over time.

#### Figure 2

Figure 2: Blood droplet on ceramic tile at 51 hour. The Raman spectrum shows characteristic peaks for biomolecules such as Heme, Typtophan, and Fibrin.

---

#### Figure 3

Figure 3: Line scan of blood droplet on ceramic tile at 51 hour. The Raman spectrum shows characteristic peaks for biomolecules such as Heme, Typtophan, and Fibrin.

#### Figure 4

Figure 4: Line scan of blood droplet on ceramic tile at 51 hour. The Raman spectrum shows characteristic peaks for biomolecules such as Heme, Typtophan, and Fibrin.

---

#### Figure 5

Figure 5: Raw Raman spectra of blood droplet on various substrates at different time stages. The plot shows several distinct peaks corresponding to various biomolecules.

#### Figure 6

Figure 6: PCA plot showing the separation of Raman spectra of blood droplets on various substrates at different time stages. The plot shows several distinct clusters corresponding to different substrates and time stages.

---

#### Figure 7

Figure 7: PCA plot showing the separation of Raman spectra of blood droplets on various substrates at different time stages. The plot shows several distinct clusters corresponding to different substrates and time stages.

#### Figure 8

Figure 8: PCA plot showing the separation of Raman spectra of blood droplets on various substrates at different time stages. The plot shows several distinct clusters corresponding to different substrates and time stages.

---

#### Figure 9

Figure 9: PCA plot showing the separation of Raman spectra of blood droplets on various substrates at different time stages. The plot shows several distinct clusters corresponding to different substrates and time stages.

#### Figure 10

Figure 10: PCA plot showing the separation of Raman spectra of blood droplets on various substrates at different time stages. The plot shows several distinct clusters corresponding to different substrates and time stages.

---

#### Figure 11

Figure 11: PCA plot showing the separation of Raman spectra of blood droplets on various substrates at different time stages. The plot shows several distinct clusters corresponding to different substrates and time stages.

#### Figure 12

Figure 12: PCA plot showing the separation of Raman spectra of blood droplets on various substrates at different time stages. The plot shows several distinct clusters corresponding to different substrates and time stages.

---

#### Figure 13

Figure 13: PCA plot showing the separation of Raman spectra of blood droplets on various substrates at different time stages. The plot shows several distinct clusters corresponding to different substrates and time stages.

#### Figure 14

Figure 14: PCA plot showing the separation of Raman spectra of blood droplets on various substrates at different time stages. The plot shows several distinct clusters corresponding to different substrates and time stages.

---

#### Figure 15

Figure 15: PCA plot showing the separation of Raman spectra of blood droplets on various substrates at different time stages. The plot shows several distinct clusters corresponding to different substrates and time stages.

#### Figure 16

Figure 16: PCA plot showing the separation of Raman spectra of blood droplets on various substrates at different time stages. The plot shows several distinct clusters corresponding to different substrates and time stages.

---

#### Figure 17

Figure 17: PCA plot showing the separation of Raman spectra of blood droplets on various substrates at different time stages. The plot shows several distinct clusters corresponding to different substrates and time stages.

#### Figure 18

Figure 18: PCA plot showing the separation of Raman spectra of blood droplets on various substrates at different time stages. The plot shows several distinct clusters corresponding to different substrates and time stages.

---

#### Figure 19

Figure 19: PCA plot showing the separation of Raman spectra of blood droplets on various substrates at different time stages. The plot shows several distinct clusters corresponding to different substrates and time stages.

#### Figure 20

Figure 20: PCA plot showing the separation of Raman spectra of blood droplets on various substrates at different time stages. The plot shows several distinct clusters corresponding to different substrates and time stages.

---

#### Figure 21

Figure 21: PCA plot showing the separation of Raman spectra of blood droplets on various substrates at different time stages. The plot shows several distinct clusters corresponding to different substrates and time stages.

#### Figure 22

Figure 22: PCA plot showing the separation of Raman spectra of blood droplets on various substrates at different time stages. The plot shows several distinct clusters corresponding to different substrates and time stages.

---

#### Figure 23

Figure 23: PCA plot showing the separation of Raman spectra of blood droplets on various substrates at different time stages. The plot shows several distinct clusters corresponding to different substrates and time stages.

#### Figure 24

Figure 24: PCA plot showing the separation of Raman spectra of blood droplets on various substrates at different time stages. The plot shows several distinct clusters corresponding to different substrates and time stages.

---

#### Figure 25

Figure 25: PCA plot showing the separation of Raman spectra of blood droplets on various substrates at different time stages. The plot shows several distinct clusters corresponding to different substrates and time stages.

#### Figure 26

Figure 26: PCA plot showing the separation of Raman spectra of blood droplets on various substrates at different time stages. The plot shows several distinct clusters corresponding to different substrates and time stages.

---

#### Figure 27

Figure 27: PCA plot showing the separation of Raman spectra of blood droplets on various substrates at different time stages. The plot shows several distinct clusters corresponding to different substrates and time stages.

#### Figure 28

Figure 28: PCA plot showing the separation of Raman spectra of blood droplets on various substrates at different time stages. The plot shows several distinct clusters corresponding to different substrates and time stages.

---

#### Figure 29

Figure 29: PCA plot showing the separation of Raman spectra of blood droplets on various substrates at different time stages. The plot shows several distinct clusters corresponding to different substrates and time stages.

#### Figure 30

Figure 30: PCA plot showing the separation of Raman spectra of blood droplets on various substrates at different time stages. The plot shows several distinct clusters corresponding to different substrates and time stages.

---

#### Figure 31

Figure 31: PCA plot showing the separation of Raman spectra of blood droplets on various substrates at different time stages. The plot shows several distinct clusters corresponding to different substrates and time stages.

#### Figure 32

Figure 32: PCA plot showing the separation of Raman spectra of blood droplets on various substrates at different time stages. The plot shows several distinct clusters corresponding to different substrates and time stages.

---

#### Figure 33

Figure 33: PCA plot showing the separation of Raman spectra of blood droplets on various substrates at different time stages. The plot shows several distinct clusters corresponding to different substrates and time stages.

#### Figure 34

Figure 34: PCA plot showing the separation of Raman spectra of blood droplets on various substrates at different time stages. The plot shows several distinct clusters corresponding to different substrates and time stages.

---

#### Figure 35

Figure 35: PCA plot showing the separation of Raman spectra of blood droplets on various substrates at different time stages. The plot shows several distinct clusters corresponding to different substrates and time stages.

#### Figure 36

Figure 36: PCA plot showing the separation of Raman spectra of blood droplets on various substrates at different time stages. The plot shows several distinct clusters corresponding to different substrates and time stages.

---

#### Figure 37

Figure 37: PCA plot showing the separation of Raman spectra of blood droplets on various substrates at different time stages. The plot shows several distinct clusters corresponding to different substrates and time stages.

#### Figure 38

Figure 38: PCA plot showing the separation of Raman spectra of blood droplets on various substrates at different time stages. The plot shows several distinct clusters corresponding to different substrates and time stages.

---

#### Figure 39

Figure 39: PCA plot showing the separation of Raman spectra of blood droplets on various substrates at different time stages. The plot shows several distinct clusters corresponding to different substrates and time stages.

#### Figure 40

Figure 40: PCA plot showing the separation of Raman spectra of blood droplets on various substrates at different time stages. The plot shows several distinct clusters corresponding to different substrates and time stages.

---

#### Figure 41

Figure 41: PCA plot showing the separation of Raman spectra of blood droplets on various substrates at different time stages. The plot shows several distinct clusters corresponding to different substrates and time stages.

#### Figure 42

Figure 42: PCA plot showing the separation of Raman spectra of blood droplets on various substrates at different time stages. The plot shows several distinct clusters corresponding to different substrates and time stages.

---

#### Figure 43

Figure 43: PCA plot showing the separation of Raman spectra of blood droplets on various substrates at different time stages. The plot shows several distinct clusters corresponding to different substrates and time stages.

#### Figure 44

Figure 44: PCA plot showing the separation of Raman spectra of blood droplets on various substrates at different time stages. The plot shows several distinct clusters corresponding to different substrates and time stages.

---

#### Figure 45

Figure 45: PCA plot showing the separation of Raman spectra of blood droplets on various substrates at different time stages. The plot shows several distinct clusters corresponding to different substrates and time stages.

#### Figure 46

Figure 46: PCA plot showing the separation of Raman spectra of blood droplets on various substrates at different time stages. The plot shows several distinct clusters corresponding to different substrates and time stages.

---

#### Figure 47

Figure 47: PCA plot showing the separation of Raman spectra of blood droplets on various substrates at different time stages. The plot shows several distinct clusters corresponding to different substrates and time stages.

#### Figure 48

Figure 48: PCA plot showing the separation of Raman spectra of blood droplets on various substrates at different time stages. The plot shows several distinct clusters corresponding to different substrates and time stages.

---

#### Figure 49

Figure 49: PCA plot showing the separation of Raman spectra of blood droplets on various substrates at different time stages. The plot shows several distinct clusters corresponding to different substrates and time stages.

#### Figure 50

Figure 50: PCA plot showing the separation of Raman spectra of blood droplets on various substrates at different time stages. The plot shows several distinct clusters corresponding to different substrates and time stages.

---

#### Figure 51

Figure 51: PCA plot showing the separation of Raman spectra of blood droplets on various substrates at different time stages. The plot shows several distinct clusters corresponding to different substrates and time stages.

#### Figure 52

Figure 52: PCA plot showing the separation of Raman spectra of blood droplets on various substrates at different time stages. The plot shows several distinct clusters corresponding to different substrates and time stages.

---

#### Figure 53

Figure 53: PCA plot showing the separation of Raman spectra of blood droplets on various substrates at different time stages. The plot shows several distinct clusters corresponding to different substrates and time stages.

#### Figure 54

Figure 54: PCA plot showing the separation of Raman spectra of blood droplets on various substrates at different time stages. The plot shows several distinct clusters corresponding to different substrates and time stages.

---

#### Figure 55

Figure 55: PCA plot showing the separation of Raman spectra of blood droplets on various substrates at different time stages. The plot shows several distinct clusters corresponding to different substrates and time stages.

#### Figure 56

Figure 56: PCA plot showing the separation of Raman spectra of blood droplets on various substrates at different time stages. The plot shows several distinct clusters corresponding to different substrates and time stages.

---

#### Figure 57

Figure 57: PCA plot showing the separation of Raman spectra of blood droplets on various substrates at different time stages. The plot shows several distinct clusters corresponding to different substrates and time stages.

#### Figure 58

Figure 58: PCA plot showing the separation of Raman spectra of blood droplets on various substrates at different time stages. The plot shows several distinct clusters corresponding to different substrates and time stages.

---

#### Figure 59

Figure 59: PCA plot showing the separation of Raman spectra of blood droplets on various substrates at different time stages. The plot shows several distinct clusters corresponding to different substrates and time stages.

#### Figure 60

Figure 60: PCA plot showing the separation of Raman spectra of blood droplets on various substrates at different time stages. The plot shows several distinct clusters corresponding to different substrates and time stages.

---

#### Figure 61

Figure 61: PCA plot showing the separation of Raman spectra of blood droplets on various substrates at different time stages. The plot shows several distinct clusters corresponding to different substrates and time stages.

#### Figure 62

Figure 62: PCA plot showing the separation of Raman spectra of blood droplets on various substrates at different time stages. The plot shows several distinct clusters corresponding to different substrates and time stages.

---

#### Figure 63

Figure 63: PCA plot showing the separation of Raman spectra of blood droplets on various substrates at different time stages. The plot shows several distinct clusters corresponding to different substrates and time stages.

#### Figure 64

Figure 64: PCA plot showing the separation of Raman spectra of blood droplets on various substrates at different time stages. The plot shows several distinct clusters corresponding to different substrates and time stages.

---

#### Figure 65

Figure 65: PCA plot showing the separation of Raman spectra of blood droplets on various substrates at different time stages. The plot shows several distinct clusters corresponding to different substrates and time stages.

#### Figure 66

Figure 66: PCA plot showing the separation of Raman spectra of blood droplets on various substrates at different time stages. The plot shows several distinct clusters corresponding to different substrates and time stages.

---

#### Figure 67

Figure 67: PCA plot showing the separation of Raman spectra of blood droplets on various substrates at different time stages. The plot shows several distinct clusters corresponding to different substrates and time stages.

#### Figure 68

Figure 68: PCA plot showing the separation of Raman spectra of blood droplets on various substrates at different time stages. The plot shows several distinct clusters corresponding to different substrates and time stages.

---

#### Figure 69

Figure 69: PCA plot showing the separation of Raman spectra of blood droplets on various substrates at different time stages. The plot shows several distinct clusters corresponding to different substrates and time stages.

#### Figure 70

Figure 70: PCA plot showing the separation of Raman spectra of blood droplets on various substrates at different time stages. The plot shows several distinct clusters corresponding to different substrates and time stages.

---

#### Figure 71

Figure 71: PCA plot showing the separation of Raman spectra of blood droplets on various substrates at different time stages. The plot shows several distinct clusters corresponding to different substrates and time stages.

#### Figure 72

Figure 72: PCA plot showing the separation of Raman spectra of blood droplets on various substrates at different time stages. The plot shows several distinct clusters corresponding to different substrates and time stages.

---

#### Figure 73

Figure 73: PCA plot showing the separation of Raman spectra of blood droplets on various substrates at different time stages. The plot shows several distinct clusters corresponding to different substrates and time stages.

#### Figure 74

Figure 74: PCA plot showing the separation of Raman spectra of blood droplets on various substrates at different time stages. The plot shows several distinct clusters corresponding to different substrates and time stages.

---

#### Figure 75

Figure 75: PCA plot showing the separation of Raman spectra of blood droplets on various substrates at different time stages. The plot shows several distinct clusters corresponding to different substrates and time stages.

#### Figure 76

Figure 76: PCA plot showing the separation of Raman spectra of blood droplets on various substrates at different time stages. The plot shows several distinct clusters corresponding to different substrates and time stages.

---

#### Figure 77

Figure 77: PCA plot showing the separation of Raman spectra of blood droplets on various substrates at different time stages. The plot shows several distinct clusters corresponding to different substrates and time stages.

#### Figure 78

Figure 78: PCA plot showing the separation of Raman spectra of blood droplets on various substrates at different time stages. The plot shows several distinct clusters corresponding to different substrates and time stages.

---